Scuola Internazionale Superiore di Studi Avanzati - Trieste

Universality: From discrete symmetry models to active matter systems

Author:

Riccardo Ben Alì Zinati

Supervisors:

Prof. Andrea Gambassi
Dr. Alessandro Codello

A thesis submitted in fulfillment of the requirements for the degree of Doctor of Philosophy in the

PhD course in Statistical Physics

Academic year 2018/2019

SISSA - Via Bonomea 265 - 34136 TRIESTE - ITALY

Preface

Nature provides countless examples in which complex collective behavior emerges spontaneously from the interactions among a large number of relatively simple individual, basic units. Many of the emergent phenomena resulting from such collective behaviors share features like scale–invariance, where different scales make contributions of equal importance. A remarkable example of this is provided by the critical points of continuous phase transitions, at which all the scales, from the microscopic to the macroscopic one, are all alike. Many features at the critical points are largely independent of small–scale details giving rise to *universality* in the large–scale behavior. The development of the scaling hypothesis and the renormalization–group theory tied everything together, providing a theoretical framework within which universality is understood in terms of attractive fixed points and, moreover, offering a method to calculate experimentally accessible quantities like critical exponents.

This thesis focuses on the universal aspects which characterize the collective behavior of many–particle classical systems along two main lines of research: In the first part of the manuscript, we study the universal properties of statistical–mechanics models characterized by discrete symmetry groups. In particular, in chapter 1 we consider the case of the permutation group of q elements. In chapter 2, the attention is devoted to the symmetry group of the regular polytopes. In the second part of the manuscript, instead, we study the collective properties of active matter, namely systems composed of individual units which convert energy to direct their motion. In particular, in chapter 3 we study a statistical–mechanics model that describes active particles interacting via a long–range force called chemotaxis.

Each of the two parts is composed of an invitation to the reading of the chapters there contained. Each chapter is provided with a brief invitation that sets the context of the forthcoming introduction and sections. Conclusions are provided at the end of each chapter.

Contents

Part I

Discrete Symmetry Groups

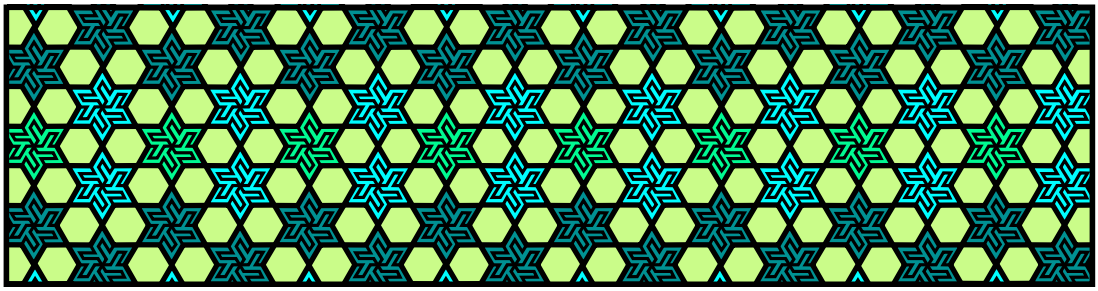

The aesthetic notion of symmetry has always been a constant source of fascination and inspiration in Arts and Sciences. Geometric ornamentation, for example, may have reached a pinnacle in the Islamic world: Mosques, minarets, and palaces are decorated with beautiful and complex patterns displaying highly ordered and symmetric tessellations. Essential to this unique style were the contributions made by Islamic mathematicians, astronomers, and other scientists, whose ideas and technical advances are indirectly reflected in the artistic tradition. Interestingly, a mathematical classification of planar repetitive patterns reveals that only 17 types of them are actually possible, almost all of which can be found in the Islamic decorative tessellations [1]. The mathematical aspects of symmetry undoubtedly played a fundamental role in Science, and even if the aesthetic side of symmetry may not be considered a guiding principle in Physics, *if one is working from the point of view of getting beauty into one's equation, . . . one is on a sure line of progress* [2].

The breakthrough in the use of symmetry in Science, however, came with the introduction of the concept of group and with the ensuing development of the technical apparatus of group theory. Within group theory, in fact, the concept of symmetry is considered as the invariance with respect to a specified group of transformations, which make it suitable to be applied not only to spatial figures, but also to abstract objects such as mathematical expressions and, more generally, physical theories. The mathematical form a physical theory may assume is indeed severely restricted by the requirement of invariance with respect to a set of fundamental transformations. General covariance, namely the invariance of the laws of nature under local changes of the space–time coordinates, is an example of how symmetry intervened in shaping Einstein's theory of general relativity. The invariance with respect to local Gauge

transformations has assumed an essential role in the fundamental theories of Nature, as they provide the basis for the pivotal standard model, i.e. the theory of the fundamental non–gravitational forces, namely the electromagnetic, weak and strong interactions. In quantum theory, the selection rules that govern the atomic spectra are consequences of rotational symmetry, while the symmetry with respect to the exchange of identical particles led to the classification of elementary particles in bosons and fermions. These are just a few examples which give a glimpse of the importance of symmetry requirements in deducing many of the most fundamental results of modern physics. An exhaustive discussion that encompasses other fundamental results is, on the other hand, beyond the scope of this brief invitation and we remind the reader to excellent articles reviewing some of these topics to different extent [3, 4].

Many of the macroscopic manifestations of matter, and more generally much of the texture of the world, can be characterized as having (spontaneously) broken symmetries. Crystals, magnetism, the structure of the unified electro–weak theory and superconductivity are just a few examples. In particular, the latter, namely superconductivity, played a special role in the formulation of what today we call Ginzburg–Landau theory of (continuous) phase transitions. To be more specific, in Landau's theory, the thermodynamic phase of a system undergoing a continuous phase transition from a high–temperature (symmetric) to a low–temperature (ordered) phase in which some symmetry is broken, is controlled by a coarse–grained local order parameter ψ. Thermodynamic quantities, on the other hand, can be derived by the free energy functional $\mathcal{F}[\psi]$ called the Ginzburg–Landau free energy which, though it can be a complicated non–linear and non–local function of the field ψ, it no longer involves the microscopic details of the system under study. It only reflects some general features of the order parameter such as the i) dimensionality of the space, ii) the number of components of the field ψ and iii) the symmetry of the ordered state, indeed. This formulation already achieved a certain level of universality since, different physical systems, with different microscopic Hamiltonians, will lead to the same Ginzburg–Landau free energy, provided they share the three basic ingredients listed above. Landau's phenomenological theory, *only* describes the universal behavior of a system undergoing a second–order phase transition and it gives no clues on non–universal numbers like the critical temperature at which

the phase transition occurs. On the other hand, Landau provided a unique formulation that could embrace at once all the critical phenomena with a given symmetry content, identifying one of the key features behind the surprising universal behavior many different phase transitions share.

However, it was understood that Landau's mean–field description of phase transitions was quantitatively inaccurate as only short–range fluctuations were considered. At the critical point at which the transition occurs, fluctuations of the order parameter occur on all scales and make non–negligible contributions which must be accounted for in determining the correct quantitative critical behavior. This consideration has been the turning point which led to the most powerful theoretical description of thermodynamic phases in terms of successive coarsening operations, the Wilson renormalization group [5, 6], in which short–scale fluctuations are progressively eliminated. The coarsening operation is then represented by a trajectory in the abstract theory space, namely the space characterized by different system Hamiltonians, whose endpoint or fixed point describes the system properties at the longest scales and thus serves to characterize the thermodynamic phase. Distinct renormalization group fixed points represent different phases of matter as well as distinct universality classes at the transition point between them: different physical systems flowing to the same fixed point belong to the same universality class.

A remarkably important conclusion emerged from the modern theory of continuous phase transitions: Different symmetries of the order parameter could lead to different fixed points of the renormalization group flow. The classification of fixed points, on the other hand, is tantamount to the classification of all possible continuous phase transitions that can occur in Nature.

In light of all this, it is therefore not surprising that one of the major problems of statistical field theory has been the classification of universality classes in arbitrary dimension and for a general symmetry group, encoded in the functional form of the Ginzburg–Landau free energy. Despite the centrality of the subject and the many decades passed since Wilson's original works, the classification is to date largely unsolved. Among the rich realm of possible different symmetry groups, in this thesis, we have been mainly interested in *discrete* global symmetries, which are characterized by a finite number of symmetry operations. Discrete groups have found numerous applications in statistical Physics and a more detailed – though not complete–

list of them is provided in the Chapter 1. Worth to mention in this respect is the central role played by the $\mathbb{Z}_2$ discrete symmetry group in the celebrated Ising universality class [7], which provided a superb example of classification. The smallest finite group, in fact, in the simplest case in which the order parameter field has a single component, culminated in Kac's classification of the infinite family of unitary universality classes provided by the conformal minimal models [8, 9]. Interestingly, by renormalization group means, the unitary minimal models have been shown to be in correspondence with the critical Ginzburg–Landau theory of an even polynomial interaction, of which they provide their exact solution at the multicritical points [10]. This connection has been of particular inspiration in our approach to the classification of universalities.

More general discrete symmetries, however, have received much less attention and the general properties of their theory spaces are still largely unexplored. Among finite groups, the permutation group S_q of q elements plays a major role, since by Cayley's theorem every group of finite order q is isomorphic to a subgroup of the permutation group S_q. Due to its major role in group theory as well as in statistical mechanics, the permutation group has been our first interest in the direction of the classification of 'discrete' universalities; the analysis of the critical behavior of the q-states Potts model [11], also called random cluster model, in its corresponding field–theoretical formulation is addressed in Chapter 1. Even more intriguing from a physical perspective is the rich set of subgroups of the permutation group. Inheriting the geometrical perspective on the construction of invariant polynomials introduced in Chapter 1, we considered the class of scalar field theories, dubbed Platonic Field Theories, characterized by the symmetry groups of regular polytopes. The motivation is quite simple: Among discrete symmetry groups, it was mainly the Potts models and the cubic models to receive larger attention. From a geometric point of view, these models are represented by the symmetries of hyper–tetrahedra and hyper–cubes which both belong to the larger family of regular polytopes and to the purposes of the classification it seemed quite natural to consider them all. Their analysis is addressed in Chapter 2.

Chapter 1

The Potts model

Originally introduced to be a natural generalization of the Ising model [7], the so–called Potts model [11] is a statistical model where at each site of a lattice there is a variable σ_i that assumes q discrete values (colors). In absence of magnetic field, the interaction only distinguishes whether nearest neighbor sites have an equal or different color so that the corresponding Hamiltonian is invariant under the group S_q of permutation of the q colors. The Potts model has been a strong surge of interest along the years and its critical behavior turned out to be richer and more general than that of the Ising model, a property that nowadays we understand in terms of its larger symmetry group. Worth to mention in this respect, are two apparently unrelated physical problems: That of determining the typical large–scale properties of connected clusters in the percolation through a porous medium [12] and that of the macroscopic properties of an electrical network in terms of its local structure [13]. What do Potts model, percolation and electrical networks have in common and how they are related to the permutation group of q objects is an interesting question. These problems remained indeed fairly distinct until Fortuin and Kasteleyn [14, 15] discovered that, in a certain way, they are all part of a family of probability measures of edge models, which were introduced as models for phase transitions and other phenomena in lattice systems, or more generally in systems with a graph structure, later termed random cluster models. In these models, Fortuin and Kasteleyn showed that formal use of the symmetry unambiguously leads to final expressions containing q as a parameter which could be varied continuously. The obvious question of the meaning of S_q symmetry for a non–integer q arises spontaneously and it should

be understood as an analytical continuation from the corresponding model of discrete variables. Interestingly, in terms of the random cluster model, the percolation problem was shown to correspond to the case $q = 1$ while the theory of electrical networks turned out to be related to $q \to 0$ limit.

Even if the phase transition of the Potts model was considered primarily of theoretical interest, experimental realizations of the various Potts models were later identified [16]. The underlying principle in the experimental realization of a spin system is the principle of universality from which one is led to seek for real systems belonging to the same universality class as the spin model in question. One is usually guided by the corresponding Ginzburg–Landau action which, for the $q \in \mathbb{R}$ Potts models, was first introduced by Zia, Wallace and Amit [17, 18]. In constructing proper invariant polynomials, Zia and Wallace adopted a geometrical approach taking advantage of an isomorphism between the symmetry group S_q and the symmetry group which maps the $(q-1)$–dimensional hyper–tetrahedra on themselves. This method has the virtue to link two of the three main ingredients defining a universality class, namely the number $(q-1)$ of components of the order parameter and the symmetry content carried by q. Interested in generalizing and extending such a constructive method for invariant polynomials, we devote an initial discussion of the present Chapter (see Section 1.2) to set up the Potts field theory, with particular attention to the construction and enumeration of (non–derivative) invariants. We then move to study the critical behavior of these (random cluster) theories for general real parameter q and in arbitrary spatial dimension d. This is particularly advantageous in the functional renormalization group formalism (fRG) where the dimension d enters as a real parameter which can be varied continuously [19, 20]. We, therefore, focused our attention on the adaptation of fRG methods to the field theory of a $(q-1)$–component scalar field with the underlying global S_q symmetry of the Potts model. Such a description constitutes the main goal of the present chapter. Even though our analysis is completely general, we have been particularly interested in the universal aspects of the original problems of percolation ($q = 1$) and electrical networks ($q = 0$). In these two cases, the numerical estimates obtained for the correlation length critical exponent ν and the correction–to–scaling exponent ω turned out to be in quite satisfactory agreement with Monte Carlo simulations and high order ε–expansion results, showing that fRG methods are indeed very effec-

tive also in the case of S_q symmetry. Apart from these first results and applications, our study serves as groundwork for future investigations of the q–states Potts model universality classes within the functional renormalization group technique.

Reference: *Journal of Statistical Mechanics* (2018) 013206

1.1 Introduction

Since its introduction in 1952 [11], the Potts model has attracted an increasing amount of attention, stimulating both theoretical and experimental research: Despite a simple definition, the model exhibits a complex and varied structure reflecting a very different class of physical situations. The three–states version of the model can describe the transition of a liquid crystal from its nematic to its isotropic phase [21, 22], the transition of a cubic crystal into a tetragonal phase [23], as well as the deconfinement phase transition in QCD at finite temperature [24–28]. The two–states version is the Ising model. As anticipated, the Potts model with a single state can describe the critical behavior of bond percolation [14, 15, 29], while the limit of zero states is related to the electrical resistor network and the relative spanning forest problem [30, 31]. The Potts model has also been a territory of controversy and debate: According to Landau's phenomenological theory, the presence of the non–zero third–order term in the corresponding effective Hamiltonian implies that it undergoes a first–order phase transition in any dimension [32, 33]. This opened the long and entangled problem of the nature of the phase transition in the Potts model. Baxter [30] proved rigorously in 1973 that in two spatial dimensions it undergoes a second–order phase transition for $q \leq 4$ and a first–order one for $q > 4$ and still is the only case known exactly. A satisfactory picture is still missing for the critical value q_c of q which marks the passage from a second–order to a first–order transition in $d > 2$. However, numerical simulations performed mainly in the 70s [34–39] and renormalization group analysis [17, 18, 32, 40–44] suggest for example that in three spatial dimensions, $2 < q_c < 3$ and therefore in $d = 3$, the three–states Potts model is believed to undergo a first–order phase transition. (The existence of a critical value q_c of q should correspond to a collapse of fixed points in the RG formalism [42]).

The main open problems concerning the q–states Potts models (from here on

called $\texttt{Potts}_q$[1]) family are the precise quantitative determination of the critical properties of $\texttt{Potts}_1$ (percolation) and $\texttt{Potts}_0$ (spanning forest) in $d \geq 3$ and the determination of the critical value q_c of q in $d > 2$ at which the phase transition ceases to be continuous. In this work we will address mainly the first of the above problems by giving estimates for the critical exponents for `Percolation` and `Spanning Forest` in $d = 4$ and $d = 5$ (and preliminary results in $d = 3$). We postpone to a future work the question related to the critical value q_c separating discontinuous from continuous phase transitions. In this respect, however, we do the preparatory work obtaining the flow equation for the effective potential in the so–called improved local potential approximation (LPA') concerning the $\texttt{Potts}_3$ case. The corresponding renormalization group flow can, in principle, be used to determine the location of a first–order phase transition as a function of d.

In section 1.2 we review and generalize the construction of the Potts field theory, i.e., the field theory for a $(q-1)$–component scalar field with discrete global symmetry S_q. In section 1.3 we implement the construction of the exact functional RG equation for the Potts field theory. One major technical difficulty has been the development of the necessary *trace machinery* to reduce the traces present in the expansion of the r.h.s. of the exact RG flow equation, unlocking in this way the computation of the renormalization group functions (beta functions) of power interactions for arbitrary q. As an alternative approach, we derive the LPA' explicitly for the $q = 2$ and $q = 3$ cases and explain how to do it for arbitrary integer $q > 1$. In section 1.4 we use the beta functions so–derived to study the critical properties of the $\texttt{Potts}_q$ universality classes. After a preliminary study that allows us to establishes a connection with known results from the ε–expansion perturbative RG formalism, we push our approach to obtain accurate estimates for the critical exponents in $d = 4$ and $d = 5$. Within the truncation scheme employed, we are able to achieve converging estimates of the critical exponents in $d = 4$ and $d = 5$, while in $d = 3$ we obtain only preliminary results.

[1] We use `typewriter` font to indicate universality classes.

1.2 Potts field theory

1.2.1 Potts Model

As anticipated at the beginning of the chapter, the Potts model is a statistical model where at each site of a lattice there is a variable σ_i that assumes q discrete values (colors). In the absence of a magnetic field, the interaction energy is given by $\gamma\,\delta(\sigma_i,\sigma_j)$, where $\delta(\sigma_i,\sigma_j) = 0$ for $i \neq j$ and 1 otherwise. The model is ferromagnetic when $\gamma > 0$ and anti–ferromagnetic when $\gamma < 0$, and the corresponding Hamiltonian reads

$$\mathcal{H} = -\gamma \sum_{\langle i\,j\rangle} \delta(\sigma_i,\sigma_j)\,. \tag{1.2.1}$$

The model can be alternatively formulated to reflect its global S_q symmetry in a $n \equiv q-1$ dimensional space [16, 17]. This is achieved by rewriting

$$\delta(\alpha,\beta) = \frac{1}{q}\left[1 + \mathrm{e}^{\alpha}\cdot\mathrm{e}^{\beta}\right]\,, \tag{1.2.2}$$

where e^{α} are the q vectors pointing along the q symmetric directions of a hyper–tetrahedron in n dimensions.[2] The formal rewriting of the interaction energy given by Eq. (1.2.2) holds since, for a n–simplex, the angle subtended by any two vertices is given by $\arccos(-1)$.[3] Geometrically the symmetries of the q–states Potts model are therefore those of an n-simplex (see Figure 1.1).

1.2.2 Universality classes

The q–states Potts model can describe the universality classes associated with the spontaneous breaking of the permutation symmetry of q colors. Baxter [45] proved that in two dimensions the transition is continuous for $q \leq 4$. Near two spatial dimensions the critical value $q_c(d)$ below which the transition is continuous, decreases rapidly as a function of d. It is known from a variational RG analysis [32] that q_c is already smaller than three in $d \simeq 2.32$ and therefore the 3–states Potts model undergoes a first–order phase transition in $d = 3$. For $q < 2$, instead, the transition is

[2] In geometry, a simplex (hyper–tetrahedron) is the generalization of a triangle or tetrahedron to arbitrary dimensions.

[3] Notice that the vectors e^{α} are normalized such that $\mathrm{e}^{\alpha}\cdot\mathrm{e}^{\alpha} = n$.

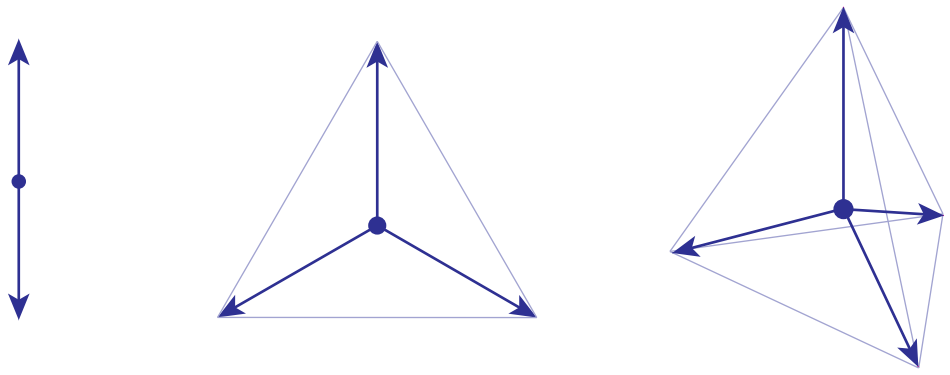

Figure 1.1: The discrete symmetries characterizing the q–states Potts model are those of the n-simplex shown here, for $n = 1, 2, 3$.

continuous in all the critical range $2 \leq d \leq 6$. The following is a summary of the present knowledge about the universality classes characterized by S_q symmetry.

- $\texttt{Potts}_q$. In their seminal paper, Fortuin and Kasteleyn showed that the Potts partition function $Z = \sum_{\{\sigma\}} \mathrm{e}^{-\mathcal{H}}$, where $\mathcal{H}$ is given by Eq. (1.2.1), can be written, up to a consequential constant, as

$$Z = \sum_{G \subseteq \mathcal{L}} p^{n_b} (1-p)^{\bar{n}_b} q^{N_c} \,, \tag{1.2.3}$$

  where G is a graph obtained placing n_b bonds on the edges of the lattice $\mathcal{L}$, each one with probability $p = 1 - e^{-\gamma} \in [0, 1]$ and $\bar{n}_b$ represents the number of edges without a bond. N_c is the number of clusters in G, with a cluster being a set of connected bonds. The configurations of the random cluster model are therefore obtained placing bonds with probability p and each of the resulting clusters can take q different colors. We notice that the probability measure in Eq. (1.2.3) is well defined for any $q \in \mathbb{R}$. In the thermodynamic limit, there exists a critical value $p_c(q)$ of the edge parameter p, separating the phase with no infinite cluster from the phase with one or more infinite clusters. By specifying the values of q to $0, 1, 2, 3, \ldots$ the model is able to capture at once the phase transition of well–known statistical models, the most important of which are listed below.

- $\texttt{Potts}_0 = \texttt{Spanning Forest}$. In graph theory, a subset F of the edge set E is called a forest of G if it contains no circuit; it is called a spanning tree if it is also connected. The electrical currents which flow in an electrical network may be expressed in terms of counts of spanning trees. Fortuin and Kasteleyn realized that the electrical network theory of a graph G is related to the limit $q \to 0$ of the random-cluster model of Eq. (1.2.3), when p is given by $p = \sqrt{q}/(1+\sqrt{q})$. In combinatorics, the generating function of spanning trees is called multivariate Tutte polynomial [46] and, in terms of relatively simple transformations, it can be shown to be equivalent to the random cluster model in the aforementioned limit [15, 47].

- $\texttt{Potts}_1 = \texttt{Percolation}$. In the limit $q \to 1$, the weight $p^{n_b}(1-p)^{\bar{n}_b}$ of a bond configuration coincides with that of the (bond) percolation problem, in which edges are randomly occupied with probability p and color plays no role. This formulation has been revisited and extended to site percolation by Wu [48].

- $\texttt{Potts}_2 = \texttt{Ising}$ thanks to the group isomorphism $\mathbb{Z}_2 \cong S_2$.

- $\texttt{Potts}_3$. It is related to the $\mathbb{Z}_3$ model since $S_3 \cong \mathbb{Z}_3 \times \mathbb{Z}_2$ and in $d = 2$ it has the same central charge ($c = 4/5$) as the $\texttt{Tricritical}$ universality class. The three–states version of the model has various connections from the nematic to isotropic phase transitions in liquid crystals [21, 33] to the deconfinment phase transition of mesons and baryons in QCD in two dimensions [24–28].

- $\texttt{Potts}_4$. The 4–states Potts model can describe the deconfinement of baryons and mesons as in the case $q = 3$ as well as tetra–quark confined states which are allowed for $q = 4$ only. Even if $\mathbb{Z}_4 \neq S_4$, the $\mathbb{Z}_4$–symmetric Ashkin–Teller model, at a particular point in the space of the couplings, can be described by a 4–states Potts model [49].

In the next section, we are going to introduce the field theoretical formulation of the Potts model (Potts field theory) which describes the scaling limit of the random cluster model for $q \in \mathbb{R}$, as well as that of the Potts ferromagnet for q integer. This theory has the Potts spin fields as fundamental fields (the Fortuin–Kasteleyn mapping relates the spin correlators in the Potts model to connectivities of clusters in the random cluster model) characterized by S_q invariance.

1.2.3 Action and invariants

As it was shown by Golner [40] and Zia and Wallace [17], the critical behavior of the $(n+1)$–states Potts model in d spatial dimensions can be studied by an n–comp. bosonic field ϕ_i $(i = 1, ..., n)$ carrying a representation of the S_{n+1}–symmetry. This representation involves the set of the $(n+1)$ vectors e_i^α $(\alpha = 1, ..., n+1)$ pointing to the vertices of a n-simplex, which have been introduced in section 1.2.1. The underlying symmetry of the model, arising from the equivalence of its $(n+1)$ states, is therefore reflected in the geometric regularity of simplexes. In fact, the indices $\alpha, \beta, \gamma, \ldots$, identifying the vertices of the n–simplex via the vectors e^α, can be permuted against each other leaving the simplex unaltered. The corresponding action is therefore symmetric under the discrete group which maps the n–dimensional hyper–tetrahedron on itself and this group isomorphic to S_{n+1} [18, 43, 50].

Properties of simplexes

In geometry, a simplex is a generalization of the notion of a triangle or a tetrahedron to arbitrary dimensions. For example, a 2–simplex is a triangle, a 3–simplex is a tetrahedron, and so on (see Figure 1.1). We can embed the regular n–dimensional simplex in $\mathbb{R}^n$ by writing directly its cartesian components. This can be achieved with the help of the following two properties:

1. All the vertices of a n–simplex are at the same distance from the center of it ,
2. the angle subtended by any two vertices is $\arccos(-1)$.

These properties allow the explicit construction of the vectors e_i^α of section 1.2.1, that we will use in the definition of the S_{n+1} polynomial invariants. Explicit manipulations of expressions involving e_i^α can be performed using the following relations:

$$\begin{aligned}
&\sum_{i=1}^{n} \mathrm{e}_i^\alpha \mathrm{e}_i^\beta = (n+1)\delta^{\alpha\beta} - 1\,, \\
&\sum_{\alpha=1}^{n+1} \mathrm{e}_i^\alpha = 0\,, \\
&\sum_{\alpha=1}^{n+1} \mathrm{e}_i^\alpha \mathrm{e}_j^\alpha = (n+1)\delta_{ij}\,.
\end{aligned} \tag{1.2.4}$$

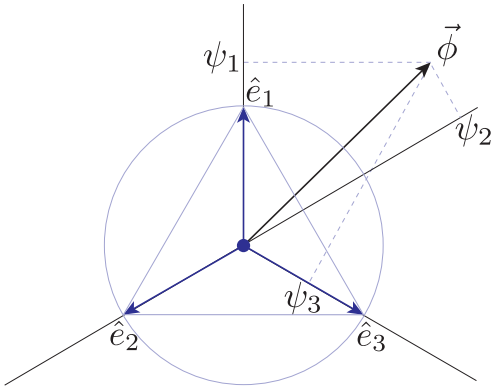

Figure 1.2: Relation between the fields ϕ_i and ψ^α in the $n = 2$ case which corresponds to the symmetry group S_3 of an equilateral triangle in the plane.

Note that in terms of the rules specified by Eqs. (1.2.4), the vectors e^α are normalised such that $\mathrm{e}^\alpha \cdot \mathrm{e}^\alpha = n$. This choice turns out to be useful in order to be able to take the limit $n \to 0$ later on. We anticipate that the set of rules in Eqs. (1.2.4) are the basic relations that we employ in section 1.3 to reduce the traces involved in the computation of the beta functions.

Invariant polynomials

A simple way to understand how to construct invariant polynomials with respect to the permutation group of $n+1$ colors, is to approach the problem geometrically. Any symmetric polynomial, can be expressed in terms of the so–called *power sum symmetric polynomials*. Consider, to this purpose, an n–comp. scalar ϕ_i in $\mathbb{R}^n$ as our fluctuating field and construct its projections ψ^α, along the vectors e^α defining the $n+1$ vertices of the hyper–tetrahedron, i.e., $\psi^\alpha \equiv \mathrm{e}^\alpha_i \cdot \phi_i$. To help the intuition, see Figure 1.2 in the case of a 2–component field $\phi \in \mathbb{R}^2$ along with the corresponding 2–simplex. The power sum symmetric polynomial P_k of degree k in $n+1$ variables is expressed as

$$P_k = \sum_{\alpha=1}^{n+1} (\psi^\alpha)^k \,, \tag{1.2.5}$$

which makes clear the symmetry with respect to any permutation of the indices α. Note that the first rule in Eqs. (1.2.4), i.e., $\sum_\alpha \mathrm{e}^\alpha_i = 0$, implies that $P_1 = \sum_\alpha \psi^\alpha = 0$,

which reflects the fact that not all the fields ψ^α are independent. Hence, any symmetric polynomial in the field variables $\psi^1, ..., \psi^{n+1}$, can be expressed in terms of the power sum symmetric polynomials P_k, which therefore constitute the basic invariant polynomials of the Potts field theory.

As a consequence of the first rule in Eqs. (1.2.4), the number $N(p)$ of invariant polynomials of degree p corresponds to the number of partitions of p objects which do not contain 1 as a part: $N(p) = \mathcal{P}(p) - \mathcal{P}(p-1)$, where by $\mathcal{P}(p)$, we intend the partition of p objects. Starting from $p = 2$, the number of invariants is then given by the sequence $N(p) = 1, 1, 2, 2, 4, 4, 7, 8, 12, 14, \ldots$ For example, for $p = 2$ and $p = 3$ the only power sum symmetric polynomials are respectively P_2 and P_3; for $p = 4$ we expect two symmetric polynomials, which, in fact, are P_4 and P_2^2; for $p = 5$ the invariants are P_5 and $P_2 P_3$; while for $p = 6$ there are four possibilities: P_6, P_3^2, $P_2 P_4$ and P_2^3; and so on.

The basic power sum symmetric polynomial P_p, can then be re–expressed in terms of the original fluctuating fields ϕ_i. For example

$$P_2 = \sum_\alpha (\psi^\alpha)^2 = \sum_\alpha \mathrm{e}_i^\alpha \mathrm{e}_j^\alpha \, \phi_i \phi_j = (n+1)\delta_{ij} \, \phi_i \phi_j \,,$$

where we used the last rules in Eqs. (1.2.4) and similarly

$$P_3 = \sum_\alpha (\psi^\alpha)^3 = \sum_\alpha \mathrm{e}_i^\alpha \mathrm{e}_j^\alpha \mathrm{e}_k^\alpha \, \phi_i \phi_j \phi_k \,.$$

In general, the k–th order power sum symmetric polynomial, is expressed as

$$P_k = \sum_\alpha \mathrm{e}_{i_1}^\alpha \ldots \mathrm{e}_{i_k}^\alpha \, \phi_{i_1} \cdots \phi_{i_k} \,, \tag{1.2.6}$$

which motivates the introduction of the following two basic tensors [4]

$$T^{(k,1)}_{i_1 \ldots i_k} \equiv \sum_\alpha \mathrm{e}_{i_1}^\alpha \ldots \mathrm{e}_{i_k}^\alpha \qquad\qquad k \geq 3 \,, \tag{1.2.7}$$

$$T^{(2,1)}_{i_1 i_2} \equiv \delta_{i_1 i_2} \qquad\qquad k = 2 \,. \tag{1.2.8}$$

The second superscript m in the definition of the basic tensor in Eq. 1.2.7, refers to

[4] An inessential factor $n+1$ is disregarded in Eq. (1.2.8)

the tensor structure: When the superscript is $m = 1$, it means that we refer to the basic tensor introduced in Eq. 1.2.7, while when $m \geq 2$ we refer to composite tensors of increasing order of complexity, see Table 1.1. When an invariant polynomial is expressed as the product of two or more power sum symmetric polynomials, in fact, it can be reduced to a product of the tensors defined in Eqs. (1.2.7) and (1.2.8). For example

$$\begin{aligned} P_2 P_4 &= \sum_\alpha (\psi^\alpha)^2 \sum_\beta (\psi^\beta)^4 = \sum_\alpha \mathrm{e}^\alpha_{i_1} \mathrm{e}^\alpha_{i_2} \sum_\beta \mathrm{e}^\beta_{i_3} \mathrm{e}^\beta_{i_4} \mathrm{e}^\beta_{i_5} \mathrm{e}^\beta_{i_6} \phi_{i_1} \cdots \phi_{i_6} \\ &= (n+1)\delta_{i_1 i_2} \sum_\beta \mathrm{e}^\beta_{i_3} \mathrm{e}^\beta_{i_4} \mathrm{e}^\beta_{i_5} \mathrm{e}^\beta_{i_6} \phi_{i_1} \cdots \phi_{i_6} = (n+1) \left\{ T^{(2,1)}_{i_1 i_2} T^{(4,1)}_{i_2 i_3 i_4 i_5} \right\} \phi_{i_1} \cdots \phi_{i_6} , \end{aligned}$$

or

$$\begin{aligned} P_3^2 &= \sum_\alpha (\psi^\alpha)^3 \sum_\beta (\psi^\beta)^3 = \left(\sum_\alpha \mathrm{e}^\alpha_{i_1} \mathrm{e}^\alpha_{i_2} \mathrm{e}^\alpha_{i_3} \right) \left(\sum_\beta \mathrm{e}^\beta_{i_4} \mathrm{e}^\beta_{i_5} \mathrm{e}^\beta_{i_6} \right) \phi_{i_1} \cdots \phi_{i_6} \\ &= \left\{ T^{(3,1)}_{i_1 i_2 i_3} T^{(3,1)}_{i_4 i_5 i_6} \right\} \phi_{i_1} \cdots \phi_{i_6} , \end{aligned}$$

and similarly for all other possible cases.[5] We finally conclude that: At any order p we can define $N(p)$ tensors $T^{(p,m)}_{i_1 \ldots i_p}$ with $m = 1, \ldots, N(p)$ as shown in Table 1.1. When these tensors are contracted with p fields ϕ_i, they constitute a basis for non–derivative invariants.

Ginzburg–Landau action

We can now express a generic action in terms of the tensors $T^{(p)}_{i_1 \ldots i_p}$ which, by construction, would result invariant under the permutation group of $n+1$ colors and in which only non–derivative interactions are considered. Indicating by $T^{(p)}_{i_1 \ldots i_p}$ the tensor coupling p fields, we can compactly write

$$\begin{aligned} S[\phi] = \int_x \Big\{ &\frac{1}{2} \partial^\mu \phi_i \partial_\mu \phi_i + \frac{1}{2} T^{(2)}_{i_1 i_2} \phi_{i_1} \phi_{i_2} + \frac{1}{3!} T^{(3)}_{i_1 i_2 i_3} \phi_{i_1} \phi_{i_2} \phi_{i_3} + \\ &+ \frac{1}{4!} T^{(4)}_{i_1 i_2 i_3 i_4} \phi_{i_1} \phi_{i_2} \phi_{i_3} \phi_{i_4} + \frac{1}{5!} T^{(5)}_{i_1 i_2 i_3 i_4 i_5} \phi_{i_1} \phi_{i_2} \phi_{i_3} \phi_{i_4} \phi_{i_5} + \ldots \Big\} , \end{aligned} \tag{1.2.9}$$

[5] Symmetrization over all indexes is understood when needed.

$T^{(p,m)}$	$m=1$	$m=2$	$m=3$	$m=4$	$N(p)$
$p=2$	δ				1
$p=3$	$\sum$eee				1
$p=4$	$\sum$eeee	$\delta\delta$			2
$p=5$	$\sum$eeeee	$\delta\sum$eee			2
$p=6$	$\sum$eeeeee	$\sum$eee$\sum$eee	$\delta\sum$eeee	$\delta\delta\delta$	4

Table 1.1: Tensor invariants $T^{(p,m)}$ defined in the text with their relative number $N(p)$. The index structure of the invariants follows the general structure of Eq. (1.2.7). We dropped the indices from e_i^α and δ_{ij} for brevity.

which implicitly defines the dimensionful couplings $\bar{\lambda}_{p,m}$ (one for each invariant of Table 1.1, according to the counting rule established in the previous section), in terms of the possible inviariant interactions

$$\begin{aligned}
T^{(3)}_{i_1 i_2 i_3} &= \bar{\lambda}_3 T^{(3,1)}_{i_1 i_2 i_3}\,, \\
T^{(4)}_{i_1 i_2 i_3 i_4} &= \bar{\lambda}_{4,1} T^{(4,1)}_{i_1 i_2 i_3 i_4} + \bar{\lambda}_{4,2} T^{(4,2)}_{i_1 i_2 i_3 i_4}\,, \\
T^{(5)}_{i_1 i_2 i_3 i_4 i_5} &= \bar{\lambda}_{5,1} T^{(5,1)}_{i_1 i_2 i_3 i_4 i_5} + \bar{\lambda}_{5,2} T^{(5,2)}_{i_1 i_2 i_3 i_4 i_5}\,, \\
T^{(6)}_{i_1 i_2 i_3 i_4 i_5 i_6} &= \bar{\lambda}_{6,1} T^{(6,1)}_{i_1 i_2 i_3 i_4 i_5 i_6} + \bar{\lambda}_{6,2} T^{(6,2)}_{i_1 i_2 i_3 i_4 i_5 i_6} + \bar{\lambda}_{6,3} T^{(6,3)}_{i_1 i_2 i_3 i_4 i_5 i_6} + \bar{\lambda}_{6,4} T^{(6,4)}_{i_1 i_2 i_3 i_4 i_5 i_6}
\end{aligned} \tag{1.2.10}$$

Finally, we can introduce a shorthand notation defining the following invariants through contraction with the fields, namely

$$I_{p,m} \equiv T^{(p,m)}_{i_1 \cdots i_p} \phi_{i_1} \cdots \phi_{i_p}\,, \tag{1.2.11}$$

which are clearly related to the invariants P_k of the preceding subsection, in terms of which one can re–write the action in Eq. (1.2.9) as

$$S[\phi] = \int_x \left\{ \frac{1}{2} \partial^\mu \phi_i \partial_\mu \phi_i + V(\phi_1, .., \phi_n) \right\}\,, \tag{1.2.12}$$

	$n=1$	$n=2$	$n=3$
I_2	φ_1^2	$\varphi_1^2+\varphi_2^2$	$\varphi_1^2+\varphi_2^2+\varphi_3^2$
I_3	0	$\frac{3}{\sqrt{2}}\varphi_2(\varphi_2^2-3\varphi_1^2)$	$\frac{4}{\sqrt{3}}\left(\sqrt{2}\varphi_1(\varphi_1^2-3\varphi_2^2)-3(\varphi_1^2+\varphi_2^2)\varphi_3+2\varphi_3^3\right)$
$I_{4,1}$	$2I_2^2$	$\frac{9}{2}I_2^2$	$8\left(\varphi_1^4+\varphi_2^4+\frac{7}{6}\varphi_3^4+\varphi_1^2(\varphi_3^2-\frac{2\sqrt{2}}{3}\varphi_1\varphi_3)+2\varphi_2^2(\varphi_1^2+\sqrt{2}\varphi_1\varphi_3+\frac{1}{2}\varphi_3^2)\right)$
$I_{4,2}$	I_2^2	I_2^2	I_2^2
$I_{5,1}$	0	$\frac{5}{2}I_2I_3$	$\frac{10}{3}I_2I_3$
$I_{5,2}$	0	I_2I_3	I_2I_3
$I_{6,1}$	$2I_2^3$	$\frac{27}{4}I_2^3+I_3^2$	$\frac{1}{3}I_3^2+3I_2I_{4,1}-8I_2^3$
$I_{6,2}$	$2I_2^3$	$\frac{9}{2}I_2^3$	$I_2I_{4,1}$
$I_{6,3}$	I_2^3	I_2^3	I_2^3
$I_{6,4}$	0	I_3^2	I_3^2

Table 1.2: Explicit form of the invariants of S_{n+1} for $n=1,2,3$. The first n invariants constitute a basis with rational coefficients, in terms of which, all other invariants defined in Eq. (1.2.11) can be expressed.

where the GL potential is constructed from the invariants in Eq. (1.2.11) as follows

$$V(\phi_1,..,\phi_n)=\sum_{p=2}^{\infty}\frac{1}{p!}\sum_{m=1}^{N(p)}\bar{\lambda}_{p,m}I_{p,m}=\frac{1}{2}\bar{\lambda}_2I_2+\frac{1}{3!}\bar{\lambda}_3I_3+\frac{1}{4!}(\bar{\lambda}_{4,1}I_{4,1}+\bar{\lambda}_{4,2}I_{4,2})+... \tag{1.2.13}$$

However, as expected, only the first n invariants are independent, as it can be seen from the explicit construction reported in Table 1.2 in the cases $n=1,2,3$. The examples of Table 1.2, exemplify the fact that rational coefficients are needed to express the dependent invariants in terms of the independent ones. To facilitate the understanding we give an explicit construction of the Potts field theory in the S_3 case in Appendix A.1.

1.3 Functional RG for Potts

1.3.1 Flow equation

The functional renormalization group (fRG) approach to quantum and statistical field theory is based on the exact flow equation satisfied by the scale–dependent effective action Γ_k (for a general review see e.g. Ref. [51]; while for a self–contained introduction focused on statistical physics see Ref. [52]). This is a scale–dependent functional which includes fluctuations between a given microscopic UV scale Λ down to a running scale $k < \Lambda$. The effective action interpolates smoothly between the bare UV action $S = \Gamma_{k=\Lambda}$ and the full effective action, or free energy, $\Gamma = \Gamma_{k=0}$ for $k \to 0$ so that all fluctuations are summed over. The scale dependence of the effective action Γ_k on the RG 'time' $t \equiv \log k$ is governed by the exact flow equation [19, 20], which for a n-comp. scalar $\varphi_i \equiv \langle \phi_i \rangle$ reads

$$\partial_t \Gamma_k[\varphi] = \frac{1}{2} \mathrm{Tr} \left(\frac{\delta^2 \Gamma_k[\varphi]}{\delta \varphi_i \delta \varphi_j} + R_{k,ij} \right)^{-1} \partial_t R_{k,ji} \,. \tag{1.3.1}$$

Here R_k is a proper infrared regulator function which suppresses the propagation of the infrared modes (of momentum smaller than k) by directly modifying the bare propagator of the theory. The so–called Wetterich equation (1.3.1) is the starting point of all our subsequent analysis.

Local potential approximation

Despite its simplicity, the Wetterich equation (1.3.1) is difficult to solve and one should rely on approximations based on non–perturbative truncations, which amounts to project the RG flow on a subset of suitable functionals. One of these truncations is called improved local potential approximation (LPA') and consist in considering the following ansatz for the effective action

$$\Gamma_k[\varphi] = \int_x \left\{ \frac{1}{2} Z_k \partial^\mu \varphi_i \partial_\mu \varphi_i + V_k(\varphi_1, ..., \varphi_n) \right\} , \tag{1.3.2}$$

where the whole theory space is projected into the infinite–dimensional functional space of the effective potentials V_k. At the first order in the derivative expansion, also called local potential approximation (LPA), one neglects the running and the field

dependence of the wave–function renormalization Z_k, i.e., $Z_k \equiv 1$. In the improved local potential approximation (LPA') we consider throughout, Z_k is a non–vanishing field–independent but scale–dependent running wave–function renormalization constant, directly related to the anomalous dimension of the fields by $\eta_k = -\partial_t \log Z_k$.

We can obtain a flow equation for the effective potential by inserting the ansatz (1.3.2) in the Wetterich equation (1.3.1). The first thing to do is to compute the Hessian which, dropping for the moment Z_k, reads

$$\frac{\delta^2 \Gamma_k}{\delta\varphi_i \delta\varphi_j} = -\partial^2 \delta_{ij} + \frac{\delta^2 V_k}{\delta\varphi_i \delta\varphi_j} =: -\partial^2 (\mathbb{I})_{ij} + (\mathbb{V})_{ij}\,, \tag{1.3.3}$$

where we introduced a matrix notation for compactness. When Eq. (1.3.3) is inserted in the flow equation (1.3.1), with the choice $R_{k,ij} = \delta_{ij} R_k$ for the matrix structure of the cutoff, we find

$$\partial_t \Gamma_k = \frac{1}{2} \mathrm{Tr} \frac{\partial_t R_k(-\partial^2)}{(-\partial^2 + R_k(-\partial^2))\mathbb{I} + \mathbb{V}}\,. \tag{1.3.4}$$

After choosing a constant field configuration, so that $\partial_t \Gamma_k = (\int \mathrm{d^d x})\, \partial_t \mathrm{V_k}$ and by performing the angular integrations, we obtain the following expression for the flow of the effective potential

$$\partial_t V_k = \frac{1}{2} \frac{1}{(4\pi)^{\frac{d}{2}} \Gamma(\frac{d}{2})} \int_0^\infty \mathrm{d}z\, z^{\frac{d}{2}-1}\, \mathrm{tr}\, \frac{\partial_t R_k(z)}{(z + R_k(z))\,\mathbb{I} + \mathbb{V}}\,. \tag{1.3.5}$$

We will adopt now the linear cutoff $R_k(z) = (k^2 - z)\theta(k^2 - z)$, where θ is the Heaviside step function, that allows a simple explicit evaluation of the integral in Eq. (1.3.5). With this choice we find the following form for the flow equation of the effective potential

$$\partial_t V_k = c_d k^{d+2}\, \mathrm{tr} \frac{1}{k^2 \mathbb{I} + \mathbb{V}}\,, \tag{1.3.6}$$

where we defined the constant $c_d^{-1} \equiv (4\pi)^{\frac{d}{2}} \Gamma(\frac{d}{2} + 1)$. This expression is the general form for the LPA of an n–comp. scalar in d spatial dimensions and as such, it is the generating function of the beta functions of the couplings $\bar{\lambda}_{p,m}$ concerning the non-derivative interactions of Eq. (1.2.13).

Unfortunately, for general n, it is not possible to obtain a closed form for the inverse of the matrix $k^2\mathbb{I} + \mathbb{V}$. Therefore, since our main interest is the study of

the limits $n \to 0$ (`Percolation`) and $n \to -1$ (`Spanning Forest`) (which we recall are the only non–trivial cases apart `Ising` in $d > 2$), we are forced to truncate the effective potential in Eq. (1.2.13). This amounts at converting Eq. (1.3.6) into a set of coupled beta functions (explicitly n–dependent) for a finite set of coupling constants, by expanding the r.h.s. of Eq. (1.3.6) in powers of $\mathbb{V}$. In this way, the problem is reduced to the evaluation of traces of these powers. This approach is presented in section 1.3.2, where the appropriate "trace machinery" will be developed and where we report the truncation up to φ^6. A different approach is based on the fact that the inversion of the matrix in Eq. (1.3.6) is instead possible whenever n is a given, conceivably small, positive integer (and thus not applicable in the `Percolation` and `Spanning Forest` cases) and in this case we are able to write the explicit form of the LPA'. This is presented in section 1.3.4 for $n = 1$ and $n = 2$.

1.3.2 Beta functions for generic n

The aim of this section is to provide a general framework to extract beta functions for any real value of $n \in \mathbb{R}$. Defining $\mathbb{V} = \bar{\lambda}_2 \mathbb{I} + \mathbb{M}$ we proceed by expanding the inverse propagator as

$$\mathrm{tr} \frac{1}{k^2 \mathbb{I} + \mathbb{V}} = \mathrm{tr} \frac{k^{-2}}{(1+\lambda_2)\mathbb{I} + \mathbb{M}/k^2} = \sum_{m=0}^{\infty} (-1)^m \frac{k^{-2-2m}}{(1+\lambda_2)^{m+1}} \mathrm{tr}\, \mathbb{M}^m \,, \tag{1.3.7}$$

where from now on we absorb the factor c_d in the definitions of the effective potential and of the field by setting $V_k \to c_d V_k$ and $\varphi_i \to c_d^{1/2} \varphi_i$. Inserting Eq. (1.3.7) into the flow equation of the effective potential (1.3.6) gives

$$\partial_t V_k = \sum_{m=0}^{\infty} (-1)^m \frac{k^{d-2m}}{(1+\lambda_2)^{m+1}} \mathrm{tr}\, \mathbb{M}^m \,. \tag{1.3.8}$$

Any field dependence on the r.h.s. of equation (1.3.8) is encoded in $\mathrm{tr}\, \mathbb{M}^m$ since, explicitly, we have

$$(\mathbb{M})_{ab} = T^{(3)}_{abi_1} \varphi_{i_1} + \frac{1}{2} T^{(4)}_{abi_1 i_2} \varphi_{i_1} \varphi_{i_2} + \frac{1}{3!} T^{(5)}_{abi_1 i_2 i_3} \varphi_{i_1} \varphi_{i_2} \varphi_{i_3} + \dots \tag{1.3.9}$$

Once the traces $\mathrm{tr}\, \mathbb{M}^m$ are computed with the help of rules (1.2.4) and expressed in terms of the basic power sum symmetric polynomial invariants of Eq. (1.2.11), the

r.h.s. of the flow equation (1.3.6) assumes the following form:

$$\partial_t V_k = \frac{1}{2}\bar{\beta}_2 I_2 + \frac{1}{3!}\bar{\beta}_3 I_3 + \frac{1}{4!}(\bar{\beta}_{4,1} I_{4,1} + \bar{\beta}_{4,2} I_{4,2}) + \frac{1}{5!}(\bar{\beta}_{5,1} I_{5,1} + \bar{\beta}_{5,2} I_{5,2}) + \dots . \quad (1.3.10)$$

From this equation, we can extract the beta functions of all the couplings included in the truncation of the potential in Eq. (1.2.13). An example of how this general procedure works in practice is given in Appendix A.2 where the simple φ^3 cubic example is shown.

Explicit beta functions

From the example given in Appendix A.2, it is clear that the computation of the general trace $\mathrm{tr}\,\mathbb{M}^m$ rapidly becomes unfeasible by hand. For a given truncation order p in the expansion (1.2.13), we need to expand the inverse propagator up to $\mathrm{tr}\,\mathbb{M}^p$ and keep all contributions up to order p. In order to tackle the "trace machinery" involved in the general computation, we have used symbolic manipulation software (the `xTensor` package for `Mathematica` [53]) for which we have written an explicit code.

Here we consider the expansion (1.2.13) up to order φ^6, which corresponds to a total of $\sum_{p=2}^{6} N(p) = 10$ dimensionless couplings:

$$\{\lambda_2, \lambda_3, \lambda_{4,1}, \lambda_{4,2}, \lambda_{5,1}, \lambda_{5,2}, \lambda_{6,1}, \lambda_{6,2}, \lambda_{6,3}, \lambda_{6,4}\}\,.$$

The beta functions of these couplings can be written in terms of the dimension–full ones as [6]

$$\beta_{m,i} = \left[m\left(\frac{d}{2} - 1 + \frac{\eta}{2}\right) - d\right]\lambda_{m,i} + k^{m\left(\frac{d}{2}-1+\frac{\eta}{2}\right)-d}\,\bar{\beta}_{m,i}\,, \quad (1.3.11)$$

and their explicit form can be extracted once the reduction of the traces up to $\mathrm{tr}\,\mathbb{M}^6$ has been performed. The final result is the following set of ten beta functions, valid for arbitrary d and n, and it is the main result of the present chapter.

$$\begin{aligned}\beta_2 = {} & (-2+\eta)\lambda_2 + \frac{2(n-1)(n+1)^2\lambda_3^2}{(1+\lambda_2)^3} \\ & - \frac{n(n+1)\lambda_{4,1} + \frac{1}{3}(n+2)\lambda_{4,2}}{(1+\lambda_2)^2}\,,\end{aligned} \quad (1.3.12)$$

[6] We just differentiate both sides of $\lambda_{m,i} = k^{m(d/2-1+\eta/2)-d}\bar{\lambda}_{m,i}$.

$$\beta_3 = \frac{1}{2}(d+3\eta-6)\lambda_3 + \frac{6\left(\frac{2}{3}\lambda_{4,2}+(n-1)(n+1)\lambda_{4,1}\right)\lambda_3}{(1+\lambda_2)^3} - \frac{n\lambda_{5,1}+\frac{1}{10}(n+6)\lambda_{5,2}}{(1+\lambda_2)^2} - \frac{6(n-2)(n+1)^2\lambda_3^3}{(1+\lambda_2)^4}, \tag{1.3.13}$$

$$\begin{aligned}\beta_{4,1} = {} & (d+2\eta-4)\lambda_{4,1} + \frac{6\left(\frac{4}{3}\lambda_{4,2}\lambda_{4,1}+(n^2-1)\lambda_{4,1}^2\right)}{(1+\lambda_2)^3} \\ & + \frac{6\frac{4}{15}(n+1)(3\lambda_{5,2}+5(n-1)\lambda_{5,1})\lambda_3}{(1+\lambda_2)^3} \\ & - \frac{24\left(\frac{3}{2}(n-2)(n+1)^2\lambda_{4,1}+(n+1)\lambda_{4,2}\right)\lambda_3^2}{(1+\lambda_2)^4} \\ & - \frac{15n\lambda_{6,1}+(n+8)\lambda_{6,3}+9(n+1)\lambda_{6,2}}{15(1+\lambda_2)^2} \\ & + \frac{24(n-3)(n+1)^3\lambda_3^4}{(1+\lambda_2)^5},\end{aligned} \tag{1.3.14}$$

$$\begin{aligned}\beta_{4,2} = {} & (d+2\eta-4)\lambda_{4,2} - \frac{24\left(\frac{3}{2}(n+1)^3\lambda_{4,1}+\frac{1}{2}(n-3)(n+1)^2\lambda_{4,2}\right)\lambda_3^2}{(1+\lambda_2)^4} \\ & + \frac{6(n+1)^2\lambda_{4,1}^2+6\frac{2}{3}n(n+1)\lambda_{4,1}\lambda_{4,2}+6\frac{1}{9}(n+8)\lambda_{4,2}^2}{(1+\lambda_2)^3} \\ & + \frac{\frac{12}{5}(n-3)(n+1)^2\lambda_3\lambda_{5,2}}{(1+\lambda_2)^3} \\ & + \frac{3(n+1)^2\lambda_{6,2}-2n(n+1)\lambda_{6,3}-(n+4)\lambda_{6,4}}{5(1+\lambda_2)^2} \\ & + \frac{48(n+1)^4\lambda_3^4}{(1+\lambda_2)^5},\end{aligned} \tag{1.3.15}$$

$$
\begin{aligned}
\beta_{5,1} = & \frac{1}{2}(3d+5\eta-10)\lambda_{5,1} + \frac{80(n+1)^2(3(n+1)(n-3)\lambda_{4,1}+2\lambda_{4,2})\lambda_3^3}{(1+\lambda_2)^5} \\
& - \frac{6(n+1)\Big(15(n+1)(n-2)\lambda_{4,1}^2+20\lambda_{4,1}\lambda_{4,2}\Big)\lambda_3}{(1+\lambda_2)^4} \\
& - \frac{12(n+1)^2(5(n-2)\lambda_{5,1}+3\lambda_{5,2})\lambda_3^2}{(1+\lambda_2)^4} \\
& + \frac{\frac{4}{3}(10\lambda_{4,2}\lambda_{5,1}+9(n+1)\lambda_{4,1}\lambda_{5,2}+15(n+1)(n-1)\lambda_{4,1}\lambda_{5,1})}{(1+\lambda_2)^3} \\
& + \frac{\frac{2}{3}(n+1)(8\lambda_{6,3}+15(n-1)\lambda_{6,1}+9(n+1)\lambda_{6,2})\lambda_3}{(1+\lambda_2)^3} \\
& - \frac{120(n-4)(n+1)^4\lambda_3^5}{(1+\lambda_2)^6}\,,
\end{aligned}
\tag{1.3.16}
$$

$$
\begin{aligned}
\beta_{5,2} = & \frac{1}{2}(3d+5\eta-10)\lambda_{5,2} - \frac{20\left(9(n+1)^2\lambda_{4,1}^2+3\left(n^2-2n-3\right)\lambda_{4,2}\lambda_{4,1}+4\lambda_{4,2}^2\right)\lambda_3}{(1+\lambda_2)^4} \\
& - \frac{6(n+1)^2\left(10\lambda_{5,1}+(4n-19)\lambda_{5,2}\right)\lambda_3^2}{(1+\lambda_2)^4} \\
& + \frac{\frac{4}{3}\left(6\lambda_{6,4}+\left(3n^2-4n-7\right)\lambda_{6,3}+3(n-4)(n+1)^2\lambda_{6,2}\right)\lambda_3}{(1+\lambda_2)^3} \\
& + \frac{2(n+1)\left(10\lambda_{5,1}+(4n-9)\lambda_{5,2}\right)\lambda_{4,1}+\left(26\lambda_{5,2}+n\left(10\lambda_{5,1}+\lambda_{5,2}\right)\right)\lambda_{4,2}}{(1+\lambda_2)^3} \\
& + \frac{80(n+1)^2\left(9(n+1)\lambda_{4,1}+(n-6)\lambda_{4,2}\right)\lambda_3^3}{(1+\lambda_2)^5} - \frac{600(n+1)^4\lambda_3^5}{(1+\lambda_2)^6}\,,
\end{aligned}
\tag{1.3.17}
$$

$$
\begin{aligned}
\beta_{6,1} = {} & (2d+3\eta-6)\,\lambda_{6,1} - \frac{600(n+1)^3\left(3\left(n^2-3n-4\right)\lambda_{4,1}+2\lambda_{4,2}\right)\lambda_3^4}{(1+\lambda_2)^6} \\
& + \frac{24(n+1)^2\left(60\lambda_{4,1}\lambda_{4,2}+45\left(n^2-2n-3\right)\lambda_{4,1}^2\right)\lambda_3^2}{(1+\lambda_2)^5} \\
& + \frac{96(n+1)^3\left(5(n-3)\lambda_{5,1}+3\lambda_{5,2}\right)\lambda_3^3}{(1+\lambda_2)^5} \\
& - \frac{24(n+1)\left(3(n+1)\left(5(n-2)\lambda_{5,1}+3\lambda_{5,2}\right)\lambda_{4,1}+10\lambda_{4,2}\lambda_{5,1}\right)\lambda_3}{(1+\lambda_2)^4} \\
& - \frac{90(n+1)\left(\left(n^2-n-2\right)\lambda_{4,1}+2\lambda_{4,2}\right)\lambda_{4,1}^2}{(1+\lambda_2)^4} \\
& - \frac{6(n+1)^2\left(15(n-2)\lambda_{6,1}+8\lambda_{6,3}+9(n+1)\lambda_{6,2}\right)\lambda_3^2}{(1+\lambda_2)^4} \\
& + \frac{20\lambda_{4,2}\lambda_{6,1}+4(n+1)\lambda_{5,1}\left(5(n-1)\lambda_{5,1}+6\lambda_{5,2}\right)}{(1+\lambda_2)^3} \\
& + \frac{2(n+1)\left(15(n-1)\lambda_{6,1}+8\lambda_{6,3}+9(n+1)\lambda_{6,2}\right)\lambda_{4,1}}{(1+\lambda_2)^3} \\
& + \frac{720(n-5)(n+1)^5\lambda_3^6}{(1+\lambda_2)^7}\,,
\end{aligned}
\tag{1.3.18}
$$

$$
\begin{aligned}
\beta_{6,2} = {} & (2d+3\eta-6)\,\lambda_{6,2} + \frac{20\left(5\lambda_{4,2}\lambda_{6,2}+\lambda_{4,1}\left(-4\lambda_{6,3}+3\left(n^2-1\right)\lambda_{6,2}\right)\right)}{5(1+\lambda_2)^3} \\
& + \frac{100\lambda_{5,1}^2+20n\lambda_{5,1}\lambda_{5,2}+(n+30)\lambda_{5,2}^2}{5(1+\lambda_2)^3} \\
& - \frac{1200(n+1)^2\left(3(n+1)\lambda_{4,1}-\lambda_{4,2}\right)\lambda_3^4}{(1+\lambda_2)^6} \\
& + \frac{48(n+1)^2\left(10\lambda_{5,1}+(n-8)\lambda_{5,2}\right)\lambda_3^3}{(1+\lambda_2)^5} \\
& + \frac{16\left(15(n+1)\left(3(n+1)\lambda_{4,1}-4\lambda_{4,2}\right)\lambda_{4,1}+5\left(9(n+1)^2\lambda_{4,1}^2+2\lambda_{4,2}^2\right)\right)\lambda_3^2}{(1+\lambda_2)^5} \\
& - \frac{6\left(-30\lambda_{4,1}^2\lambda_{4,2}+6(n+1)\left(10\lambda_{5,1}+(n-4)\lambda_{5,2}\right)\lambda_3\lambda_{4,1}\right)}{(1+\lambda_2)^4} \\
& - \frac{6\left(3(n+1)^2(2n-7)\lambda_3\lambda_{6,2}-8\left((n+1)\lambda_3\lambda_{6,3}-2\lambda_{4,2}\lambda_{5,2}\right)\right)\lambda_3}{(1+\lambda_2)^4} \\
& + \frac{2160(n+1)^4\lambda_3^6}{(1+\lambda_2)^7}\,,
\end{aligned}
\tag{1.3.19}
$$

$$
\begin{aligned}
\beta_{6,3} = {} & (2d+3\eta-6)\,\lambda_{6,3} + \frac{16(n+1)\left(60(n+1)^2\lambda_{5,1}-63\lambda_{5,2}\right)\lambda_3^3}{(1+\lambda_2)^5} \\
& + \frac{16(n+1)\left(9n^3-45n^2-117n\right)\lambda_3^3\lambda_{5,2}}{(1+\lambda_2)^5} \\
& + \frac{16(n+1)\left(180(n+1)^2\lambda_{4,1}^2+15\left(3n^2-11n-14\right)\lambda_{4,1}\lambda_{4,2}+50\lambda_{4,2}^2\right)\lambda_3^2}{(1+\lambda_2)^5} \\
& - \frac{6(n+1)\left(7\left(n^2-2n-3\right)\lambda_{6,3}-18(n+1)^2\lambda_{6,2}\right)\lambda_3^2}{(1+\lambda_2)^4} \\
& - \frac{18(n+1)\left(5(n+1)\lambda_{6,1}+4\lambda_{6,4}\right)\lambda_3^2}{(1+\lambda_2)^4} \\
& - \frac{30\left(9(n+1)^2\lambda_{4,1}^2+3\left(n^2-1\right)\lambda_{4,2}\lambda_{4,1}+8\lambda_{4,2}^2\right)\lambda_{4,1}}{(1+\lambda_2)^4} \\
& - \frac{12(n+1)\left(2\left(5(n-3)\lambda_{5,1}+9\lambda_{5,2}\right)\lambda_{4,2}+3(n+1)\left(10\lambda_{5,1}+3(n-5)\lambda_{5,2}\right)\lambda_{4,1}\right)\lambda_3}{(1+\lambda_2)^4} \\
& + \frac{18(n+1)\left(10(n-3)\lambda_{5,1}+9\lambda_{5,2}\right)\lambda_{5,2}}{15(1+\lambda_2)^3} \\
& + \frac{10\left(15n\lambda_{6,1}+(n+38)\lambda_{6,3}+9(n+1)\lambda_{6,2}\right)\lambda_{4,2}}{15(1+\lambda_2)^3} \\
& + \frac{30\left(15(n+1)\lambda_{6,1}+\left(7n^2+n-6\right)\lambda_{6,3}+12\lambda_{6,4}-18(n+1)^2\lambda_{6,2}\right)\lambda_{4,1}}{15(1+\lambda_2)^3} \\
& - \frac{600(n+1)^3\left(12(n+1)\lambda_{4,1}+(n-7)\lambda_{4,2}\right)\lambda_3^4}{(1+\lambda_2)^6} \\
& + \frac{4320(n+1)^5\lambda_3^6}{(1+\lambda_2)^7}, \qquad (1.3.20)
\end{aligned}
$$

$$
\begin{aligned}
\beta_{6,4} = {} & (2d+3\eta-6)\,\lambda_{6,4} + \frac{600(n+1)^4\,(3(n+1)\lambda_{4,1}-4\lambda_{4,2})\lambda_3^4}{(1+\lambda_2)^6} \\
& + \frac{8(n+1)^2\left(-90(n+1)^2\lambda_{4,1}^2+72(n+1)^2\lambda_3\lambda_{5,2}\right)\lambda_3^2}{(1+\lambda_2)^5} \\
& + \frac{8(n+1)^2\left(150(n+1)\lambda_{4,1}\lambda_{4,2}+5(3n-23)\lambda_{4,2}^2\right)\lambda_3^2}{(1+\lambda_2)^5} \\
& - \frac{108(n+1)^2\,(6(n+1)\lambda_{4,1}+(n-7)\lambda_{4,2})\;\lambda_3\lambda_{5,2}}{3(1+\lambda_2)^4} \\
& - \frac{54(n+1)^2\,(2(n+1)\lambda_{6,3}+(n-5)\lambda_{6,4}+3(n+1)^2\lambda_{6,2})\lambda_3^2}{3(1+\lambda_2)^4} \\
& - \frac{10\left(-27(n+1)^3\lambda_{4,1}^3+27(n+1)^2\lambda_{4,1}^2\lambda_{4,2}+9n(n+1)\lambda_{4,1}\lambda_{4,2}^2+(n+26)\lambda_{4,2}^3\right)}{3(1+\lambda_2)^4} \\
& + \frac{2\left(6(n+1)^2\lambda_{4,1}\lambda_{6,3}+9(n+1)^3\lambda_{4,1}\lambda_{6,2}+14\lambda_{4,2}\lambda_{6,4}\right)}{(1+\lambda_2)^3} \\
& + \frac{2\left(3n(n+1)\lambda_{4,1}\lambda_{6,4}+2n(n+1)\lambda_{4,2}\lambda_{6,3}+n\lambda_{4,2}\lambda_{6,4}-3(n+1)^2\lambda_{4,2}\lambda_{6,2}\right)}{(1+\lambda_2)^3} \\
& + \frac{9(n-7)(n+1)^2\lambda_{5,2}^2}{5(1+\lambda_2)^3} - \frac{1440(n+1)^6\lambda_3^6}{(1+\lambda_2)^7}\,.
\end{aligned}
\tag{1.3.21}
$$

This system of beta functions, in the truncation scheme considered, encode the critical properties of the random cluster model for arbitrary n and d. The anomalous dimension η entering these expressions will be computed in the next subsection.

While the beta functions (1.3.12)–(1.3.21) are written using the linear cutoff, it is easy to generalize them to a general cutoff function $R_k(z)$ by the substitution [7]

$$
\frac{1}{(1+\lambda_2)^m} \;\to\; k^{2m-2-d}\,\frac{d}{4}\int_0^\infty dz\, z^{d/2-1} G_k^m(z)\partial_t R_k(z)\,.
$$

The generalization to arbitrary cutoffs, on the other hand, is crucial for the study of the cutoff dependence and for the optimization of convergence of the numerical results [54]. We leave this task to a future study, since, as we will show in section 1.4.2, within the $p = 6$ truncation, convergence of the critical exponents is fully achieved only in $d = 5$. This indicates that higher order truncations in the expansion

[7] For a definition of $G_k(z)$, see Eq. (1.3.24).

(1.2.13) are needed in $d = 4$ and in $d = 3$.

1.3.3 Anomalous dimension

The computation of the anomalous dimension η_k requires the computation of the flow of the wave–function renormalization Z_k since $\eta_k = -\partial_t \log Z_k$. It is clear from Eq. (1.3.2) that Z_k corresponds to the term in Γ_k which is quadratic in the fields and in the momentum. Accordingly,

$$\partial_t Z_k \, \delta_{ij} = \lim_{p^2 \to 0} \frac{d^2}{dp^2} \frac{\delta^2}{\delta\varphi_i(p)\delta\varphi_j(-p)} \partial_t \Gamma_k[\varphi] \Big|_{\varphi=0} . \tag{1.3.22}$$

The flow of Z_k is therefore related to that of the two-point function whose flow equation reads

$$[\partial_t \Gamma_k^{(2)}(p^2)]_{ij} = -\frac{1}{2} \int_q [\Gamma_k^{(4)}(q, p, -p, -q)]_{aija} G_k^2(q^2) \partial_t R_k(q^2)$$

$$+ \int_q [\Gamma_k^{(3)}(q, p, -q-p)]_{aib} G_k((q+p)^2) [\Gamma_k^{(3)}(q+p, -p, -q)]_{bja} G_k^2(q^2) \partial_t R_k(q^2) \,, \tag{1.3.23}$$

where we introduced the regularized propagator (at $\varphi = 0$), namely

$$[G_k(q^2)]^{-1} = \Gamma_k^{(2)}(q^2) + R_k(q^2) = Z_k q^2 + \bar{\lambda}_2 + R_k(q^2) \,. \tag{1.3.24}$$

Equation (1.3.23) depends on the three– and four–point functions, but the only contribution proportional to p^2 comes from the integral involving the first. Hence without loss of generality, we can consider the effective action (1.3.2) where the potential (1.2.13) is truncated at order $p = 3$, obtaining

$$\partial_t Z_k \delta_{ij} = \bar{\lambda}_3^2 \, T^{(3)}_{aib} T^{(3)}_{ajb} \int_q G_k((q+p)^2) G_k^2(q^2) \partial_t R_k(q^2) \Big|_{p^2} . \tag{1.3.25}$$

By employing the linear cutoff (including the wave–function renormalization Z_k) $R_k(z) = Z_k(k^2 - z)\theta(k^2 - z)$, we obtain

$$\int_q G_k((q+p)^2) G_k^2(q^2) \partial_t R_k(q^2) \Big|_{p^2} = -Z_k^2 c_d \left(1 - \frac{\eta_k}{d+2}\right) \frac{k^{d+2}}{(Z_k k^2 + \bar{\lambda}_2)^4} \,. \tag{1.3.26}$$

At this point we are left with the task of computing the trace $T^{(3)}_{aib}T^{(3)}_{ajb}$, which has been computed in Appendix A.2. Equation (1.3.25) then becomes

$$\partial_t Z_k = -Z_k^2 c_d \left(1 - \frac{\eta_k}{d+2}\right) \frac{k^{d+2}}{(Z_k k^2 + \bar{\lambda}_2)^4} (n-1)(n+1)^2 \, \bar{\lambda}_3^2 \,.$$

Finally, switching to dimensionless variables $\bar{\lambda}_m = Z_k^{m/2} k^{d-m(d/2-1)} \lambda_m$ and after re–absorbing the factor c_d in a field redefinition as before, we find the following simple expression for the anomalous dimension

$$\eta_k = (n-1)(n+1)^2 \frac{\lambda_3^2}{(1+\lambda_2)^4} \left(1 - \frac{\eta_k}{d+2}\right) . \tag{1.3.27}$$

The anomalous dimension term on the r.h.s of this equation originates from the non–perturbative part of the flow equation. We will omit it in the following, since its contributions turns out to be negligible in $d = 4$ and $d = 5$, provided that the correction due to the anomalous dimension η is small in that range of dimensions. We remark here that, in the LPA′ approximation scheme, the anomalous dimension receives contributions only from the three–point function at $\varphi = 0$, i.e., from the trilinear coupling λ_3, irrespectively of the number of LPA′ couplings considered. We therefore expect no further corrections to Eq. (1.3.27) when the potential (1.2.13) is truncated at higher orders. Beyond the LPA′ approximation scheme instead, the expression for the anomalous dimension would receive additional contributions, but this will not be considered in this work.

1.3.4 LPA′ at fixed n

The flow equation (1.3.6) can be expressed exactly using the Cayley–Hamilton theorem to compute $(k^2\mathbb{I} + \mathbb{V})^{-1}$. In linear algebra, the Caley–Hamilton theorem asserts that, for a general $m \times m$ invertible matrix A, i.e. with non–zero determinant, A^{-1} can be expressed as a $(m-1)$–polynomial expression in A. The theorem amounts at the following identity

$$A^m + c_{m-1} A^{m-1} + \cdots + c_1 A + (-1)^m \det(A)\, \mathbb{I}_m = 0 \,. \tag{1.3.28}$$

The coefficientes c_i are given by the elementary symmetric polynomials of the eigenvalues of A, which can then be expressed in terms of power sum symmetric polynomials. By multiplying both sides of Equation (1.3.28) by A^{-1}, one is led to an expression for the inverse of A, namely

$$A^{-1} = \frac{(-1)^{m-1}}{\det(A)} \left(A^{m-1} + c_{m-1} A^{m-2} + \cdots + c_1 \mathbb{I}_m \right) . \tag{1.3.29}$$

By applying the Caley–Hamilton theorem for $n = 1, 2, 3$, we find the following explicit forms

$$\partial_t V_k = k^{d+2} \frac{1}{k^2 + \mathrm{tr}\mathbb{V}} \qquad n = 1 , \tag{1.3.30}$$

$$\partial_t V_k = k^{d+2} \frac{2k^2 + \mathrm{tr}\mathbb{V}}{k^4 + k^2 \mathrm{tr}\mathbb{V} + \det \mathbb{V}} \qquad n = 2 , \tag{1.3.31}$$

$$\partial_t V_k = k^{d+2} \frac{3k^4 + 2k^2 \mathrm{tr}\mathbb{V} - \frac{1}{2}\left(\mathrm{tr}(\mathbb{V}^2) - (\mathrm{tr}\mathbb{V})^2\right)}{k^6 + k^4 \mathrm{tr}\mathbb{V} - \frac{1}{2}k^2 \left(\mathrm{tr}(\mathbb{V}^2) - (\mathrm{tr}\mathbb{V})^2\right) + \det \mathbb{V}} \qquad n = 3 . \tag{1.3.32}$$

These are just the flow equations for an n–component scalar φ_i since the symmetry has not been considered yet. The information on the discrete symmetry S_{n+1}, enters via the form of the invariants which the potential depends on. In general, the LPA' for S_{n+1} depends on n independent invariants, as can be seen explicitly for the $n = 1, 2, 3$ cases in Table 1.2. In what follows any k dependence is understood.

In the `Ising` case $n = 1$ the only invariant is $\rho = \varphi_1^2$ so we define $U(\rho) \equiv V(\varphi_1)$. Since by change of variables, the second functional derivative V_{11} of the effective potential w.r.t. φ_1 reads $V_{11} = 2U_\rho + 4\rho U_{\rho\rho}$, the LPA' Eq. (1.3.30) takes the well–known form

$$\partial_t U = \frac{k^{d+2}}{k^2 + 2U_\rho + 4\rho U_{\rho\rho}} . \tag{1.3.33}$$

Standard `Ising` beta functions are retrieved once we consider, for example, the following φ^6 truncation

$$U(\rho) = \frac{1}{2}\bar{g}_2 \rho + \frac{1}{4!}\bar{g}_4 \rho^2 + \frac{1}{6!}\bar{g}_6 \rho^3 .$$

By inserting this expression into equation (1.3.33) and by switching to dimensionless

variables we can compare equal powers of the fields. The result reads:

$$\begin{aligned}
\beta_2 &= (-2+\eta)g_2 - \frac{g_4}{(1+g_2)^2}\,, \\
\beta_4 &= (d+2\eta-4)g_4 + \frac{6g_4^2}{(1+g_2)^3} - \frac{g_6}{(1+g_2)^2}\,, \\
\beta_6 &= (2d+3\eta-6)g_6 - \frac{90g_4^3}{(1+g_2)^4} + \frac{30g_6g_4}{(1+g_2)^3}\,.
\end{aligned} \tag{1.3.34}$$

We can compare these beta functions with the general beta functions of section 1.3.2 for $n = 1$ [55]. Having in mind the result of Table 1.2 we find the following mapping between the two representations

$$g_2 = \lambda_2 \qquad g_4 = 2\lambda_{4,1} + \lambda_{4,2} \qquad g_6 = 2\lambda_{6,1} + 2\lambda_{6,3} + \lambda_{6,4}\,. \tag{1.3.35}$$

If we now take the corresponding linear combinations of the general beta functions of section 1.3.2 and set $n = 1$, we find that they are correctly expressed only in terms of the couplings g_1, g_2, g_3 as indicated in Eq. (1.3.34). We remark that this is a non–trivial check of the formalism introduced in previous sections.

In the same fashion we turn to the $n = 2$ case, which is characterized by the following two invariants (see Table 1.2)

$$\rho = \varphi_1^2 + \varphi_2^2\,, \qquad \tau = \frac{3}{\sqrt{2}}\varphi_2(\varphi_2^2 - 3\varphi_1^2)\,, \tag{1.3.36}$$

and, accordingly, the effective potential can be expressed as $U(\rho,\tau) \equiv V(\varphi_1,\varphi_2)$. We can therefore express the flow equation for a two–component scalar field in terms of the S_3 invariants (ρ,τ). The derivatives needed to evaluate Eq. (1.3.31) are

$$V_{11} = 2U_\rho + 4U_{\rho\rho}\varphi_1^2 - 9\varphi_2\left[\sqrt{2}U_\tau + 2\varphi_1^2\left(2\sqrt{2}U_{\rho\tau} - 9U_{\tau\tau}\varphi_2\right)\right]\,,$$
$$V_{22} = 2U_\rho + \frac{81}{2}\left[\left(\varphi_1^2 - \varphi_2^2\right)^2 U_{\tau\tau} + \varphi_2\left(4\varphi_2 U_{\rho\rho} - 18\sqrt{2}\left(\varphi_1^2 - \varphi_2^2\right)\right)U_{\rho\tau} + 9\sqrt{2}U_\tau\right]\,,$$

and

$$V_{12} = V_{21} = -\varphi_1\varphi_2\left[81\left(\varphi_2^2 - \varphi_1^2\right)U_{\tau\tau} - 4U_{\rho\rho}\right] - 9\sqrt{2}\varphi_1\left(\varphi_1^2 + \varphi_2^2\right)U_{\rho\tau} + 9\sqrt{2}U_\tau\,.$$

Note that these relations are not yet expressed solely in terms of the invariants ρ and τ, as only the matrix invariants $\mathrm{tr}\,\mathbb{V}$ and $\det\mathbb{V}$ are. In fact, we can write

$$\mathrm{tr}\,\mathbb{V} = V_{11} + V_{22} = \frac{81\rho^2 U_{\tau\tau}}{2} + 4\rho U_{\rho\rho} + 4U_\rho + 12\tau U_{\rho\tau}\,,$$

$$\begin{aligned}\det\mathbb{V} &= V_{11}V_{22} - (V_{12})^2 \\ &= 4U_\rho^2 + U_\rho\left(81\rho^2 U_{\tau\tau} + 8\rho U_{\rho\rho} + 24\tau U_{\rho\tau}\right) - 6U_{\rho\rho}\left[3\left(2\tau^2 - 9\rho^3\right)U_{\tau\tau} + 4\tau U_\tau\right] \\ &\quad -18\left(9\rho^3 - 2\tau^2\right)U_{\rho\tau}^2 - 324\rho^2 U_{\rho\tau}U_\tau - 81\rho U_\tau\left(3\tau U_{\tau\tau} + 2U_\tau\right)\,.\end{aligned}$$

We can now insert these expressions into the flow equation (1.3.31) for $V(\varphi_1, \varphi_2)$ to get the flow equation for $U(\rho, \tau)$

$$\begin{aligned}\partial_t U_k = &\left\{2k^2 + 4U_\rho + 4\rho U_{\rho\rho} + 12\tau U_{\rho\tau} + \frac{81}{2}\rho^2 U_{\tau\tau}\right\}\left\{k^4 + k^2\left(4U_\rho + 4\rho U_{\rho\rho} + 12\tau U_{\rho\tau} + \frac{81}{2}\rho^2 U_{\tau\tau}\right)\right. \\ &+4U_\rho^2 + U_\rho\left(8\rho U_{\rho\rho} + 24\tau U_{\rho\tau} + 81\rho^2 U_{\tau\tau}\right) - 18\left(9\rho^3 - 2\tau^2\right)\left(U_{\rho\tau}^2 - U_{\tau\tau}U_{\rho\rho}\right) \\ &\left.-162\rho U_\tau^2 - 3U_\tau\left(8\tau U_{\rho\rho} + 108\rho^2 U_{\rho\tau} + 81\rho\tau U_{\tau\tau}\right)\right\}^{-1}\,. \qquad (1.3.37)\end{aligned}$$

This is the explicit form of the LPA′ with $n = 2$. As an application we can take advantage of the flow equation in this form to extract the beta functions of the corresponding S_3–symmetric potential. Considering the following φ^6 truncation

$$U(\rho, \tau) = \frac{1}{2!}\bar{g}_2\rho + \frac{1}{3!}\bar{g}_3\tau + \frac{1}{4!}\bar{g}_4\rho^2 + \frac{1}{5!}\bar{g}_5\rho\tau + \frac{1}{6!}(\bar{g}_{6,1}\rho^3 + \bar{g}_{6,2}\tau^2)\,, \qquad (1.3.38)$$

we obtain the following system of dimensionless beta functions

$$
\begin{aligned}
\beta_2 &= (-2+\eta)g_2 + \frac{18g_3^2}{(1+g_2)^3} - \frac{4g_4}{3(1+g_2)^2}\,,\\
\beta_3 &= \frac{1}{2}(d+3\eta-6)g_3 + \frac{4g_3g_4}{(1+g_2)^3} - \frac{4g_5}{5(1+g_2)^2}\,,\\
\beta_4 &= (d+2\eta-4)g_4 + \frac{972g_3^4}{(1+g_2)^5} - \frac{216g_3^2g_4}{(1+g_2)^4} + \frac{648g_3g_5+100g_4^2}{15(1+g_2)^3}\\
&\quad - \frac{12g_{6,1}+27g_{6,2}}{10(1+g_2)^2}\,,\\
\beta_5 &= \frac{1}{2}(3d+5\eta-10)g_5 + \frac{720g_3^3g_4}{(1+g_2)^5} - \frac{216g_3^2g_5}{(1+g_2)^4}\\
&\quad + \frac{56g_4g_5 - 240g_3g_4^2 + 24g_3g_{6,1} + 189g_3g_{6,2}}{3(1+g_2)^3}\,,\\
\beta_{6,1} &= (2d+3\eta-6)g_{6,1} + \frac{131220g_3^6}{(1+g_2)^7} - \frac{48600g_3^4g_4}{(1+g_2)^6} + \frac{4680g_3^2g_4^2+11664g_3^3g_5}{(1+g_2)^5}\\
&\quad - \frac{729g_3^2(4g_{6,1}+9g_{6,2}) - 560g_4^3 - 7776g_3g_4g_5}{6(1+g_2)^4}\\
&\quad + \frac{5g_4(32g_{6,1}+27g_{6,2}) + 324g_5^2}{5(1+g_2)^3}\,,\\
\beta_{6,2} &= (2d+3\eta-6)g_{6,2} + \frac{160g_3^2g_4^2}{(1+g_2)^5} - \frac{96g_3g_5g_4}{(1+g_2)^4} + \frac{100g_4g_{6,2}+32g_5^2}{5(1+g_2)^3}\,.
\end{aligned}
\tag{1.3.39}
$$

We can compare this result with the general beta functions of section 1.3.2, now evaluated for $n = 2$. Having in mind the results of Table 1.2 in the case $n = 2$, we get the following mapping between couplings

$$
g_2 = \lambda_2 \qquad g_3 = \lambda_3 \qquad g_4 = \frac{9}{2}\lambda_{4,1} + \lambda_{4,2}
$$

$$
g_5 = \frac{5}{2}\lambda_{5,1} + \lambda_{5,2} \qquad g_{6,1} = \frac{27}{4}\lambda_{6,1} + \frac{9}{2}\lambda_{6,3} + \lambda_{6,4} \qquad g_{6,2} = \frac{1}{3}\lambda_{6,1} + \lambda_{6,2}\,.
$$

The matching between the beta functions of section 1.3.2 for $n = 2$ with those of Eqs. (1.3.39) is a non–trivial check. Finally, it is clear that for any integer n it is possible to find corresponding expressions for the relative LPA', but these flow equations become extremely complicated as n increases.

1.4 Applications

1.4.1 Cubic interaction

As a first application of the so–developed fRG formalism to the study of the critical behavior of S_{n+1}–symmetric theories, we consider the simplest case where only a mass term (i.e., quadratic term) and the trilinear coupling are present.

Referring to the general system of dimensionless beta functions of section 1.3.2, we switch off all couplings but λ_2 and λ_3 so that the corresponding dimensionless beta functions of Eqs. (1.3.12) and (1.3.13) is reduced to:

$$\beta_2 = -2\lambda_2 + \eta\lambda_2 + 2\frac{(n-1)(n+1)^2}{(1+\lambda_2)^3}\lambda_3^2\,,$$
$$\beta_3 = \frac{1}{2}\lambda_3(d-6+3\eta) - 6\frac{(n-2)(n+1)^2}{(1+\lambda_2)^4}\lambda_3^3\,.$$

Fixed point solutions $\beta_i = 0$ describe the critical behavior of such theories in the corresponding theory space. Apart from the trivial Gaussian fixed point ($\lambda_2^* = 0$, $\lambda_3^* = 0$) we find the following non-trivial fixed point

$$\lambda_2^* = -\frac{(d-6)(n-1)}{d(n-1)-18n+30}\,, \qquad \lambda_3^* = \pm\frac{24\sqrt{3}\sqrt{(d-6)(n-2)}(n-2)}{\sqrt{(n+1)^2(d(n-1)-18n+30)^4}}\,, \tag{1.4.1}$$

which, as expected, reduce to the Gaussian one in $d = 6$. Note that in $d < 6$ and $n > 2$ the fixed point is imaginary and, as a consequence, the theory is non–unitary, as in the case of the `Lee-Yang` universality class [56]. But for $n < 2$ the fixed point is real and so it is the corresponding Landau–Ginzburg action.

We can now linearize the RG flow around the non–trivial fixed given above to acquire a qualitative understanding of the flow and to extract the critical exponents. The stability matrix $M_{ij} = \frac{\partial\beta_i}{\partial\lambda_j}\Big|_*$ around the fixed point has the following compo-

nents,

$$
\begin{aligned}
M_{11} &= -\frac{[d(n-1)-8]\,[12(n-3)+d(n-1)]}{(3n-7)\,[d-(d-24)n-48]}\,,\\
M_{12} &= \frac{2(6-d)^{3/2}\,[d-(d-24)n-48]}{3\,[d(n-1)-12n+20]\,\sqrt{21-9n}(n+1)}\,,\\
M_{21} &= \frac{24\sqrt{3}\,[d(n-1)-12n+20]\,\sqrt{(d-6)(3n-7)}\,(n^2-1)}{[d-(d-24)n-48]^2}\,,\\
M_{22} &= 6-d\,,
\end{aligned}
$$

with corresponding eigenvalues

$$
\theta_{\pm} = \frac{1}{2}\left(M_{11}+M_{22}-\sqrt{M_{11}^2-2M_{22}M_{11}+M_{22}^2+4M_{12}M_{21}}\right)\,.
$$

At this point one can obtain analytical expressions for the critical exponents simply considering that the correlation length critical exponent ν is related to the inverse of the negative eigenvalue $\nu = -\theta_-^{-1}$ while the correction–to–scaling critical exponent ω can be obtained as the first positive eigenvalue of the stability matrix which in this case is $\omega = \theta_+$. The anomalous dimension instead is obtained once the fixed point values (1.4.1) are substituted into equation (1.3.27), obtaining

$$
\eta = \frac{(d-6)(n-1)}{3(7-3n)}\,. \tag{1.4.2}
$$

The critical exponents obtained in this approximation provide the blue curves reported in Figure 1.3 in the next subsection, where they are plotted as functions of the dimension d in the relevant cases of `Percolation` and `Spanning forest`.

We conclude this section specializing the analysis to $d = 6-\epsilon$ dimensions to make contact with the known results from the perturbative renormalization group calculations in the ε-expansion [43]. Expanding to first order in ϵ our results we find

$$
\nu = \frac{1}{2}+\frac{5(n-1)}{12(3n-7)}\epsilon+O(\epsilon^2) \qquad\qquad \eta = \frac{n-1}{3(7-3n)}\epsilon+O(\epsilon^2) \tag{1.4.3}
$$

and $\omega = \epsilon + O(\epsilon^2)$ independently of n [57]. Notice that setting $n = 1$ here, renders

the Ising mean–field critical exponents, consistently with the fact that Ising is described at least by a quartic interaction term which, on the other hand, sets the upper critical dimension d_c to $d_c = 4$. The explicit results for the Percolation are [44, 58]

$$\nu = \frac{1}{2} + \frac{5}{84}\epsilon + O(\epsilon^2)\,, \qquad \eta = -\frac{\epsilon}{21} + O(\epsilon^2)\,, \tag{1.4.4}$$

while for the Spanning Forest universality class we obtain [59]

$$\nu = \frac{1}{2} + \frac{1}{12}\epsilon + O(\epsilon^2)\,, \qquad \eta = -\frac{\epsilon}{15} + O(\epsilon^2)\,. \tag{1.4.5}$$

Notice that, for $n \geq 2$ we find $\nu < \nu_{\rm MF}$ where one expects, on the other hand, that the phase transition is first–order. Finally, we remark that the Ising ε-expansion results, can be recovered upon expanding the beta functions (1.3.34) around $d_c = 4 - \epsilon$.

1.4.2 General Analysis

The full set of beta functions presented in section 1.3.2 can be studied only numerically. As anticipated, we focus on the non–trivial universality classes in $d > 2$ which, apart from Ising, are Percolation and Spanning Forest. The numerical analysis proceeds in various steps: For all values $3 \leq p \leq 6$ we first solve numerically the algebraic system $\beta_{i,m} = 0$ with $i = 2, ..., p$ and $m = 1, ..., N(p)$ to extract the fixed–point coordinates; we compute the stability matrix $M_{ij} = \frac{\partial \beta_i}{\partial \lambda_j}$ symbolically and then we evaluate it at the numerical fixed–point; finally we extract their eigenvalues. At each truncation order we find just one negative eigenvalue θ_- from which we can extract the correlation–length critical exponent $\nu = -\theta_-^{-1}$; the first positive eigenvalue θ_+ gives, instead, the correction–to–scaling exponent $\omega = \theta_+$; the anomalous dimension is computed from Eq. (1.3.27). At every order of the truncation p, we repeated the procedure for any $3 \leq d \leq 6$. The results for the critical exponents $\nu(d), \omega(d), \eta(d)$ as functions of the dimensionality d up to truncation order $p = 6$ are shown in Figure 1.3 for the relevant cases of Percolation and Spanning Forest cases.

It is immediately clear from the plots that, as the order of the truncation p increases, the curves for the critical exponents converge non–uniformly: For values d closer to the upper critical dimension $d_c = 6$, few orders suffice to obtain a stable estimate (which is intended to be when the curves, at different truncation or-

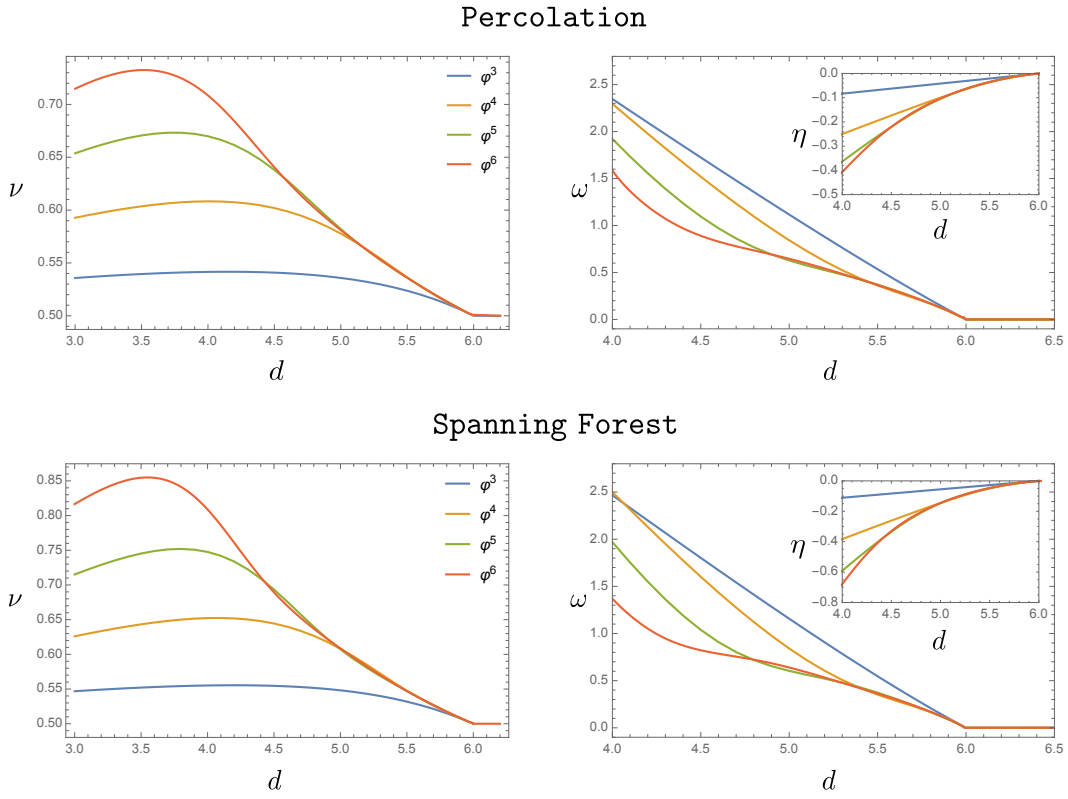

Figure 1.3: `Percolation` (upper plots) and `Spanning Forest` (lower plots) critical exponents ν (left), ω (right) and η (inset) as a function of the dimensionality d for increasing order of the truncation. For both universality classes, convergence is evident down to $d = 5$. In lower dimensions, e.g., in $d = 4$ and $d = 3$, convergence is expected only at higher–orders in the truncation.

ders, overlap each other). For the critical exponent ν, in $d = 5$, the truncation order $p = 4$ already gives good estimates with respect to the known results indicated in Tables 1.3, 1.4 and 1.5; in $d = 4$, instead, the maximum order available $p = 6$ is not enough to see convergence; in $d = 3$ dimension, convergence is still far from being reached: This suggest that an improvement of the truncation is needed [8]. In Table 1.3 we report the precise numerical values for the correlation length critical

[8] As a first guess one can interpolate the curves using the converging parts; the result is consistent with the estimates for ν even in $d = 3$. This gives us a reason to expect that higher–order truncations can deal also with this case.

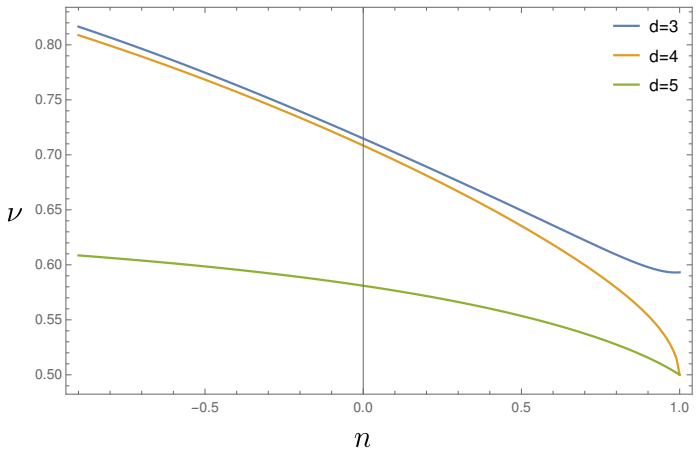

Figure 1.4: The correlation length critical exponent ν as a function of n for $d = 3, 4, 5$ in the φ^6 truncation. Curves interpolate smoothly between `Spanning Forest` and `Ising`: In $d = 4$ and $d = 5$ the critical exponent converges to $\nu = 1/2$ for $n = 1$ since above $d_c = 4$, `Ising` is correctly described by mean–field theory; in $d = 3$ instead the curve approaches $\nu = 0.593$ which is the `Ising` estimate for the correlation–length critical exponent at order φ^6 in the LPA′.

exponent. For the critical exponent ω, the convergence is, as expected, slower than for ν and the numerical estimates are reported in Table 1.4, while the results for the anomalous dimension can be found in Table 1.5. The estimates for ν are quite satisfactory and testify the success of polynomial truncations in the determination of this exponent. A satisfactory determination of the exponent ω, would require an improvement of the truncation, while the significant departure of the numerical value of the exponent η from known results, is a general trend in LPA′–like approximations. In particular, it is difficult to see how the anomalous dimension can change in sign in lower dimensions, as expected from $d = 3$ estimates and the exact results in $d = 2$, thus questioning the validity of Eq. (1.3.27) below four dimensions.

In Figure 1.4 and Figure 1.5 we explore the n–dependence of the correlation–length critical exponent. In the first figure we plot $\nu(n)$ for $d = 3, 4, 5$ in the range $-1 \leq n \leq 1$; in the second picture we plot $\nu(d)$ for values of n between $-1 \leq n \leq 1$.

As shown in section 1.2, the number of couplings grows rapidly with the order p of the truncation. Even if the general analysis presented above indicates that

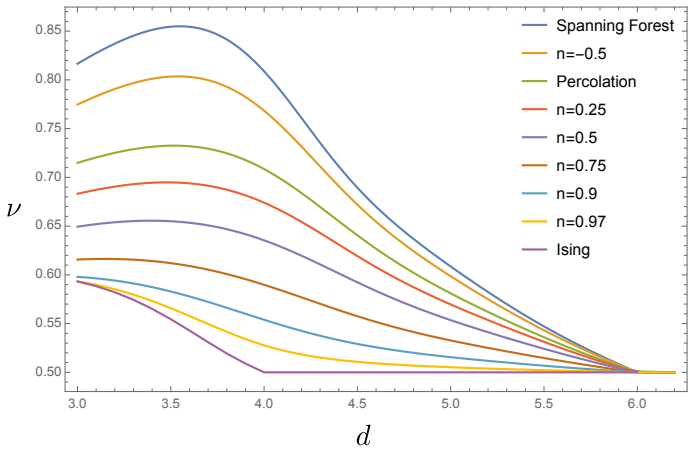

Figure 1.5: Critical exponent ν as a function of d for various values of n in the φ^6 truncation. As n increases, the critical exponent in the $d > 4$ region flattens toward the $n = 1$ mean field value $\nu = \frac{1}{2}$ (`Ising`).

higher–order truncations have the strength to fully determine the spectrum down to three dimensions, an explicit derivation of beta functions beyond those reported in section 1.3.2 demands a significant amount of further work. Finally, while in $d = 5$ a study of scheme dependence is possible already at $p = 6$ since convergence has been achieved, we postpone this study to a future work when also convergence in the other two physically relevant dimensions $d = 3$ and $d = 4$ is obtained.

1.5 Conclusions and perspectives

In this chapter we have been mainly interested in the adaption of the functional RG (fRG) methods to the field theory of an n–comp. scalar with the underlying global S_{n+1} symmetry of the Potts model. Approaching this problem requires an in–depth understanding of the underlying representation theory of the permutation group. Zia and Wallace [17] paved the way showing that invariant polynomials can be constructed geometrically, in terms of the isomorphism connecting the group S_{n+1} to the symmetry group which maps the n–hyper–tetrahedra on themselves. We generalized this construction to invariant polynomials of arbitrary power interactions in order to develop an algorithm able to compute the beta functions for the couplings

dim.	n	φ^3	φ^4	φ^5	φ^6	best	ref.
5	-1	0.5481	0.6059	0.6071	0.6085	0.59	[59]
	0	0.5358	0.5777	0.5820	0.5810	0.575	[60]
4	-1	0.5551	0.6492	0.7476	0.8087	0.80	[59]
	0	0.5415	0.6083	0.6698	0.7084	0.692	[60]
3	-1	0.5468	0.6238	0.7151	0.8170	1.28	[59]
	0	0.5357	0.5927	0.6537	0.7148	0.897	[60]

Table 1.3: Correlation length critical exponent ν for `Percolation` ($n = 0$) and `Spanning Forest` ($n = -1$) in $d = 5, 4, 3$. Estimates obtained in the various truncations considered are presented and convergent digits are denoted in blue. Comparison is made with available Monte Carlo simulations or re-summed high order ϵ-expansion estimates.

dim.	n	φ^3	φ^4	φ^5	φ^6	best	ref.
5	-1	1.157	0.8413	0.603	0.639		
	0	1.116	0.842	0.627	0.645	0.718	[60]
4	-1	2.466	2.500	1.969	1.368		
	0	2.346	2.295	1.922	1.587	1.2198	[60]

Table 1.4: Critical exponent ω for `Percolation` ($n = 0$) and `Spanning Forest` ($n = -1$) in $d = 5, 4$. Estimates obtained in the various truncations considered are presented and convergent digits (in the LPA') are denoted in blue. Comparison is made with available re-summed high order ϵ-expansion estimates in the $n = 0$ case. No estimates have been found in the literature for $n = -1$.

appearing in the effective potential. We applied the formalism to perform explicit computations up to order φ^6, from which we obtained a system of coupled ordinary differential equations describing the RG flow of the ten couplings present at this order, for arbitrary d and n.

A characterizing property of the S_{n+1}–symmetry is that the LPA' is a partial differential equation of $(n+1)$–variables, since n independent invariants can be built out of the field multiplet, even without introducing derivatives. In this respect, the

dim	n	φ^3	φ^4	φ^5	φ^6	best	ref
5	-1	-0.055	-0.145?	-0.145?	-0.1458	-0.08	[59]
	0	-0.041	-0.099	-0.104	-0.102	-0.0565	[60]
4	-1	-0.110	-0.382	-0.590	-0.678	-0.16	[59]
	0	-0.0833	-0.250	-0.363	-0.406	-0.0954	[60]

Table 1.5: Anomalous dimension η for `Percolation` ($n = 0$) and `Spanning Forest` ($n = -1$) in $d = 5, 4$. Estimates obtained in the various truncations considered are presented and convergent digits (in the LPA') are denoted in blue. Comparison is made with available Monte Carlo simulations or re-summed high order ϵ-expansion. As generally happens with LPA' truncations, the estimates for the anomalous dimension are much poorer that those for ν or ω.

generalization of a single component $\mathbb{Z}_2$–scalar to a multi–component scalar is more involved in the S_{n+1} case than, for example, in the $O(n)$ case. In this respect what is still missing is the fRG improved local potential approximation (LPA') for arbitrary n: this would unlock a fully functional analysis of the physically interesting limits of `Percolation` and `Spanning-Forest`. A large–n limit will also become available.

Higher–order truncations, as well as the use of the principle of minimal sensitivity (PMS) [61], proved to be crucial in the optimization of numerical results as obtained from the fRG [54]. In this respect, it would be interesting to improve our results in order to see full numerical convergence in $d = 3$ where we reported preliminary estimates.

A physically relevant question that attracted lot of attention, is the disputed critical value d_c of d at which the phase transition of the three–states Potts model ceases to be continuous and becomes of the first–order type. We suggest that in order to tackle such a problem, one needs to study the two variables partial differential equation (1.3.31) which encodes the RG flow in the LPA' approximation scheme for $n = 2$. Since no expansion around a particular upper critical dimension is needed, we consider the fRG a preferred computational framework to answer this question.

Recently, the authors in Ref. [62] studied the multi–critical phases of the $\texttt{Potts}_q$ models by means conformal field theory and functional perturbative renormalization group methods.

Appendix A

A.1 Explicit construction of the invariants in the $n = 2$ case

In the following, we give an explicit construction of the Potts field theory in the S_3 case. The coordinates of the vertices of a regular triangle in the plane, as shown in Figure 1.2, are

$$\mathrm{e}^1 = \sqrt{2}\begin{pmatrix} 0 \\ 1 \end{pmatrix}, \qquad \mathrm{e}^2 = \sqrt{2}\begin{pmatrix} -\sqrt{3}/2 \\ -1/2 \end{pmatrix}, \qquad \mathrm{e}^3 = \sqrt{2}\begin{pmatrix} \sqrt{3}/2 \\ -1/2 \end{pmatrix}. \tag{A.1.1}$$

The matrix representation of the $|S_3| = 3! = 6$ elements of S_3, which leave invariant the triangle, are

$$I = \begin{pmatrix} 1 & 0 \\ 0 & 1 \end{pmatrix}, \qquad R = \begin{pmatrix} -1/2 & -\sqrt{3}/2 \\ +\sqrt{3}/2 & -1/2 \end{pmatrix}, \qquad R^{-1} = \begin{pmatrix} -1/2 & \sqrt{3}/2 \\ -\sqrt{3}/2 & -1/2 \end{pmatrix},$$
$$\mu_1 = \begin{pmatrix} -1 & 0 \\ 0 & 1 \end{pmatrix}, \qquad \mu_2 = \begin{pmatrix} +1/2 & +\sqrt{3}/2 \\ +\sqrt{3}/2 & -1/2 \end{pmatrix}, \qquad \mu_3 = \begin{pmatrix} +1/2 & -\sqrt{3}/2 \\ -\sqrt{3}/2 & -1/2 \end{pmatrix}. \tag{A.1.2}$$

Clearly I is the identity, R the (counter–clockwise) rotation of $2\pi/3$ and R^{-1} its inverse, while μ_i for $i = 1, 2, 3$ are the reflections along the axis passing through the i-th vertex of the triangle. The two $n = 2$ invariants are, from Table 1.2, the following

$$\rho \equiv I_2 = 3(\varphi_1^2 + \varphi_2^2), \qquad \tau \equiv I_3 = \frac{3}{\sqrt{2}}\varphi_2(\varphi_2^2 - 3\varphi_1^2).$$

We can check explicitly ρ and τ are indeed invariant under the transformations (A.1.2). Consider, for example, the rotation R:

$$\begin{pmatrix} \varphi_1 \\ \varphi_2 \end{pmatrix} \longmapsto \begin{pmatrix} \tilde{\varphi}_1 \\ \tilde{\varphi}_2 \end{pmatrix} = R \begin{pmatrix} \varphi_1 \\ \varphi_2 \end{pmatrix} = \begin{pmatrix} -\frac{1}{2}\varphi_1 - \frac{\sqrt{3}}{2}\varphi_2 \\ \frac{\sqrt{3}}{2}\varphi_1 - \frac{1}{2}\varphi_2 \end{pmatrix} .$$

Its easy to check the invariance of ρ and τ

$$\begin{aligned} \tilde{\rho} &= 3(\tilde{\varphi}_1^2 + \tilde{\varphi}_2^2) \\ &= \frac{3}{4}\varphi_1^2 + \frac{9}{4}\varphi_2^2 + \frac{3\sqrt{3}}{2}\varphi_1\varphi_2 + \frac{3}{4}\varphi_2^2 + \frac{9}{4}\varphi_1^2 - \frac{3\sqrt{3}}{2}\varphi_1\varphi_2 \\ &= 3(\varphi_1^2 + \varphi_2^2) = \rho\,, \end{aligned}$$

$$\begin{aligned} \tilde{\tau} &= \frac{3}{\sqrt{2}}\tilde{\varphi}_2(\tilde{\varphi}_2^2 - 3\tilde{\varphi}_1^2) \\ &= \frac{3}{\sqrt{2}}\left(\frac{\sqrt{3}}{2}\varphi_1 - \frac{1}{2}\varphi_2\right)\left[\left(\frac{\sqrt{3}}{2}\varphi_1 - \frac{1}{2}\varphi_2\right)^2 - 3\left(-\frac{1}{2}\varphi_1 - \frac{\sqrt{3}}{2}\varphi_2\right)^2\right] \\ &= \frac{3}{\sqrt{2}}\varphi_2(\varphi_2^2 - 3\varphi_1^2) = \tau\,. \end{aligned}$$

Similarly one can check all the other transformations in Eqs. (A.1.2). We therefore showed explicitly that the field theory characterized by the potential in Eq. (1.2.13)

$$V(\varphi_1, \varphi_2) = \frac{\bar{\lambda}_2}{2} 3\left(\varphi_1^2 + \varphi_2^2\right) + \frac{\bar{\lambda}_3}{3!}\frac{3}{\sqrt{2}}\varphi_2(\varphi_2^2 - 3\varphi_1^2) + ... \tag{A.1.3}$$

is invariant under the action of the elements of S_3.

A.2 Trace machinery: Cubic example

When we truncate the expansion (1.2.13) at order $p = 3$, only the trilinear coupling and the quadratic terms are present in the corresponding effective action Γ_k. Accordingly, the non–diagonal part of the Hessian is just $\mathbb{M} = \bar{\lambda}_3 T^{(3)}_{abi}\varphi_i$ and therefore we have to consider the contributions $\mathrm{tr}\,\mathbb{M}$, $\mathrm{tr}\,\mathbb{M}^2$, $\mathrm{tr}\,\mathbb{M}^3$. Contributions of the type $\mathrm{tr}\,\mathbb{M}^m$ for $m \geq 4$ are beyond the truncation with $p = 3$ and can be disregarded. In

order to show explicitly how the computation of these traces works, we use a colour code for the rules (1.2.4) in order to highlight when they play a role in the evaluation

$$\sum_{\alpha} \mathrm{e}_i^{\alpha} = 0 \qquad , \mathrm{e}_i^{\alpha}\mathrm{e}_i^{\beta} = (n+1)\delta^{\alpha\beta} - 1 \qquad , \mathrm{e}_i^{\alpha}\mathrm{e}_j^{\alpha} = (n+1)\delta_{ij}\,. \tag{A.2.1}$$

The first contribution, namely $\mathrm{tr}\mathbb{M}$, vanishes identically since

$$\mathrm{tr}\,\mathbb{M} = \bar{\lambda}_3\, T^{(3)}_{aai}\, \varphi_i = \bar{\lambda}_3 \sum_{\alpha} \mathrm{e}_a^{\alpha}\mathrm{e}_a^{\alpha}\mathrm{e}_i^{\alpha}\, \varphi_i = n\,\bar{\lambda}_3 \sum_{\alpha} \mathrm{e}_i^{\alpha} = 0\,. \tag{A.2.2}$$

Non–trivial contributions come from the trace of the square

$$\begin{aligned}
\mathrm{tr}\,\mathbb{M}^2 &= T^{(3,1)}_{aji_1}\varphi_{i_1} T^{(3,1)}_{jai_2}\varphi_{i_2} \\
&= \bar{\lambda}_3^2 \left[\sum_{\alpha\beta} \mathrm{e}_a^{\alpha}\mathrm{e}_j^{\alpha}\mathrm{e}_{i_1}^{\alpha}\mathrm{e}_j^{\beta}\mathrm{e}_a^{\beta}\mathrm{e}_{i_2}^{\beta}\right]\varphi_{i_1}\varphi_{i_2} \\
&= \bar{\lambda}_3^2 \left[(n+1)\sum_{\alpha} \mathrm{e}_j^{\alpha}\mathrm{e}_{i_1}^{\alpha}\mathrm{e}_j^{\alpha}\mathrm{e}_{i_2}^{\alpha} - \sum_{\alpha\beta} \mathrm{e}_j^{\alpha}\mathrm{e}_{i_1}^{\alpha}\mathrm{e}_j^{\beta}\mathrm{e}_{i_2}^{\beta}\right]\varphi_{i_1}\varphi_{i_2} \\
&= \bar{\lambda}_3^2 \left[n(n+1)^2\delta_{i_1 i_2} - (n+1)\sum_{\alpha} \mathrm{e}_{i_1}^{\alpha}\mathrm{e}_{i_2}^{\alpha} - \sum_{\alpha}\mathrm{e}_{i_1}^{\alpha}\sum_{\beta}\mathrm{e}_{i_2}^{\beta}\right]\varphi_{i_1}\varphi_{i_2} \\
&= \bar{\lambda}_3^2 (n+1)^2(n-1) I_2\,,
\end{aligned} \tag{A.2.3}$$

and from the trace of the cube

$$
\begin{aligned}
\operatorname{tr}\mathbb{M}^3 &= T^{(3,1)}_{abi_1}\varphi_{i_1}T^{(3,1)}_{bci_2}\varphi_{i_2}T^{(3,1)}_{cai_3}\varphi_{i_3} \\
&= \bar{\lambda}_3^3\sum_{\alpha\beta\gamma} \mathrm{e}_a^\alpha \mathrm{e}_b^\alpha \mathrm{e}_{i_1}^\alpha \mathrm{e}_b^\beta \mathrm{e}_c^\beta \mathrm{e}_{i_2}^\beta \mathrm{e}_c^\gamma \mathrm{e}_a^\gamma \mathrm{e}_{i_3}^\gamma \varphi_{i_1}\varphi_{i_2}\varphi_{i_3} \\
&= \bar{\lambda}_3^3\left[(n+1)\sum_{\alpha\beta} \mathrm{e}_b^\alpha \mathrm{e}_{i_1}^\alpha \mathrm{e}_b^\beta \mathrm{e}_c^\beta \mathrm{e}_{i_2}^\beta \mathrm{e}_c^\alpha \mathrm{e}_{i_3}^\alpha - \sum_{\alpha\beta\gamma} \mathrm{e}_b^\alpha \mathrm{e}_{i_1}^\alpha \mathrm{e}_b^\beta \mathrm{e}_c^\beta \mathrm{e}_{i_2}^\beta \mathrm{e}_c^\gamma \mathrm{e}_{i_3}^\gamma\right]\varphi_{i_1}\varphi_{i_2}\varphi_{i_3} \\
&= \bar{\lambda}_3^3\Bigg[(n+1)^2\sum_{\alpha} \mathrm{e}_{i_1}^\alpha \mathrm{e}_c^\alpha \mathrm{e}_{i_2}^\alpha \mathrm{e}_c^\alpha \mathrm{e}_{i_3}^\alpha - (n+1)\sum_{\alpha\beta} \mathrm{e}_{i_1}^\alpha \mathrm{e}_c^\beta \mathrm{e}_{i_2}^\beta \mathrm{e}_c^\alpha \mathrm{e}_{i_3}^\alpha \\
&\quad -(n+1)\sum_{\alpha\gamma} \mathrm{e}_{i_1}^\alpha \mathrm{e}_c^\alpha \mathrm{e}_{i_2}^\alpha \mathrm{e}_c^\gamma \mathrm{e}_{i_3}^\gamma + \sum_{\alpha\beta\gamma} \mathrm{e}_{i_1}^\alpha \mathrm{e}_c^\beta \mathrm{e}_{i_2}^\beta \mathrm{e}_c^\gamma \mathrm{e}_{i_3}^\gamma\Bigg]\varphi_{i_1}\varphi_{i_2}\varphi_{i_3} \\
&= \bar{\lambda}_3^3\Bigg[n(n+1)^2\sum_{\alpha} \mathrm{e}_{i_1}^\alpha \mathrm{e}_{i_2}^\alpha \mathrm{e}_{i_3}^\alpha - (n+1)^2\sum_{\alpha} \mathrm{e}_{i_1}^\alpha \mathrm{e}_{i_2}^\alpha \mathrm{e}_{i_3}^\alpha + \\
&\quad +(n+1)\sum_{\alpha\beta} \mathrm{e}_{i_1}^\alpha \mathrm{e}_{i_2}^\beta \mathrm{e}_{i_3}^\alpha - (n+1)^2\sum_{\alpha} \mathrm{e}_{i_1}^\alpha \mathrm{e}_{i_2}^\alpha \mathrm{e}_{i_3}^\alpha + (n+1)\sum_{\alpha\beta\gamma} \mathrm{e}_{i_1}^\alpha \mathrm{e}_{i_2}^\alpha \mathrm{e}_{i_3}^\gamma\Bigg]\varphi_{i_1}\varphi_{i_2}\varphi_{i_3} \\
&= \bar{\lambda}_3^3\left[n(n+1)^2\sum_{\alpha} \mathrm{e}_{i_1}^\alpha \mathrm{e}_{i_2}^\alpha \mathrm{e}_{i_3}^\alpha - 2(n+1)^2\sum_{\alpha} \mathrm{e}_{i_1}^\alpha \mathrm{e}_{i_2}^\alpha \mathrm{e}_{i_3}^\alpha\right]\varphi_{i_1}\varphi_{i_2}\varphi_{i_3} \\
&= \bar{\lambda}_3^3(n+1)^2(n-2)I_3\,.
\end{aligned}
\tag{A.2.4}
$$

Inserting these traces into Eq. (1.3.8), and comparing the result with the flow equation in the form (1.3.10), we can immediately read off the (dimensionful) beta functions

$$
\bar{\beta}_2 = k^{d-4}\frac{2(n-1)(n+1)^2}{(1+\lambda_2)^3}\bar{\lambda}_3^2\,, \qquad \bar{\beta}_3 = -k^{d-6}\frac{6(n-2)(n+1)^2}{(1+\lambda_2)^4}\bar{\lambda}_3^3\,.
$$

Chapter 2

Platonic field theories

In this Chapter we study the scalar field theories endowed with the discrete symmetry groups of the regular polytopes, i.e., the generalization of the regular polygons and the regular polyhedra to an arbitrary number of spatial dimensions. Because of their extremely symmetric nature, these geometrical structures have an outstanding history of study, unmatched by almost any other geometric object. The breakthrough in the mathematical study of regular polytopes, came only with group theory, in terms of which the early approaches to the study of regular polytopes were consolidated and the foundations were laid for a unified approach to the regularity of figures [63]. In particular, even if the symmetry groups $\mathcal{G}$ characterizing the regular polytopes in arbitrary dimension were identified and classified [64], the determination of all the possible invariant polynomials under representations of the discrete groups $\mathcal{G}$ is, in general, a very non–trivial task.

Inheriting the geometrical perspective introduced in chapter 1,, in the context of hyper–tetrahedra, in section 2.2 we propose a constructive method to determine basic $\mathcal{G}$–invariant polynomials: These constitutes the building blocks in terms of which one expresses the corresponding $\mathcal{G}$–invariant Ginzburg–Landau (GL) actions of what we dub *Platonic Field Theories* (PFTs). Typically, it emerges that the so–obtained invariant polynomials, are characterized by having (relatively) high polynomial degree. In this respect, we recall that, an interaction term characterized by a polynomial of degree m, is marginal at the upper critical dimension $d_c = \frac{2m}{m-2}$ with $m \geq 2$, and a brief inspection reveals that, mostly, upper critical dimensions are rational (fractional). Above d_c, fluctuations of the order parameter are weak and the

theory is essentially captured by the Gaussian mean–field theory; below the upper critical dimension d_c, instead, fluctuations of the order parameter are strong and they change the scaling properties of the theory. This change in behavior at d_c is captured by the renormalization group, whose fixed points govern the universal, scale–invariant properties at a phase transition.

As it was originally proposed by K. Wilson [5] in the framework of the so–called ε–expansion, the universal properties can be obtained as a Taylor series in the parameter $0 < \varepsilon \equiv d_c - d \ll 1$; this led to the identification of the well–known Wilson–Fisher fixed point in $d = 3$. By the argument above concerning the upper critical dimension for high–order invariant polynomials, this entails, in general, that the renormalization procedure has to be carried out in fractional critical dimensions. In Wilson's spirit, field theories which are marginal at a fractional d_c, could in principle provide accurate predictions for physical phase transitions when analytically continued to an integer spacetime dimension. However, the renormalization of scalar field theories in rational spacetime dimensions has not been systematically analyzed until recently [65–68], since, in general, it requires the computation of high–order loop Feynman diagrams, which are typically quite complicated. Such a systematic approach can be achieved once the functional perspective typical of the fRG is encoded in the perturbative expansion: This leads to a functional reformulation of the perturbative renormalization group (fpRG). We briefly review the salient features of this technique in Appendix B.3.

What emerged from the application of the fpRG is that, already for the case in which the order parameter is a single–component field, the functional constraints are very efficient in re–organizing the information contained in the standard perturbative RG. The functional constraints, in fact, allow the direct computation of renormalization group functions for *any* fractional critical dimension [65, 66]. A second key feature of the fpRG is that it gives access to some of the conformal field theory (CFT) universal data, like the operator product expansion (OPE) coefficients[69]. Finally, one of the most remarkable consequences of the functional constraints is the following: The renormalization group functions for a multi–component field theory (i.e., a field theory whose order parameter is a multi–component field), can be obtained from their single–component counterparts without performing any additional computation. (Additional arguments are provided in Appendix B.3).

This crucial fact unlocks the access to the renormalization group functions of the marginal couplings appearing in the effective potential of the PFTs. The analysis of the corresponding critical behavior is contained in Table 2.3 and Table 2.4, which constitute the *atlas* of the universality classes spanned by the symmetry groups of the regular polytopes. A surprising result of our general analysis is the identification of a new fixed point, and therefore a new candidate universality class, in $d = 3$, based on the dihedral symmetry group $\mathbb{D}_5$ of the Pentagon.

Reference: *Journal of High Energy Physics* (2019)152.

2.1 Introduction

In recent years the ε–expansion has been reconsidered [66, 70, 71] since it provides a simple method to approach the general classification of universality classes in arbitrary dimension and for a general symmetry group, as exotic and complex as it may be. As anticipated, the analysis of the single–component scalar field theories with ϕ^k interactions reveals which are the possible upper critical dimensions $d_c(k)$ around which the ε–expansion can be performed. The standard cases ϕ^3, ϕ^4 and ϕ^6 corresponding, respectively, to integer $d_c = 6, 4, 3$ and have been extensively studied [43, 44, 60, 65, 72–77]. However, since in the case of rational upper critical dimensions, the universal leading order (LO) and next–to–leading order (NLO) contributions appear in the perturbative expansion at loop orders higher than one, they have attracted attention only recently [65–68]. In the fpRG formalism, the multi–component beta functionals describing the renormalization group flow of the effective potential V and that of a wave–function renormalization functional Z, can be obtained straightforwardly, in any d_c, from their single–component counterparts. No additional loop computations are needed to obtain the LO beta functions relevant for the analysis of the critical behavior. This important fact, for a long time unnoticed, paves the way for the general analysis of the multi–component universality classes in dimension greater than two.

One of the typical approaches to the classification of universality classes, is to fix the number of components N of the field ϕ, without assuming any symmetry for the models considered. The analysis at fixed $N > 1$ is a non–trivial algebraic problem in $\binom{k+N-1}{k}$ variables (number of marginal couplings), and can be carried

out in a fully analytical way only in the $N = 2$ case (see [70] for the cases $d_c = 6, 4, 3$ and [78] for the new case $d_c = {}^{10}/_{3}$). A higher number of components have been considered under the trace condition in $d_c = 4$ for $N = 3, 4, 6$ [79–83], while the general problem in the absence of this condition becomes rapidly algebraically intractable. A complementary approach, that is the one adopted in this chapter, is a "symmetry perspective" where one explores scalar field theories characterized by a given family of symmetry groups $\mathcal{G}$s, with the appropriate N–comp. representations, and considering the upper critical dimensions implied by the functional form of the corresponding $\mathcal{G}$s–invariant GL Lagrangians.

Among the simplest families that exist for arbitrary N and that have been the main object of study for decades, we recall the $O(N)$ symmetric theories in $d_c = 4$, the Potts S_{N+1} families in $d_c = 6$ and the Cubic$_N$ ones in $d_c = 4$ (see [70] for a recent review and [84] for the state of the art). From a geometrical point of view, these symmetry groups correspond respectively to the $(N-1)$–sphere, the N–simplex and the N–cube. While the first is the simplest among continuous groups, the other two belong to the discrete group family of the regular polytopes and they are the only two which are present in any N–dimension[1]. All the other regular polytopes can be constructed only in two (polygons), three (Platonic solids) and four (hyper–Platonic solids) N–dimensions. In particular, $N = 2$ regular polytopes are the polygons and they are infinitely many. In $N = 3$ we have only three cases up to duality: the Tetrahedron, the dual Octahedron/Cube pair, and the dual Icosahedron/Dodecahedron pair. Finally, in $N = 4$ there are four cases: the 5-cell (hyper–Tetrahedron), the dual 8-cell/16-cell pair (hyper–Cube/hyper–Octahedron), the 24–Cell and the dual 600–cell/120–cell pair (hyper–Icosahedron/hyper–Dodecahedron).

In this chapter, we perform a systematic study of scalar field theories characterized by the symmetry groups of these geometrical objects by using the fpRG formalism. Depending on the N–dimension considered, the related PFTs have order parameter with $N = 2, 3, 4$ components and show up many possible upper critical dimensions; the ones we examined are $d_c = 6, 4, {}^{10}/_{3}, 3, {}^{14}/_{5}, {}^{8}/_{3}, {}^{5}/_{2}, {}^{12}/_{5}$.

The chapter is organized as follows. In Section 2.2 we introduce the Platonic

[1] We refer to N-dimension as the dimension of the geometrical object considered ruling the internal symmetry of our theory, which is not to be confused with the physical space dimension d.

Field Theories and the relative method to construct $\mathcal{G}$–invariant polynomials. We then determine the set of all possible upper critical dimensions d_c the corresponding PFTs entail. In Section 2.3 we explain how to derive the beta functions for the marginal couplings generalizing the single–component beta functionals to their multi–component version. The known cases of $d_c = 6, 4, {}^{10}/_{3}, 3$ are reviewed and we give the new beta functionals for the cases $d_c = {}^{8}/_{3}, {}^{14}/_{5}, {}^{5}/_{2}, {}^{12}/_{5}$ (the last two cases are given in Appendix B.2). In Section 2.4 we report a detailed analysis of all the fixed points and universality classes found (all the analytical details are contained in Appendix B.1). This section should be intended as a *guide map* to Table 2.3 and Table 2.4 which constitute the main results of our work and contain the relevant information regarding the critical behavior of each polytope, namely for any admissible upper critical dimension, the corresponding fixed points, and critical exponents. Concluding remarks and further perspectives are provided in Section 2.5.

2.2 Platonic Field Theories

The $N = 2$ Platonic solids are nothing else than the regular polygons; a n-gonal regular polygon is represented by Schläfli symbol $\{n\}$. $N = 3$ Platonic solids are regular convex polyhedra: their faces are polygons $\{p\}$, q surrounding each vertex and they are denoted by Schläfli symbol $\{p, q\}$. The possible values of p and q can be enumerated and can have any other values than $\{3,3\}$, $\{3,4\}$, $\{4,3\}$, $\{3,5\}$, $\{5,3\}$, which identify the five Platonic solids in three dimensions. Platonic solids in $N = 4$ (4–polytopes) are the analogs of the regular polyhedra in three dimensions and the regular polygons in two dimensions. The corresponding Schläfli symbol $\{p, q, r\}$ identifies a solid with $\{p\}$ faces and $\{q, r\}$ vertex figures. The Schläfli's criterion [63] for the existence of a regular figure corresponding to a symbol $\{p, q, r\}$ selects the only 6 admissible 4–polytopes to be $\{3,3,3\}$, $\{3,3,4\}$, $\{4,3,3\}$, $\{3,4,3\}$, $\{3,3,5\}$ and $\{5,3,3\}$. The symmetry groups $\mathcal{G}$ of the polytopes $\mathcal{P}$ considered are listed in Table 2.1.

In the RG approach to critical phenomena, the critical behavior of PFTs can be described in terms of an N–comp. scalar field ϕ_i which carries an irreducible representation of a given polytope's symmetry group $\mathcal{G}$. Accordingly, the corresponding

	Polytope	Schläfli	$\mathcal{G}$	Molien Series $M(t)$
$N=2$	n-Polygon	$\{n\}$	$\mathbb{D}_n$	$[(1-t^2)(1-t^n)]^{-1}$
$N=3$	Tetrahedron	$\{3,3\}$	S_4	$[(1-t^2)(1-t^3)(1-t^4)]^{-1}$
	Octahedron	$\{3,4\}$	$S_4 \times \mathbb{Z}_2$	$[(1-t^2)(1-t^4)(1-t^6)]^{-1}$
	Cube	$\{4,3\}$	$S_4 \times \mathbb{Z}_2$	
	Icosahedron	$\{3,5\}$	$A_5 \times \mathbb{Z}_2$	$[(1-t^2)(1-t^6)(1-t^{10})]^{-1}$
	Dodecahedron	$\{5,3\}$	$A_5 \times \mathbb{Z}_2$	
$N=4$	5-cell	$\{3,3,3\}$	S_5	$[(1-t^2)(1-t^3)(1-t^4)(1-t^5)]^{-1}$
	16-cell	$\{3,3,4\}$	$(\mathbb{Z}_2)^4 \rtimes S_4$	$[(1-t^2)(1-t^4)(1-t^6)(1-t^8)]^{-1}$
	8-cell	$\{4,3,3\}$	$(\mathbb{Z}_2)^4 \rtimes S_4$	
	24-cell	$\{3,4,3\}$	F_4	$[(1-t^2)(1-t^6)(1-t^8)(1-t^{12})]^{-1}$
	120-cell	$\{3,3,5\}$	H_4	$[(1-t^2)(1-t^{12})(1-t^{20})(1-t^{30})]^{-1}$
	600-cell	$\{5,3,3\}$	H_4	

Table 2.1: Polytopes symmetry groups $\mathcal{G}$ along with the corresponding Molien series. The groups F_4 and H_4 are named according to the Coxeter notation.

field theory will be described by a GL action

$$S = \int \mathrm{d}^d x \left\{ \frac{1}{2} \partial\phi_i \partial\phi_i + V(\phi_i) \right\} , \tag{2.2.1}$$

where the GL potential $V(\phi_i)$ will be eventually expressed as a $\mathcal{G}$–invariant polynomial in the components ϕ_i. Basic $\mathcal{G}$–invariant polynomials of degree k, namely $I^{(k)}(\phi_i)$, can be constructed geometrically taking advantage of the strong symmetry of regular polytopes. To this purpose, let's consider the set of versors $\{\mathrm{e}^\alpha\}$ defining the n vertices of a given polytope $\mathcal{P}$. In terms of these versors, as in chapter 1, we

construct the k^{th} order invariant polynomial as [2]

$$I^{(k\geq 2)}(\phi_i) = \sum_{\alpha=1}^{n} e^{\alpha}_{a_1} \dots e^{\alpha}_{a_k} \phi_{a_1} \dots \phi_{a_k} , \tag{2.2.2}$$

where summation over repeated indices is intended and we have chosen the versors to be normalized to one. In general the explicit forms of the invariant polynomials $I^{(k)}$ depend on the choice of the (cartesian) coordinates which identify the vertices of $\mathcal{P}$, however, polynomials which are transformed into each other by a mere change of reference frame in the space of the ϕ_i components are physically equivalent and should not be distinguished.

Not all the invariants $I^{(k)}$ are independent, as can be inferred from Table 2.2. For each polytope, we identify the basic N independent ones by increasing the polynomial degree k. To this purpose, it is useful to consider the Molien series which, for a given symmetry group $\mathcal{G}$, counts the number of homogeneous polynomials of a given degree k that are invariants w.r.t. $\mathcal{G}$ itself [85]. It is defined as:

$$M(t) = \frac{1}{|\mathcal{G}|} \sum_{g\in\mathcal{G}} \frac{1}{\det[\mathbb{I} - t\, \rho(g)]} , \tag{2.2.3}$$

where ρ is a linear representation of the group $\mathcal{G}$ on the underlying N dimensional vector space. Once the series is expanded, the coefficient of the monomial t^m gives the number of linearly independent homogeneous invariants of degree m; the Molien series furthermore suggests which is the polynomial degree of the basic N independent invariant polynomials, as it can be understood cross–checking Tables 2.1 and 2.2. We always find only one quadratic independent invariant[3] which we call $\rho := I^{(2)}$, while, independently of the order at which they first appear, we call τ the second and, when present, σ and ω respectively the third and the fourth ones (see Table 2.2). Let's call $B_{\mathcal{P}}$ the set given by the basic N independent invariants of a given polytope $\mathcal{P}$. In terms of the elements of $B_{\mathcal{P}}$ we can consider $P^{(k)}(\rho, \tau, \sigma, \omega)$ as the most general homogeneous $\mathcal{G}$–invariant polynomial of degree k; in general it

[2] A regular polytope is easily seen to have a *centre* from which all the vertices are at the same distance and therefore by construction it is always true that $I^{(1)} = 0$. See Eqs (1.2.4).

[3] A single quadratic invariant guarantees that the underlying fundamental representation of $O(N)$ remains irreducible under $\mathcal{G}$ and that we have only one phase transition.

$I^{(k)}$	$\{3\}$	$\{4\}$	$\{5\}$	$\{6\}$	$\{7\}$	$\{8\}$
$I^{(2)}$	$\rho =$ (B.1.1)	$\rho =$ (B.1.6)	$\rho =$ (B.1.12)	$\rho =$ (B.1.17)	$\rho =$ (B.1.23)	$\rho =$ (B.1.28)
$I^{(3)}$	$\tau =$ (B.1.2)	0	0	0	0	0
$I^{(4)}$		$\tau =$ (B.1.7)	$\frac{3\rho^2}{10}$	$\frac{\rho^2}{4}$	$\frac{3\rho^2}{14}$	$\frac{3\rho^2}{16}$
$I^{(5)}$			$\tau =$ (B.1.13)	0	0	0
$I^{(6)}$				$\tau =$ (B.1.18)	$\frac{5\rho^3}{98}$	$\frac{5\rho^3}{128}$
$I^{(7)}$					$\tau =$ (B.1.24)	0
$I^{(8)}$						$\tau =$ (B.1.29)
$I^{(k)}$	$\{3,3\}$	$\{3,4\}$	$\{3,5\}$	$\{3,3,3\}$	$\{3,3,4\}$	$\{3,4,3\}$
$I^{(2)}$	$\rho =$ (B.1.34)	$\rho =$ (B.1.44)	$\rho =$ (B.1.56)	$\rho =$ (B.1.67)	$\rho =$ (B.1.82)	$\rho =$ (B.1.103)
$I^{(3)}$	$\tau =$ (B.1.35)	0	0	$\tau =$ (B.1.68)	0	0
$I^{(4)}$	$\sigma =$ (B.1.36)	$\tau =$ (B.1.45)	$\frac{3\rho^2}{20}$	$\sigma =$ (B.1.69)	$\tau =$ (B.1.83)	$\frac{\rho^2}{12}$
$I^{(5)}$		0	0	$\omega =$ (B.1.70)	0	0
$I^{(6)}$		$\sigma =$ (B.1.46)	$\tau =$ (B.1.57)		$\sigma =$ (B.1.84)	$\tau =$ (B.1.104)
$I^{(7)}$			0		0	0
$I^{(8)}$			$-\frac{7\rho^4}{960}+\frac{7\rho\tau}{15}$		$\omega =$ (B.1.85)	$\sigma =$ (B.1.105)
$I^{(9)}$			0			0
$I^{(10)}$			$\sigma =$ (B.1.58)			$\frac{7\rho^5}{41472}-\frac{7\rho^2\tau}{144}+\frac{3\rho\sigma}{8}$
$I^{(11)}$						0
$I^{(12)}$						$\omega =$ (B.1.106)

Table 2.2: For each polytope $\mathcal{P}$, we give the basic $\mathcal{G}$-invariant polynomials $I^{(k)}$, expressed in terms of the elements of the relative $B_{\mathcal{P}}$, making reference to the corresponding equation in the main text. The Table makes clear the order at which the independent invariants appear. For any case related by duality, we give only the ones treated in the text and for simplicity we omit the 600-cell case.

can be expressed as

$$P^{(k)}(\rho,\tau,\sigma,\omega) = \sum_{\mu=1}^{r} g_\mu \, M_\mu^{(k)}(\rho,\tau,\sigma,\omega)\,, \tag{2.2.4}$$

where $M_\mu^{(k)}(\rho,\tau,\sigma,\omega)$ are monomials given by powers and products of elements of

$B_{\mathcal{P}}$ such that their overall polynomial degree is k, g_μ are some real coefficients [82] and the number r of homogeneous polynomials of degree k that are invariant under $\mathcal{G}_{\mathcal{P}}$, is provided by the Molien series as explained above. In the framework of the ε–expansion we are going to renormalize PFTs in $d = d_c - \varepsilon$, where the upper critical dimension d_c is uniquely determined by the degree of the homogeneous polynomials $P^{(k)}$. In fact, we can express the GL $\mathcal{G}$–invariant potential $V(\phi_i) \equiv U(\rho, \tau, \sigma, \omega)$ simply as

$$U(\rho, \tau, \sigma, \omega) = \sum_{k=2} \frac{1}{k!} P^{(k)}(\rho, \tau, \sigma, \omega)\,, \tag{2.2.5}$$

and we understand that the coefficients g_μ play the role of coupling constants. By imposing the GL potential U to be marginal (remember that ϕ has dimensions $\frac{d-2}{2}$ as it can be gleaned out inspecting the kinetic part of the action (2.2.1)) we obtain the upper critical dimensions as

$$d_c(k) = \frac{2k}{k-2}\,. \tag{2.2.6}$$

In this chapter, for any polytope $\mathcal{P}$, we considered all the possible upper critical dimensions d_c corresponding to the allowed $P^{(k \leq k_{\max})}$, where $k_{\max}$ is the degree of the highest order polynomial in $B_{\mathcal{P}}$. [4] We exclude from the analysis, those d_c related to polynomials $P^{(k)}$ which are expressed as powers of ρ only, since they will simply describe the corresponding $O(N)$ symmetric theory.

Let us make all this more concrete and give an example for the Square polygon $\{4\}$. First we construct the basic $\mathbb{D}_4$–symmetric invariant polynomials $I^{(k)}$. To this purpose, we fix the versors $\{\mathrm{e}^\alpha\}$ choosing the four vertices of the Square to be the permutations of the coordinates $(\pm 1/\sqrt{2}, \pm 1/\sqrt{2})$. We then proceed performing the sum in Eq. (2.2.2) which, in this case, extends up to $N = 2$ field components and to $n = 4$ basic vertices. Starting from $k = 2$ we find

$$I^{(2)} = 2\left(\phi_1^2 + \phi_2^2\right)\,, \tag{2.2.7}$$

$$I^{(3)} = 0\,, \tag{2.2.8}$$

$$I^{(4)} = \phi_1^4 + 6\phi_2^2\phi_1^2 + \phi_2^4\,, \tag{2.2.9}$$

and therefore the two elements of $B_{\{4\}}$ are $\rho_{\{4\}} \equiv I^{(2)}$ and $\tau_{\{4\}} \equiv I^{(4)}$. Since the

[4] We identify $\mathcal{P}$ by its Schläfli symbol, see Table 2.1.

Square interaction term is represented by the invariant polynomial $\tau_{\{4\}}$ of degree $k = 4$, the only interesting upper critical dimension in this case is $d_c = 4$. The Molien Series for the Square group $\mathbb{D}_4$ is given by

$$M(t) = [(1-t^2)(1-t^4)]^{-1} = 1 + t^2 + 2t^4 + 2t^6 + O(t^8)\,, \tag{2.2.10}$$

from which we understand that the $r = 2$ monomials of degree 4 are $M_1^{(4)} = \rho^2$ and $M_2^{(4)} = \tau$, so that the corresponding marginal potential $U(\rho, \tau)$ is finally given by

$$U(\rho,\tau) = \frac{1}{4!}P_4(\rho,\tau) = \frac{1}{4!}\left(X\,\rho_{\{4\}}^2 + Y\,\tau_{\{4\}}\right)\,, \tag{2.2.11}$$

where we named the coupling constants $g_1 = X$ and $g_2 = Y$.

As a further example, consider the case of the dual pair $\{3,4\}$, $\{4,3\}$ namely the Octahedron and the Cube. We fix the versors $\{e^\alpha\}$ choosing the eight Cube vertices as the permutations of the coordinates $\sqrt{4/3}(\pm 1, \pm 1, \pm 1)$ so that, once we perform the sum in Eq. (2.2.2) which now extends up to $N = 3$ and $n = 8$, we find that the three elements of $B_{\{4,3\}}$ in the Cube basis are

$$\rho_{\{4,3\}} \equiv I^{(2)} = \frac{8}{3}\left(\phi_1^2 + \phi_2^2 + \phi_3^2\right)\,, \tag{2.2.12}$$

$$\tau_{\{4,3\}} \equiv I^{(4)} = \frac{8}{9}\left(\phi_1^4 + 6\left(\phi_2^2 + \phi_3^2\right)\phi_1^2 + \phi_2^4 + \phi_3^4 + 6\phi_2^2\phi_3^2\right)\,, \tag{2.2.13}$$

$$\begin{aligned}\sigma_{\{4,3\}} \equiv I^{(6)} = \frac{8}{27}\Big(&\phi_1^6 + 15\left(\phi_2^2 + \phi_3^2\right)\phi_1^4 + 15\left(\phi_2^4 + 6\phi_3^2\phi_2^2 + \phi_3^4\right)\phi_1^2 + \phi_2^6 \\ &+\phi_3^6 + 15\phi_2^2\phi_3^4 + 15\phi_2^4\phi_3^2\Big)\,.\end{aligned} \tag{2.2.14}$$

In the Octahedron basis the independent invariants are given in Appendix B.1. The duality between the two Platonic solids is expressed as a map between the invariants (ρ, τ, σ) in the two representations which, in the case of the Octahedron/Cube reads

$$\begin{aligned}\rho_{\{4,3\}} &= \frac{4}{3}\,\rho_{\{3,4\}}\,,\\ \tau_{\{4,3\}} &= \frac{2}{3}\,\rho_{\{3,4\}}^2 - \frac{8}{9}\,\tau_{\{3,4\}}^2\,,\\ \sigma_{\{4,3\}} &= \frac{5}{6}\,\rho_{\{3,4\}}^3 - \frac{20}{9}\,\rho_{\{3,4\}}\tau_{\{3,4\}} + \frac{64}{27}\,\sigma_{\{3,4\}}\,.\end{aligned} \tag{2.2.15}$$

The map between invariants translates in a smooth map between couplings and thus their RG properties are trivially the same.

Due to their interest in statistical physics [86–88], we notice, as a final remark, that $\mathbb{Z}_n$–symmetric models may be described, in the continuum limit, in terms of a complex order parameter $(\phi, \bar{\phi})$ and mapped into a Lagrangian whose interaction term in general can be written as $(\lambda\phi^n + \bar{\lambda}\bar{\phi}^n)$. Imposing the reality of this interaction, formally amounts at enlarging the $\mathbb{Z}_n$ group to the corresponding dihedral one $\mathbb{D}_n$ and the $\mathbb{Z}_n$ invariants are nothing but the corresponding polygon ones. As an example consider the $\mathbb{Z}_5$ theory described by $(\lambda\phi^5 + \bar{\lambda}\bar{\phi}^5)$; requiring $\lambda = \bar{\lambda}$ and changing representation to $\phi = \phi_1 + i\,\phi_2$, gives exactly the $\mathbb{D}_5$ Pentagon invariant considered in Eq. (B.1.13).

2.3 Multicomponent beta functionals

In order to study the RG flow of PFTs, as presented in the previous section, we adopt the fpRG formalism [66, 70]. In particular we use minimal subtraction scheme ($\overline{\text{MS}}$) in $d = d_c - \varepsilon$ where, for each PFT, the upper critical dimensions d_c are uniquely identified by Eq. (2.2.6) and specify the dimensions where to expect non–trivial universality classes. For each polytope the upper critical dimensions considered are listed in Table 2.3. The beta functions of the couplings appearing in the marginal potential $V(\phi)$ can be extracted from the beta functional β_V while the flow of β_Z fixes the anomalous dimension η, where by $Z(\phi)$ we denote a field–dependent wave–function (we refer to Ref. [66] and to Appendix B.3 for more details).

For even potentials, namely when $k = 2m$ with integer $m > 1$, the upper critical dimensions d_c in Eq. (2.2.6) read $d_c = \frac{2m}{m-1}$ and the corresponding single component LO and NLO contributions are known in general [65]. LO beta functionals in the even case have been given recently for general N in [76]. While for $d_c = 4$ and $d_c = 3$ the NLO corrections are well known[5] [70], there are no general expressions for the NLO multi–component beta functionals for arbitrary m. But it is here that the functional constraints come to help. In fact, by analyzing the form of the $N = 1$ beta functionals given in [65], one realizes that there is only one way to enhance them to the multicomponent case.

[5] In $d_c = 4$ higher loop corrections are also known, but they are not universal and we do not consider them in the present paper.

For example let's consider the $d_c = 4$ case. The knowledge of the single component beta functionals $\beta_V = {}^1/_2(V^{(2)})^2 - {}^1/_2 V^{(2)}(V^{(3)})^2$ and $\beta_Z = -{}^1/_6(V^{(4)})^2$, leads directly to their multi–component version since there is only way to "promote" the monomials to the $N > 1$ case: $(V^{(2)})^2 \to V_{a_1a_2}V_{a_1a_2}$ and $V^{(2)}(V^{(3)})^2 \to V_{a_1a_2}V_{a_1a_3a_4}V_{a_2a_3a_4}$; similarly, taking care of the uncontracted indexes for β_Z, $(V^{(4)})^2 \to V_{a_1a_2a_3a_4}V_{a_1a_2a_3a_4}$. We finally obtain

$$d_c = 4$$

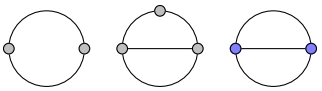

$$\begin{aligned} \beta_V &= \frac{1}{2}V_{a_1a_2}V_{a_1a_2} - \frac{1}{2}V_{a_1a_2}V_{a_1a_3a_4}V_{a_2a_3a_4} \\ (\beta_Z)_{a_1a_2} &= -\frac{1}{6}V_{a_1a_3a_4a_5}V_{a_2a_3a_4a_5}\,, \end{aligned} \tag{2.3.1}$$

where we reported the corresponding perturbative diagrams using hereafter, as a color code, grey for β_V's and blue for β_Z's. Similarly, in the $d_c = 3$ case one can avoid performing a direct multi–component computation simply generalizing the $\beta_V = \frac{1}{3}(V^{(3)})^2 + \frac{1}{6}V^{(2)}(V^{(5)})^2 - \frac{4}{3}V^{(3)}V^{(4)}V^{(5)} - \frac{\pi^2}{12}(V^{(4)})^3$ as well as $\beta_Z = -\frac{1}{45}(V^{(6)})^2$ to the multi–component cases, namely

$$d_c = 3$$

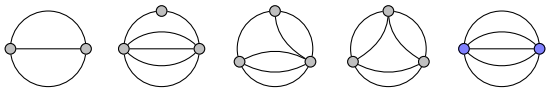

$$\begin{aligned} \beta_V &= \frac{1}{3}V_{a_1a_2a_3}V_{a_1a_2a_3} + \frac{1}{6}V_{a_1a_2}V_{a_1a_3a_4a_5a_6}V_{a_2a_3a_4a_5a_6} \\ &\quad - \frac{4}{3}V_{a_1a_2a_3}V_{a_3a_4a_5a_6}V_{a_1a_2a_4a_5a_6} - \frac{\pi^2}{12}V_{a_1a_2a_3a_4}V_{a_3a_4a_5a_6}V_{a_1a_2a_5a_6} \\ (\beta_Z)_{a_1a_2} &= -\frac{1}{45}V_{a_1a_3a_4a_5a_6a_7}V_{a_2a_3a_4a_5a_6a_7}\,. \end{aligned} \tag{2.3.2}$$

We are now in the position to infer the beta functionals for the even potential's upper critical dimensions we are interested in, namely $d_c = {}^8/_3, {}^5/_2, {}^{12}/_5$, generalizing

the single component ones given in [65]. The result for $d_c = 8/3$ is given in Eq. (2.3.3), while the cases $d_c = 5/2$ and $d_c = 12/5$ are given respectively in Eq. (B.2.1) and Eq. (B.2.2).

$$d_c = \frac{8}{3}$$

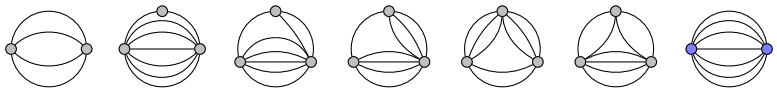

$$\begin{aligned}
\beta_V = & \frac{1}{8} V_{a_1a_2a_3a_4} V_{a_1a_2a_3a_4} + \frac{1}{160} V_{a_1a_2} V_{a_1a_3a_4a_5a_6a_7a_8} V_{a_2a_3a_4a_5a_6a_7a_8} \\
& + \frac{9}{80} V_{a_1a_2a_3} V_{a_3a_4a_5a_6a_7a_8} V_{a_1a_2a_4a_5a_6a_7a_8} \\
& - \frac{3}{8} V_{a_1a_2a_3a_4} V_{a_2a_3a_4a_5a_6a_7a_8} V_{a_1a_5a_6a_7a_8} \\
& - \frac{\Gamma(1/3)^3}{24} V_{a_1a_2a_3a_4a_5a_6} V_{a_1a_2a_3a_7a_8} V_{a_4a_5a_6a_7a_8} \\
& + \frac{3}{64} \left[\sqrt{3}\pi - 3(2 + \log 3) \right] V_{a_1a_2a_3a_4} V_{a_1a_2a_5a_6a_7a_8} V_{a_3a_4a_5a_6a_7a_8} \\
(\beta_Z)_{a_1a_2} = & -\frac{1}{1120} V_{a_1a_3a_4a_5a_6a_7a_8a_9} V_{a_2a_3a_4a_5a_6a_7a_8a_9} \, .
\end{aligned} \tag{2.3.3}$$

We underline two interesting aspects about these expressions: First, as it can be noted from the diagrams above, they are of relatively high–loop order since the LO contribution β_V arises from a $(m-1)$–loop computation while the NLO functionals β_V and β_Z appear at $2(m-1)$–loops; second all the coefficients reported are universal, i.e. independent of the specific RG scheme adopted [89]. Even if it is not difficult to write down the beta functionals for general m and N, their expressions become rapidly cumbersome and we won't report them here. In any case, we have checked that the general LO contributions agree with those recently derived by CFT methods in [76] generalizing to the multicomponent case the results of [62].

In the odd case where $k = 2m+1$ with integer $m \geq 1$ and the upper critical dimensions read $d_c = 2 + \frac{4}{2m-1}$, we consider only the leading contributions for two reasons: First, as reported in [66] we have a general formula for the beta functionals only at LO; second, the enhancement from the single to the multicomponent case works only at LO for even theories, since the presence of higher powers of $V^{(2)}$

in the NLO beta functionals makes the $N = 1$ case degenerate with respect to the multi–component case.

The $d_c = 6$ case is well known and the NLO contributions can be found in [43, 70]. We report here the LO contributions, which are those that can be inferred from the single–component case

$$
\begin{aligned}
&d_c = 6 \\
&\text{ 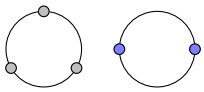 } \\
&\beta_V = -\frac{1}{6} V_{a_1 a_2} V_{a_2 a_3} V_{a_3 a_1} \\
&(\beta_Z)_{a_1 a_2} = -\frac{1}{6} V_{a_1 a_3 a_4} V_{a_2 a_3 a_4} \,.
\end{aligned}
\tag{2.3.4}
$$

The $d_c = 10/3$ single component case has been reported recently in [67]. The generalization to its multi–component version is straightforward and reads[6]

$$
\begin{aligned}
&d_c = \frac{10}{3} \\
&\text{ 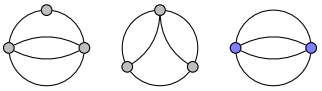 } \\
&\beta_V = \frac{3}{4} V_{a_1 a_2} V_{a_1 a_3 a_4 a_5} V_{a_2 a_3 a_4 a_5} - \frac{27}{8} V_{a_1 a_2 a_3} V_{a_1 a_4 a_5} V_{a_2 a_3 a_4 a_5} \\
&(\beta_Z)_{a_1 a_2} = -\frac{3}{40} V_{a_1 a_3 a_4 a_5 a_6} V_{a_2 a_3 a_4 a_5 a_6} \,.
\end{aligned}
\tag{2.3.5}
$$

Finally we analysed the $m = 3$ case obtaining, as a new result, the beta functionals referring to the upper critical dimension $d_c = 14/5$; the result is as follows

[6] We use a different normalization with respect to [67, 78]

$$d_c = \frac{14}{5}$$

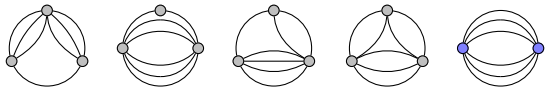

$$\begin{aligned}
\beta_V =& -\frac{125}{72} V_{a_1a_2a_3a_4a_5a_6} V_{a_1a_2a_3a_7} V_{a_4a_5a_6a_7} + \frac{5}{144} V_{a_1a_2} V_{a_1a_3a_4a_5a_6a_7} V_{a_2a_3a_4a_5a_6a_7} \\
&+ \frac{125}{144} V_{a_1a_2a_3} V_{a_1a_4a_5a_6a_7} V_{a_2a_3a_4a_5a_6a_7} \\
&- \frac{125(\sqrt{5}-1)\Gamma(3/10)\Gamma(6/5)}{96\, 2^{2/5}\sqrt{\pi}} V_{a_1a_2a_3a_4} V_{a_1a_2a_5a_6a_7} V_{a_3a_4a_5a_6a_7} \\
(\beta_Z)_{a_1a_2} =& -\frac{5}{1008} V_{a_1a_3a_4a_5a_6a_7a_8} V_{a_2a_3a_4a_5a_6a_7a_8} \,.
\end{aligned} \tag{2.3.6}$$

As an example we show how to extract the beta functions in the case of the Square polygon $\{4\}$. Since the upper critical dimension in this case is $d_c = 4$, we then refer to the beta functional in Eq. (2.3.1) to obtain the couplings' beta functions. To this purpose, consider the Square potential, as expressed in Eq. (2.2.11), in terms of which we can define straightforwardly

$$\beta_V = \frac{1}{4!}\left(\beta_X\, \rho^2_{\{4\}} + \beta_Y\, \tau_{\{4\}}\right) . \tag{2.3.7}$$

We then proceed computing the r.h.s of Eq. (2.3.1), which reads [7]

$$\begin{aligned}
\frac{1}{2} V_{a_1a_2} V_{a_1a_2} - \frac{1}{2} V_{a_1a_2} V_{a_1a_3a_4} V_{a_2a_3a_4} =& -\frac{1}{54}\rho^2\, X\left(256X^2 + 6X(24Y-5) + 9Y(2Y-1)\right) \\
&- \frac{1}{36}\tau\, Y(8X+3Y)(32X+12Y-3) \,.
\end{aligned} \tag{2.3.8}$$

One then inserts (2.3.7) and (2.3.8), respectively, on the l.h.s. and r.h.s. of Eq. (2.3.1) and equates equal powers of the invariants on both sides to read off the corresponding dimension–full beta functions. Switching to dimensionless variables is straightforward [8] and the resulting system of beta functions is given in Eqs. (B.1.9), (B.1.10).

[7] Note that functional derivatives are first taken w.r.t. the fields $\{\phi_i\}$ and then the result is re-expressed in the natural basis of the invariants $\{\rho, \tau\}$.

[8] With abuse of notation we use the same symbols for dimensionless and dimensional couplings.

2.4 Universality Classes

The result of our analysis is reported in Table 2.3, which together with Table 2.4, constitute the main results of this work. This Section should be intended as the guide to these two Tables which the reader should have at hand. Table 2.3 is basically composed of three columns: the first lists the polytopes; the second one reports the upper critical dimensions examined, which we remember are those where the relative PFT homogeneous invariant polynomials $P^{(k)}$ (interactions) are marginal (see Section 2.2); the third one lists all the real FPs found, i.e. all the real zeros of the corresponding system of beta functions, whose solutions are labeled with the name of the `universality class` to which they correspond. Table 2.4 instead reports the critical exponents η and ν for all those universality classes for which we were able to compute both of them.

We start our analysis considering the polygons, namely the $N = 2$ case. Since there are an infinite number of polygons, we limited our analysis up to the Octagon, which is enough to show the general critical pattern emerging from the two families of *even* and *odd* n-gons. The Triangle in $d_c = 6$ is the well known $\texttt{Potts}_3$ [17, 18, 40, 41, 43] which has a real FP [but note the unusual fact: $\nu < \nu_{\rm MF} = 1/2$ as in Eq.(1.4.1) for $n = 2$]. It is well known that $\texttt{Potts}_3$ is not present in $d = 3$ [90], and this is an indication that even near $d = 6$ it doesn't have a clear status (one can construct an argument using the NLO beta functions to claim the same [18, 41]). The Square FPs in $d_c = 4$ are the `O(2)` and two copies of `Ising`. Particular to the $N = 2$ case is a mapping in terms of which it is true that $\texttt{Cubic}_2\texttt{=Ising}$ [70, 84] and therefore the cubic FP is not present in this case. Cubic FPs emerge instead in the $N = 3$ and $N = 4$ cases as we shall see below. The first surprise among polygons is the `Pentagon` universality class. The upper critical dimension in this case is $d_c = 10/3$ and therefore it is a candidate to give a non–trivial critical behavior in $d = 3$. The corresponding critical exponents are reported in Table 2.4. It is reassuring to see that $\nu > \nu_{\rm MF}$ contrary to what found in the single field case [67] for this upper critical dimension. Note also that the anomalous dimension is quite large in $d = 3$ where it assumes the value $\eta = 1/5$; it is natural therefore to consider this universality class in three dimensions where the ε-expansion may have well behaved convergence properties since, we just have to set $\varepsilon = 1/3$. The next polygon is the Hexagon which is analysed in $d_c = 3$. In this case only a FP which identifies the tri-critical version of

the O(2), namely the Tri-O(2), is present. The corresponding anomalous dimension is $\eta = \frac{1}{392}\varepsilon^2$. The Heptagon case in $d_c = 14/5$ shows a behavior analogous to the Pentagon, namely there is real FP representative of this universality class with 'well behaved' critical exponents given in Table 2.4. Even though this universality class is new, it is less interesting w.r.t. the Pentagon one since it does not exist in three dimensions and possibly exists only in $d = 2$. Finally we analysed the Octagon in $d_c = 8/3$ which exhibits a critical behavior analogous to the Hexagon case. In particular we find only the tetra-critical version of the O(2) FP, namely only the Tetra-O(2), with anomalous dimension given by $\eta = \frac{9}{59858}\varepsilon^2$. We expect the *even* family of n–gons with $n > 8$ to reproduce the series of multi–critical O(2) FPs[9]. Even though, within the formalism presented in Section 2.3 and in Appendix B.2, we could consider polygons $\{n\}$ with $n > 8$ being *even* or *odd* generalising to the multicomponent case the beta functionals of [66, 70], we will not pursue this analysis here. It is anyway of interest to understand if the appearing of a non-trivial FP as for the Pentagon and the Heptagon is a general feature of all the *odd* $\{n\}$ theories or if there is a critical number of edges after which the fluctuations drive the FP to the corresponding O(2) universality class.

We now move to the $N = 3$ case, where we encounter the famous five Platonic solids. We first analyzed the Tetrahedron, which belongs to the family of simplexes; in this case, the possible upper critical dimensions are $d_c = 6$ and $d_c = 4$. The first gives rise to no real FP, mirroring the fact that no real $\texttt{Potts}_4$ FP is known in $d \geq 3$ [90]; in $d_c = 4$, due to the fact that for $N = 3$ the tetrahedral group is isomorphic to the cubic one ($\mathcal{G} = S_4 \times \mathbb{Z}_2$, see Table 2.1), the tetrahedral FPs coincide with the cubic ones [17, 70]. The three universality classes that emerge are therefore $3\times$Ising, O(3) and $\texttt{Cubic}_3$, a case that has been extensively studied [84, 91–94]. We considered the Cube/Octahedron pair in the Octahedron basis where the invariant polynomials assume a simpler form, see Appendix B.1. As explained above, due to the group isomorphism between the Tetrahedron and the Cube, the universal content in $d_c = 4$ coincides. The second allowed upper critical dimension is $d_c = 3$ where we find the tri-critical version of the previous FPs. In particular the ϕ^6–$\texttt{Cubic}_3$ FP is new and should be intended as a ϕ^6–theory with cubic symmetry[10]. Its critical exponents are

[9] In particular, an even n–gon is characterized by the $n/2$-th multi–critical O(2) FP.

[10] In order to determine the exact degree of multi-criticality one has to analyze the corresponding

given in Table 2.4. While it is clear [70, 87, 95] that no icosahedral FPs can be found in $d = 4 - \varepsilon$ since the first invariant polynomial is of degree 6, our analysis revealed that as we study the icosahedral theory in $d_c = 5/2$ by means of the marginal potential in Eq. (B.1.64), there emerge two icosahedral FPs for which we were able to compute the anomalous dimensions

$$\eta_1 = 7.95024 \times 10^{-6}\, \epsilon^2\,, \tag{2.4.1}$$

$$\eta_2 = 8.93795 \times 10^{-6}\, \epsilon^2\,. \tag{2.4.2}$$

Apart from the new icosahedral FPs, we find the `Tri-O(3)` FP in $d_c = 3$, the `Tetra-O(3)` FP in $d_c = 8/3$ and finally the `Penta-O(3)` FP in $d_c = 5/2$, the last two being new to our knowledge. The critical exponents are reported in Table 2.4 while for the `Penta-O(3)` FP we computed only the anomalous dimension $\eta = \frac{231}{25694761}\epsilon^2$, due to the high complexity of the NLO terms. We have analyzed the Icosahedron/Dodecahedron pair in the icosahedral basis; details on the invariant polynomials and on the duality map can be found in Appendix B.1.

Finally we considered the 4–polytopes, namely the $N = 4$ hyper–Platonic solids. The PFT associated to the 5-cell (hyper-Simplex) entails upper critical dimensions $d_c = 6, 4, 10/3$. As expected, to the 5-cell in $d_c = 6$ corresponds no real FP [90]. In $d_c = 4$ instead, apart from the `O(4)` symmetric FP, the restricted Potts case gives rise to a $\texttt{Quartic-Potts}_5$ FP [70], while the new information is that there is no real FP in $d_c = 10/3$. We explored 8–cell/16–cell symmetry in the basis of the 16–cell (hyper-Octahedron), where invariant polynomials are much simpler; details on the duality map are given in Appendix B.1. The analogy is perfect with the $N = 3$ cubic case apart from the fact that no $\texttt{Cubic}_4$ FP is present in $d_c = 4$ but only $4\times\texttt{Ising}$ and `O(4)` universality classes emerge [70]. In $d_c = 3$ the FPs correspond to the ϕ^6–$\texttt{Cubic}_4$ and to the tri–critical version of $4\times\texttt{Ising}$ and `O(4)` while in $d_c = 8/3$ they simply are the ϕ^8-$\texttt{Cubic}_4$ and the tetra–critical version of $4\times\texttt{Ising}$ and `O(4)`. All the new critical exponents are reported in the Table 2.4. The 24–cell symmetry is peculiar to the $N = 4$ case. In $d_c = 3$ and $d_c = 8/3$ we respectively find only the `Tri-O(4)` and the `Tetra-O(4)` FPs. Beside the `Penta-O(4)` with anomalous dimensions given by $\eta = \frac{1}{83544}\varepsilon^2$, in $d_c = 5/2$ we find two 24–cell FPs characterized by the same anomalous

stability matrix.

dimension[11]

$$\eta_{1,2} = 1.15365 \cdot 10^{-5}\, \varepsilon^2 \,. \tag{2.4.3}$$

In $d_c = {}^{12}/_{5}$ instead, there emerge two distinct 24-cell FPs with anomalous dimensions given by

$$\eta_1 = 3.77524 \cdot 10^{-7}\, \varepsilon^2 \,,$$
$$\eta_2 = 0.00171903\, \varepsilon^2 \,,$$

along with the `Hexa-O(4)` FP, whose anomalous dimensions reads $\eta = \frac{25}{53014528}\varepsilon^2$. Any of these universality classes can be present only in two dimensions. The analysis of the 600–cell/120–cell symmetry starts to be very complicated even if straightforward. We considered this dual pair of polytopes at the upper critical dimensions $d_c = {}^{12}/_{5}, {}^{20}/_{9}, {}^{15}/_{7}$, but for simplicity we omit to report the corresponding invariants and beta functions though easily accessible along the line of reasoning of Sections 2.2 and 2.3. The analysis of the FPs for this dual pair revealed no other real FP except for the multi–critical `O(4)` FPs (see Table 2.3)[12]. This result is somehow expected since, due to the high number of points on the unit 4–sphere it can be considered very close to the `O(4)` model. We notice here that we could have analyzed the 600–cell/120 pair in all the intermediate accessible upper critical dimensions, but since the analysis at the highest polynomial of degree $k_{\max} = 30$ revealed no 600–cell FP, we expect the aforementioned d_c to correspond only to the $O(4)$ multi–critical FPs.

It is natural to consider extensions of the present analysis based on the regular N–polytopes for general $N \geq 5$. However, we have that apart from N–simplexes (hyper-Tetrahedra) studied in [78], just hyper–Cubes (hyper–Octahedra) are present and both their critical content is, on the other hand, already known.

[11] These two FPs can be related by an $O(4)$ field redefinition.

[12] In Table 2.3 we called `Triaconta--O(4)` the multi–critical `O(4)` FP associated to a ϕ^{30} theory.

	Polytope	d_c	Fixed Points
$N=2$	 Triangle	6	$\texttt{Potts}_3$
	 Square	4	$2\times\texttt{Ising}$, $\texttt{O(2)}$
	 Pentagon	$10/3$	$\texttt{Pentagon}$
	 Hexagon	3	$\texttt{Tri-O(2)}$
	 Heptagon	$14/5$	$\texttt{Heptagon}$
	 Octagon	$8/3$	$\texttt{Tetra-O(2)}$
	⋮ ⋮	⋮	⋮
$N=3$	 Tetrahedron	6	No real FP
		4	$3\times\texttt{Ising}$, $\texttt{O(3)}$, $\texttt{Cubic}_3$
	 Octahedron	4	$3\times\texttt{Ising}$, $\texttt{O(3)}$, $\texttt{Cubic}_3$
		3	$3\times\texttt{Tri-Ising}$, $\texttt{Tri-O(3)}$, ϕ^6-$\texttt{Cubic}_3$
		3	$\texttt{Tri-O(3)}$
	 Icosahedron	$8/3$	$\texttt{Tetra-O(3)}$
		$5/2$	$\texttt{Penta-O(3)}$, $\texttt{Ico}_{1\leq i\leq 2}$
$N=4$		6	No real FP
	 5-cell	4	$\texttt{O(4)}$, $\texttt{Quartic-Potts}_5$
		$10/3$	No real FP
		4	$4\times\texttt{Ising}$, $\texttt{O(4)}$
	 16-cell	3	$4\times\texttt{Tri-Ising}$, $\texttt{Tri-O(4)}$, ϕ^6-$\texttt{Cubic}_4$
		$8/3$	$4\times\texttt{Tetra-Ising}$, $\texttt{Tetra-O(4)}$, ϕ^8-$\texttt{Cubic}_4$
		3	$\texttt{Tri-O(4)}$
	 24-cell	$8/3$	$\texttt{Tetra-O(4)}$
		$5/2$	$\texttt{Penta-O(4)}$, $\texttt{24-cell}_1$
		$12/5$	$\texttt{Hexa-O(4)}$, $\texttt{24-cell}_{1\leq i\leq 2}$
		$12/5$	$\texttt{Hexa-O(4)}$
		⋮	⋮
	 600-cell	$20/9$	$\texttt{Deca-O(4)}$
		⋮	⋮
		$15/7$	$\texttt{Triaconta-O(4)}$

Table 2.3: N–dimensional regular polytopes along with the upper critical dimensions d_c around which the corresponding PFT can be studied in the ε-expansion. For each polytope and d_c we report the real FPs found in our analysis.

	Universality Class	d_c	η	ν
$N=1$	Ising	4	$\frac{1}{54}\varepsilon^2$	$\frac{1}{2}+\frac{1}{12}\varepsilon+\frac{7}{162}\varepsilon^2$
	Tri-Ising	3	$\frac{1}{500}\varepsilon^2$	$\frac{1}{2}+\frac{1}{125}\varepsilon^2$
	Tetra-Ising	$\frac{8}{3}$	$\frac{9}{85750}\varepsilon^2$	$\frac{1}{2}+\frac{27}{68600}\varepsilon^2$
$N=2$	Potts_3	6	$\frac{1}{3}\varepsilon$	$\frac{1}{2}-\frac{5}{12}\varepsilon$
	O(2)	4	$\frac{1}{50}\varepsilon^2$	$\frac{1}{2}+\frac{1}{10}\varepsilon+\frac{11}{200}\varepsilon^2$
	Pentagon	$\frac{10}{3}$	$\frac{3}{5}\varepsilon$	$\frac{1}{2}+\frac{3}{20}\varepsilon$
	Tri-O(2)	3	$\frac{1}{392}\varepsilon^2$	$\frac{1}{2}+\frac{1}{98}\varepsilon^2$
	Heptagon	$\frac{14}{5}$	$\frac{10}{7}\varepsilon$	$\frac{1}{2}+\frac{5}{14}\varepsilon$
	Tetra-O(2)	$\frac{8}{3}$	$\frac{9}{59858}\varepsilon^2$	$\frac{1}{2}+\frac{135}{239432}\varepsilon^2$
$N=3$	O(3)	4	$\frac{5}{242}\varepsilon^2$	$\frac{1}{2}+\frac{5}{44}\varepsilon+\frac{345}{5324}\varepsilon^2$
	Cubic_3	4	$\frac{5}{243}\varepsilon^2$	$\frac{1}{2}+\frac{1}{9}\varepsilon+\frac{599}{8748}\varepsilon^2$
	Tri-O(3)	3	$\frac{35}{11532}\varepsilon^2$	$\frac{1}{2}+\frac{35}{2883}\varepsilon^2$
	ϕ^6-Cubic_3	3	$0.00261529\,\varepsilon^2$	$\frac{1}{2}+0.0104612\,\varepsilon^2$
	Tetra-O(3)	$\frac{8}{3}$	$\frac{945}{4798802}\varepsilon^2$	$\frac{1}{2}+\frac{14175}{19195208}\varepsilon^2$
$N=4$	O(4)	4	$\frac{1}{48}\varepsilon^2$	$\frac{1}{2}+\frac{1}{8}\varepsilon+\frac{7}{96}\varepsilon^2$
	Quartic-Potts_5	4	$\frac{55}{2646}\varepsilon^2$	$\frac{1}{2}+\frac{5}{42}\varepsilon+\frac{22465}{222264}\varepsilon^2$
	Tri-O(4)	3	$\frac{1}{289}\varepsilon^2$	$\frac{1}{2}+\frac{4}{289}\varepsilon^2$
	ϕ^6-Cubic_4	3	$0.00322216\,\varepsilon^2$	$\frac{1}{2}+0.0128886\,\varepsilon^2$
	Tetra-O(4)	$\frac{8}{3}$	$\frac{9}{36980}\varepsilon^2$	$\frac{1}{2}+\frac{27}{29584}\varepsilon^2$
	ϕ^8-Cubic_4	$\frac{8}{3}$	$0.000196765\,\varepsilon^2$	$\frac{1}{2}+0.000737867\,\varepsilon^2$

Table 2.4: Critical exponents η and ν for the universality classes with $d_c = 6, 4, {}^{10}/_3, 3, {}^{14}/_5, {}^{8}/_3$ (for which we know both of them) ordered by the number of field components.

2.5 Conclusions and perspectives

In this chapter, we systematically analyzed the critical behavior of Platonic Field Theories (PFTs) within the ε–expansion. We devised a method to construct invariant polynomials w.r.t the discrete symmetry groups of the regular polytopes, in terms of which we expressed the first N independent invariants by increasing polynomial order. Since the upper critical dimensions the corresponding PFTs entail are generally non–integer (though still rational), we derived the relative novel RG flow by generalising the single component beta functionals β_V and β_Z to their multicomponent counterparts in all the relevant d_c considered. New results in this respect regard $d_c = {}^{14}/_5, {}^{8}/_3, {}^{5}/_2, {}^{12}/_5$ for which we reported the corresponding beta functionals in the main text and in Appendix B.2.

A very interesting result of this analysis regards a new candidate universality class in $d = 3$ dimensions with the symmetry group $\mathbb{D}_5$ of the Pentagon. Validating its existence, as well as measuring its critical properties by other methods surely deserves attention. Numerical Monte Carlo investigations are currently being pursued in this direction [96]. Moreover being the upper critical dimension very close to three ($\varepsilon = {}^1/_3$) it would be an ideal testing ground for the fpRG. It would also be desirable to have an accurate estimate of the critical exponents of this universality class by means of CFT bootstrap methods in terms of which hyper–Tetrahedral and hyper–Cubic theories have recently been analyzed [97]. Other interesting results concern new Icosahedron fixed points in $d < 3$ as well as the fixed points of the 24–Cell. As a by–product of the present analysis, we found many new multi–critical $O(N)$ and ϕ^n–Cubic universality classes.

Since the recent renewed interest in the multi–critical $O(N)$–models [98, 99], future perspectives regard the analogous analysis of the multi–critical behavior of Cubic theories. In this respect, it would be desirable, as well as interesting, to approach the problem within both fpRG and fRG formalisms, as the first easily tackles the multicritical fixed point structure of the theory, while the second can shed light on possible non–trivial behavior linked to the emergence of non–perturbative fixed points in the large–N limit [98]. We also notice that the universality classes with $d_c < 3$ may correspond to some novel unitary $2d$ CFTs with discrete global symmetry and of central charge $c > 1$; these theories are likely to be irrational CFTs and can be examined with numerical conformal bootstrap methods [100].

As it has been studied in Ref. [101] for $\mathbb{Z}_2$ scalar theories, it would also be interesting to systematically analyze polygons, in particular, with respect to the $d \to 2$ limit where a countable infinity of FPs corresponding to para–fermionic CFTs is expected [102]. Further studies can be directed to the application of the formalism to the study of the "chiral" platonic field theories, namely those field theories characterized by the chiral version of the symmetry groups of regular polytopes, as it may be relevant in particle physics.

We emphasize that, the general method for the construction of invariant polynomials that we introduced in the previous chapters, is suitable to construct invariant polynomials of *any* geometrical regular object.

Appendix B

B.1 Analytical Details

B.1.1 $N = 2$

Triangle $\{3\}$

The Triangle $\{3\}$ $\mathbb{D}_3$ symmetry is encoded in the following two invariants

$$\rho_{\{3\}} = \frac{3}{2}\left(\phi_1^2 + \phi_2^2\right), \tag{B.1.1}$$

$$\tau_{\{3\}} = \frac{3}{4}\phi_2\left(\phi_2^2 - 3\phi_1^2\right). \tag{B.1.2}$$

Since the non–trivial invariant polynomial $\tau_{\{3\}}$ is of order $k = 3$, we study the Triangle in $d_c = 6$ and therefore we consider the following marginal potential

$$U(\tau) = \frac{1}{3!} X\, \tau_{\{3\}}. \tag{B.1.3}$$

The beta function β_X and the anomalous dimension η are obtained from the general formulae (2.3.4) and they read

$$\beta_X = -\frac{1}{2}\varepsilon X + \frac{9}{32}X^3, \tag{B.1.4}$$

$$\eta = \frac{3}{16}X^2. \tag{B.1.5}$$

We find that the universality class associated to the Triangle is the well known $\texttt{Potts}_3$.

Square $\{4\}$

The two invariants for the Square $\{4\}$ $\mathbb{D}_4$ symmetry are

$$\rho_{\{4\}} = 2\left(\phi_1^2 + \phi_2^2\right), \tag{B.1.6}$$

$$\tau_{\{4\}} = \phi_1^4 + 6\phi_2^2\phi_1^2 + \phi_2^4. \tag{B.1.7}$$

We immediately note that $\tau_{\{4\}}$ can be related to $\phi_1^4 + \phi_2^4$ by a field redefinition allowed by the $\mathtt{O(2)}$ symmetry (in fact one can check that $\mathtt{Cubic_2 = Ising}$ [70]) and, given that $\tau_{\{4\}}$ is of polynomial order $k = 4$, we study the Square in $d_c = 4$. The corresponding marginal potential reads

$$U(\rho, \tau) = \frac{1}{4!}\left(X\rho_{\{4\}}^2 + Y\tau_{\{4\}}\right). \tag{B.1.8}$$

In terms of the general formulae (2.3.1), the beta functions and the anomalous dimension read

$$\beta_X = -\varepsilon X + \frac{40}{3}X^2 + 4XY - \frac{1024}{9}X^3 - 64X^2Y - 8XY^2, \tag{B.1.9}$$

$$\beta_Y = -\varepsilon Y + 6Y^2 + 16XY - \frac{512}{3}X^2Y - 128XY^2 - 24Y^3, \tag{B.1.10}$$

$$\eta = \frac{32}{9}X^2 + \frac{8}{3}XY + \frac{2}{3}Y^2. \tag{B.1.11}$$

The LO fixed point potentials are

$$V(\phi_1, \phi_2) = \frac{\varepsilon}{144}\left(\phi_1^4 + 6\phi_2^2\phi_1^2 + \phi_2^4\right),$$
$$V(\phi_1, \phi_2) = \frac{\varepsilon}{80}\left(\phi_1^2 + \phi_2^2\right)^2,$$
$$V(\phi_1, \phi_2) = \frac{\varepsilon}{72}\left(\phi_1^4 + \phi_2^4\right).$$

The first and last potentials represent two copies of $\mathtt{Ising}$ related by the aforementioned field redefinition, while the middle one is the $\mathtt{O(2)}$ class. The computation of the critical exponents at NLO confirms this picture.

Pentagon $\{5\}$

The interesting $\mathbb{D}_5$–symmetric Pentagon $\{5\}$ case can be studied considering the following two invariant polynomials

$$\rho_{\{5\}} = \frac{5}{2}\left(\phi_1^2 + \phi_2^2\right), \tag{B.1.12}$$

$$\tau_{\{5\}} = \frac{5}{16}\left(\phi_2^5 - 10\phi_1^2\phi_2^3 + 5\phi_1^4\phi_2\right). \tag{B.1.13}$$

Since the invariant polynomial $\tau_{\{5\}}$ is of field order $k = 5$, the corresponding upper critical dimension around which the ε-expansion is performed is $d_c = 10/3$. Since ρ and its powers are even in the fields, there is only one marginal coupling and consequently the marginal potential reads

$$U(\tau) = \frac{1}{5!} X\, \tau_{\{5\}}\,. \tag{B.1.14}$$

Beta functionals in $d_c = 10/3$ are given in Eq. (2.3.5). Since the beta functional β_V in $d_c = 10/3$ does not contain $V_{a_1a_2a_3a_4a_5}$, the beta function β_X receives non-tree level contributions only from the anomalous dimension and it reads

$$\beta_X = -\frac{3}{2}\varepsilon X + \frac{625}{384}X^3\,, \tag{B.1.15}$$

with anomalous dimension given by

$$\eta = \frac{125}{192}X^2\,. \tag{B.1.16}$$

The solution $X_* = \frac{24}{25}\sqrt{\varepsilon}$ defines the `Pentagon` universality class with critical exponents reported in Table 2.4.

Hexagon {6}

The Hexagon {6} dihedral symmetry $\mathbb{D}_6$ can be expressed in terms of the following two independent invariant polynomials

$$\rho_{\{6\}} = 3\left(\phi_1^2 + \phi_2^2\right) , \tag{B.1.17}$$

$$\tau_{\{6\}} = \frac{3}{16}\left(11\phi_1^6 + 15\phi_2^2\phi_1^4 + 45\phi_2^4\phi_1^2 + 9\phi_2^6\right) . \tag{B.1.18}$$

Since $\tau_{\{6\}}$ is of polynomial order $k = 6$, the corresponding upper critical dimension is $d_c = 3$ and accordingly we consider the following marginal potential

$$U(\rho, \tau) = \frac{1}{6!}\left(X\,\rho_{\{6\}}^3 + Y\,\tau_{\{6\}}\right) . \tag{B.1.19}$$

The LO beta functions and the anomalous dimension can be obtained from the general formulae (2.3.2); the result is as follows

$$\beta_X = -2\varepsilon\, X + \frac{1008}{5}X^2 + 18XY + \frac{5}{16}Y^2 , \tag{B.1.20}$$

$$\beta_Y = -2\varepsilon\, Y + 144XY + 10Y^2 , \tag{B.1.21}$$

$$\eta = \frac{648}{25}X^2 + \frac{18}{5}XY + \frac{11}{80}Y^2 , \tag{B.1.22}$$

and they are enough to show that the only real fixed point belongs to the `O(2)` class.

Heptagon {7}

The heptagonal symmetry $\mathbb{D}_7$ can be expressed in terms of the following two independent invariant polynomials

$$\rho_{\{7\}} = \frac{7}{2}\left(\phi_1^2 + \phi_2^2\right) , \tag{B.1.23}$$

$$\tau_{\{7\}} = \frac{7}{64}\left(\phi_2^7 - 21\phi_1^2\phi_2^5 + 35\phi_1^4\phi_2^3 - 7\phi_1^6\phi_2\right) . \tag{B.1.24}$$

In this case the invariant $\tau_{\{7\}}$ is of field order $k = 7$, so that the corresponding upper critical dimension is $d_c = 14/5$; we notice that the Heptagon is the first polygon for which $d_c < 3$. As for the `Pentagon`, there is only one marginal coupling since $\rho_{\{7\}}$ and its powers are even in the fields and therefore the corresponding marginal

potential reads

$$U(\tau) = \frac{1}{7!} X \, \tau_{\{7\}} \, . \tag{B.1.25}$$

The beta function β_X receives a non vanishing contribution only from the anomalous dimension since the beta functional β_V in Eq. (2.3.6) is identically zero in this case. We have

$$\beta_X = -\frac{5}{2}\varepsilon X + \frac{245}{73728} X^3 \, , \tag{B.1.26}$$

$$\eta = \frac{35}{18432} X^2 \, . \tag{B.1.27}$$

The solution $X_* = \frac{192}{7}\sqrt{\varepsilon}$ represents the `Heptagon` FP with critical exponents reported in Table 2.4.

Octagon {8}

In the Octagon case the two independent invariants are

$$\rho_{\{8\}} = 4 \left(\phi_1^2 + \phi_2^2 \right) \, , \tag{B.1.28}$$

$$\tau_{\{8\}} = \frac{1}{8} \left(17\phi_1^8 + 84\phi_2^2\phi_1^6 + 70\phi_2^4\phi_1^4 + 84\phi_2^6\phi_1^2 + 17\phi_2^8 \right) \, . \tag{B.1.29}$$

The invariant $\tau_{\{8\}}$ is of field order $k = 8$ and we therefore analyse the theory in $d_c = 8/3$. As for the Hexagon and the Square, there are two marginal couplings and the corresponding marginal potential reads

$$U(\rho, \tau) = \frac{1}{8!} \left(X \, \rho_{\{8\}}^4 + Y \, \tau_{\{8\}} \right) \, . \tag{B.1.30}$$

The beta functions and anomalous dimension can both be extracted from Eq. (2.3.3) and they read

$$\beta_X = -3\varepsilon X + \frac{88576}{35} X^2 + \frac{69}{2} XY + \frac{455}{4096} Y^2 \, , \tag{B.1.31}$$

$$\beta_Y = -3\varepsilon Y + 1024 XY + \frac{35}{4} Y^2 \, , \tag{B.1.32}$$

$$\eta = \frac{131072}{1225} X^2 + \frac{64}{35} XY + \frac{9}{1120} Y^2 \, . \tag{B.1.33}$$

The solution $\{X_* = \frac{105}{88576}\varepsilon, Y_* = 0\}$ represents the `Tetra-O(2)` universality class with exponents reported in Table 2.4.

B.1.2 $N = 3$

Tetrahedron $\{3,3\}$

The Tetrahedron (Potts$_4$) S_4 symmetry has been widely analysed and can be studied in terms of the following polynomial invariants

$$\rho_{\{3,3\}} = \frac{4}{3}\left(\phi_1^2 + \phi_2^2 + \phi_3^2\right), \tag{B.1.34}$$

$$\tau_{\{3,3\}} = \frac{4}{9}\left(\sqrt{2}\phi_1^3 - 3\phi_3\phi_1^2 - 3\sqrt{2}\phi_2^2\phi_1 + 2\phi_3^3 - 3\phi_2^2\phi_3\right), \tag{B.1.35}$$

$$\sigma_{\{3,3\}} = \frac{4}{27}\Big[6\phi_1^4 - 4\sqrt{2}\phi_3\phi_1^3 + 6\left(2\phi_2^2 + \phi_3^2\right)\phi_1^2 + 12\sqrt{2}\phi_2^2\phi_3\phi_1 + 6\phi_2^4 + 7\phi_3^4 + 6\phi_2^2\phi_3^2\Big] \tag{B.1.36}$$

Since $\tau_{\{3,3\}}$ and $\sigma_{\{3,3\}}$ appear respectively at order $k = 3$ and $k = 4$, the upper critical dimensions in the Tetrahedron case are $d_c = 6, 4$. In $d_c = 6$ we have only one marginal coupling

$$U(\tau) = \frac{1}{3!} X\, \tau_{\{3,3\}}, \tag{B.1.37}$$

and at LO the beta function β_X and anomalous dimension can be obtained from Eq. (2.3.4) as

$$\beta_X = -\frac{1}{2}\varepsilon X - \frac{8}{27}X^3, \tag{B.1.38}$$

$$\eta = \frac{16}{81}X^2, \tag{B.1.39}$$

and it does not have any non-trivial real FP. In $d_c = 4$ instead we have two marginal couplings and the marginal potential is given by

$$U(\rho, \tau) = \frac{1}{4!}\left(X\,\rho_{\{3,3\}}^2 + Y\,\sigma_{\{3,3\}}\right). \tag{B.1.40}$$

At NLO we find the following beta functions and anomalous dimension

$$\beta_X = -\varepsilon X - \frac{5888}{243}X^3 - \frac{1408}{81}X^2Y + \frac{176}{27}X^2 - \frac{1136}{243}XY^2 + \frac{8}{3}XY - \frac{16}{27}Y^3 + \frac{1}{3}Y^2, \tag{B.1.41}$$

$$\beta_Y = -\varepsilon Y - \frac{24832}{729}X^2Y - \frac{2176}{81}XY^2 + \frac{64}{9}XY - \frac{1328}{243}Y^3 + \frac{8}{3}Y^2, \tag{B.1.42}$$

$$\eta = \frac{640}{729}X^2 + \frac{64}{81}XY + \frac{56}{243}Y^2. \tag{B.1.43}$$

As already pointed out in Section 2.4, by symmetry enhancement the universal content of the $d_c = 4$ Tetrahedron is the same as the $d_c = 4$ Cube one (see Table 2.3 with corresponding critical exponents reported in Table 2.4).

Octahedron $\{3,4\}$ – Cube $\{4,3\}$

The Octahedron-Cube $S_4 \times \mathbb{Z}_2$ symmetry can be easily expressed in the Octahedron basis, in terms of which the invariant polynomials assume a very simple form

$$\rho_{\{3,4\}} = 2\left(\phi_1^2 + \phi_2^2 + \phi_3^2\right), \tag{B.1.44}$$

$$\tau_{\{3,4\}} = 2\left(\phi_1^4 + \phi_2^4 + \phi_3^4\right), \tag{B.1.45}$$

$$\sigma_{\{3,4\}} = 2\left(\phi_1^6 + \phi_2^6 + \phi_3^6\right). \tag{B.1.46}$$

The duality map that relates the Octahedron invariants to the Cube ones is given in Eq. (2.2.15). The non-trivial invariant polynomials $\tau_{\{3,4\}}$ and $\sigma_{\{3,4\}}$ are respectively of order $k = 4$ and $k = 6$ and consequently the upper critical dimensions we consider in this case are $d_c = 4, 3$.

In $d_c = 4$ there are only two marginal couplings since $\sigma_{\{3,4\}}$ is irrelevant and the marginal potential reads

$$U(\rho, \tau) = \frac{1}{4!}\left(X\,\rho_{\{3,4\}}^2 + Y\,\tau_{\{3,4\}}\right), \tag{B.1.47}$$

with NLO beta functions and anomalous dimension computed from the general ex-

pressions (2.3.1)

$$\beta_X = -\varepsilon X + \frac{44}{3}X^2 + 4XY - \frac{20}{3}XY^2 - \frac{368}{3}X^3 - \frac{176}{3}X^2Y\,, \tag{B.1.48}$$

$$\beta_Y = -\varepsilon Y + 6Y^2 + 16XY - \frac{1552}{9}X^2Y - \frac{368}{3}XY^2 - \frac{68}{3}Y^3\,, \tag{B.1.49}$$

$$\eta = \frac{40}{9}X^2 + \frac{8}{3}XY + \frac{2}{3}Y^2\,. \tag{B.1.50}$$

This systems has three non-trivial fixed points that correspond to three copies of `Ising`, `O(3)` and $\texttt{Cubic}_3$ universality classes. Their GL potentials are, respectively,

$$\begin{aligned} V_{3\times\texttt{Ising}} &= \frac{\varepsilon}{72}(\phi_1^4 + \phi_2^4 + \phi_3^4)\,, \\ V_{\texttt{O(3)}} &= \frac{\varepsilon}{88}\left(\phi_1^2 + \phi_2^2 + \phi_3^2\right)^2\,, \\ V_{\texttt{Cubic}_3} &= \frac{\varepsilon}{72}\left(\phi_1^2 + \phi_2^2 + \phi_3^2\right)^2 - \frac{\varepsilon}{216}\left(\phi_1^4 + \phi_2^4 + \phi_3^4\right)\,. \end{aligned}$$

The critical exponents are reported in Table 2.4.

In $d_c = 3$ instead there are three marginal couplings

$$U(\rho,\tau,\sigma) = \frac{1}{6!}\left(X\,\rho^3_{\{3,4\}} + Y\,\rho_{\{3,4\}}\tau_{\{3,4\}} + Z\,\sigma_{\{3,4\}}\right)\,, \tag{B.1.51}$$

and we give here the LO beta functions and anomalous dimension

$$\beta_X = -2\varepsilon X + \frac{992}{15}X^2 + \frac{64}{5}XY + \frac{8}{15}Y^2\,, \tag{B.1.52}$$

$$\beta_Y = -2\varepsilon Y + \frac{208}{15}Y^2 + \frac{448}{5}XY + 32XZ + \frac{16}{3}YZ\,, \tag{B.1.53}$$

$$\beta_Z = -2\varepsilon Z + \frac{40}{3}Z^2 + \frac{128}{3}XZ + \frac{224}{9}Y^2 + \frac{128}{3}YZ\,, \tag{B.1.54}$$

$$\eta = \frac{448}{135}X^2 + \frac{448XY}{225}XY + \frac{32XZ}{45}XZ + \frac{272}{675}Y^2 + \frac{16}{45}YZ + \frac{4}{45}Z^2\,. \tag{B.1.55}$$

The non-trivial FPs turn out to be, as expected, the tri-critical version of the three FPs in $d_c = 4$. Their critical exponents are reported in Table 2.4.

Icosahedron $\{3,5\}$ – Dodecahedron $\{5,3\}$

In the Icosahedron basis, the $A_5 \times \mathbb{Z}_2$ symmetric independent invariant polynomials read

$$\rho_{\{3,5\}} = 4(\phi_1^2 + \phi_2^2 + \phi_3^2)\,, \tag{B.1.56}$$

$$\begin{aligned}\tau_{\{3,5\}} = \frac{4}{25}[&10\phi_1^6 + 6\phi_3\phi_1^5 + 15\left(2\phi_2^2 + 3\phi_3^2\right)\phi_1^4 - 60\phi_2^2\phi_3\phi_1^3 \\ &+15\left(2\phi_2^4 + 6\phi_3^2\phi_2^2 + \phi_3^4\right)\phi_1^2 + 30\phi_2^4\phi_3\phi_1 + 10\phi_2^6 \\ &+13\phi_3^6 + 15\phi_2^2\phi_3^4 + 45\phi_2^4\phi_3^2]\,,\end{aligned} \tag{B.1.57}$$

$$\begin{aligned}\sigma_{\{3,5\}} = \frac{4}{625}\Big[&127\phi_1^{10} + 360\phi_3\phi_1^9 + 45\left(13\phi_2^2 + 35\phi_3^2\right)\phi_1^8 - 120\left(24\phi_2^2\phi_3 - 7\phi_3^3\right)\phi_1^7 \\ &+210\left(7\phi_2^4 + 30\phi_3^2\phi_2^2 + 10\phi_3^4\right)\phi_1^6 - 252\left(-\phi_3^5 + 30\phi_2^2\phi_3^3 + 20\phi_2^4\phi_3\right)\phi_1^5 \\ &+210\left(5\phi_2^6 + 45\phi_3^2\phi_2^4 + 30\phi_3^4\phi_2^2 + 3\phi_3^6\right)\phi_1^4 - 840\left(3\phi_2^2\phi_3^5 + 5\phi_2^4\phi_3^3\right)\phi_1^3 \\ &+45\left(15\phi_2^8 + 140\phi_3^2\phi_2^6 + 140\phi_3^4\phi_2^4 + 28\phi_3^6\phi_2^2 + \phi_3^8\right)\phi_1^2 \\ &+60\left(30\phi_3\phi_2^8 + 70\phi_3^3\phi_2^6 + 21\phi_3^5\phi_2^4\right)\phi_1 \\ &+125\phi_2^{10} + 313\phi_3^{10} + 45\phi_2^2\phi_3^8 + 630\phi_2^4\phi_3^6 + 2100\phi_2^6\phi_3^4 + 1575\phi_2^8\phi_3^2\Big]\,,\end{aligned} \tag{B.1.58}$$

which can be expressed, by duality, in the Dodecahedron basis in terms of the following map

$$\begin{aligned}\rho_{\{5,3\}} =& \frac{5}{3}\rho_{\{3,5\}}\,, \\ \tau_{\{5,3\}} =& \frac{5}{72}\rho_{\{3,5\}}^3 - \frac{25}{27}\tau_{\{3,5\}}\,, \\ \sigma_{\{5,3\}} =& \frac{35}{2592}\rho_{\{3,5\}}^5 - \frac{175}{324}\rho_{\{3,5\}}^2\tau_{\{3,5\}} + \frac{625}{243}\sigma_{\{3,5\}}\,.\end{aligned} \tag{B.1.59}$$

Since the field power of $\tau_{\{3,5\}}$ and $\sigma_{\{3,5\}}$ are respectively $k = 6$ and $k = 10$ the interesting upper critical dimensions are $d_c = 3, {}^8/_3, {}^5/_2$.

In $d_c = 3$ the marginal potential is

$$U(\rho,\tau) = \frac{1}{6!}\left(X\,\rho_{\{3,5\}}^3 + Y\,\tau_{\{3,5\}}\right)\,, \tag{B.1.60}$$

and the corresponding LO beta functions, computed from Eq. (2.3.2), read

$$\beta_X = -2\varepsilon\, X + \frac{7936}{15}X^2 + \frac{96}{5}XY + \frac{3}{25}Y^2\,, \tag{B.1.61}$$

$$\beta_Y = -2\varepsilon\, Y + \frac{32}{3}Y^2 + \frac{1024}{3}XY\,, \tag{B.1.62}$$

with anomalous dimension

$$\eta = \frac{28672}{135}X^2 + \frac{512}{45}XY + \frac{208}{1125}Y^2\,. \tag{B.1.63}$$

This system exhibits no other real fixed point than `Tri-O(3)` for which the critical exponents are given in Table 2.4.

Also in $d_c = 8/3$ we find only `Tetra-O(3)`, whose critical exponents are reported in Table 2.4. To find a real icosahedral fixed point we have to shift to the third possible upper critical dimension which is $d_c = 5/2$ for which the marginal potential assumes the following form

$$U(\rho,\tau,\sigma) = \frac{1}{10!}\left(X\,\rho^5_{\{3,5\}} + Y\,\rho^2_{\{3,5\}}\tau_{\{3,5\}} + Z\,\sigma_{\{3,5\}}\right)\,. \tag{B.1.64}$$

The LO beta function system in this case reads

$$\begin{aligned}
\beta_X &= -4\varepsilon X + \frac{10381312}{945}X^2 + \frac{3968}{15}XY - \frac{896}{45}XZ + \frac{19601}{23625}Y^2 - \frac{1817}{4500}YZ + \frac{203}{200000}Z^2\,,\\
\beta_Y &= -4\varepsilon Y + \frac{11429888}{945}XY + \frac{68864}{45}XZ + \frac{232928}{945}Y^2 + \frac{7024}{225}YZ - \frac{7}{250}Z^2\,,\\
\beta_Z &= -4\varepsilon Z + \frac{32768}{15}XZ + \frac{13568}{21}Y^2 + \frac{3776}{15}YZ + \frac{84}{5}Z^2\,,
\end{aligned} \tag{B.1.65}$$

with anomalous dimension

$$\eta = \frac{2883584}{42525}X^2 + \frac{360448}{99225}XY + \frac{2048}{14175}XZ + \frac{381952}{7441875}Y^2 + \frac{1664}{354375}YZ + \frac{1252}{8859375}Z^2\,. \tag{B.1.66}$$

Apart from the `Penta-O(3)` FP (see Table 2.4) there are two pure icosahedral real FPs.

B.1.3 $N = 4$

5-cell $\{3,3,3\}$

The S_5 symmetric 5–cell can be studied in terms of the following polynomial invariants

$$\rho_{\{3,3,3\}} = \frac{5}{4}\left(\phi_1^2+\phi_2^2+\phi_3^2+\phi_4^2\right), \tag{B.1.67}$$

$$\tau_{\{3,3,3\}} = \frac{15\left[\phi_3\phi_1^2+\left(\phi_3^2+\left(2\phi_2-\phi_4\right)\phi_4\right)\phi_1-\phi_2\phi_3\left(\phi_2+2\phi_4\right)\right]}{8\sqrt{2}}, \tag{B.1.68}$$

$$\begin{aligned}\sigma_{\{3,3,3\}} = \frac{5}{32}\Big[&3\phi_1^4+4\phi_3\phi_1^3+6\left(\phi_2^2-2\phi_4\phi_2+2\left(\phi_3^2+\phi_4^2\right)\right)\phi_1^2+4\phi_3\left(-3\phi_2^2+\phi_3^2-3\phi_4^2\right)\phi_1\\&+3\,\phi_2^4+3\left(\phi_3^2+\phi_4^2\right)^2+4\phi_2^3\phi_4+12\phi_2^2\left(\phi_3^2+\phi_4^2\right)+4\phi_2\left(3\phi_3^2\phi_4-\phi_4^3\right)\Big],\end{aligned} \tag{B.1.69}$$

$$\begin{aligned}\omega_{\{3,3,3\}} = \frac{5}{64\sqrt{2}}\Big[&\phi_1^5+20\phi_3\phi_1^4-10\left(\phi_2^2-4\phi_4\phi_2-3\phi_3^2+3\phi_4^2\right)\phi_1^3+30\left(\phi_3^3+\phi_4\left(\phi_4-2\phi_2\right)\phi_3\right)\phi_1^2\\&+5\left(\phi_2^4+8\phi_4\phi_2^3+6\left(\phi_3^2-\phi_4^2\right)\phi_2^2+12\phi_4\left(\phi_3^2+\phi_4^2\right)\phi_2+4\left(\phi_3^4-\phi_4^4\right)\right)\phi_1\\&+\phi_3\left(-20\phi_2^4-60\phi_4\phi_2^3-30\left(\phi_3^2+\phi_4^2\right)\phi_2^2-40\phi_4\left(\phi_3^2+\phi_4^2\right)\phi_2+\phi_3^4+5\phi_4^4-10\phi_3^2\phi_4^2\right)\Big].\end{aligned} \tag{B.1.70}$$

The Invariants $\tau_{\{3,3,3\}}$, $\sigma_{\{3,3,3\}}$ and $\omega_{\{3,3,3\}}$ appear respectively at order $k = 3,4,5$ and therefore we study the critical behavior of the 5-cell at the upper critical dimensions $d_c = 6, 4, {}^{10}/_{3}$.

In $d_c = 6$ we have only one marginal coupling and the corresponding potential reads

$$U(\tau) = \frac{1}{6} X\,\tau_{\{3,3,3\}}, \tag{B.1.71}$$

with the corresponding LO beta function β_X and anomalous dimension η given by

$$\beta_X = -\frac{1}{2}\varepsilon\, X - \frac{125}{256}X^3, \tag{B.1.72}$$

$$\eta = \frac{25}{128}X^2. \tag{B.1.73}$$

In $d_c = 4$ instead we have two marginal couplings

$$U(\rho,\tau) = \frac{1}{4!}\left(X\,\rho_{\{3,3,3\}}^2 + Y\,\sigma_{\{3,3,3\}}\right), \tag{B.1.74}$$

and at NLO we find the following system of beta functions along with the corre-

sponding anomalous dimension

$$\beta_X = -\varepsilon X - \frac{8125}{384}X^3 - \frac{1375}{96}X^2Y + \frac{25}{4}X^2 - \frac{2525}{768}XY^2 + \frac{5}{2}XY - \frac{45}{128}Y^3 + \frac{3}{16}Y^2\,, \tag{B.1.75}$$

$$\beta_Y = -\varepsilon Y - \frac{10625}{384}X^2Y - \frac{4625}{192}XY^2 + \frac{25}{4}XY - \frac{4175}{768}Y^3 + \frac{45}{16}Y^2\,, \tag{B.1.76}$$

$$\eta = \frac{625}{768}X^2 + \frac{125}{192}XY + \frac{325}{1536}Y^2\,. \tag{B.1.77}$$

Finally in $d_c = 10/3$ we also have two marginal couplings and the potential reads

$$U(\rho,\tau,\omega) = \frac{1}{5!}\left(X\,\rho_{\{3,3,3\}}\tau_{\{3,3,3\}} + Y\,\omega_{\{3,3,3\}}\right)\,, \tag{B.1.78}$$

and we find the following LO beta functions β_X, β_Y and anomalous dimension η

$$\beta_X = -\frac{3}{2}\varepsilon X - \frac{6525}{4096}X^3 + \frac{17325}{2048}X^2Y + \frac{98775}{8192}XY^2 + \frac{8025}{2048}Y^3\,, \tag{B.1.79}$$

$$\beta_Y = -\frac{3}{2}\varepsilon Y - \frac{138375}{1024}X^3 - \frac{2948625}{8192}X^2Y - \frac{640125}{2048}XY^2 - \frac{732675}{8192}Y^3\,, \tag{B.1.80}$$

$$\eta = \frac{1125}{4096}X^2 + \frac{225}{512}XY + \frac{765}{4096}Y^2\,. \tag{B.1.81}$$

16–Cell $\{3,3,4\}$ – 8–Cell $\{4,3,3\}$

The four polynomial invariants in the 16–cell basis are very simple and read

$$\rho_{\{3,3,4\}} = 2\left(\phi_1^2 + \phi_2^2 + \phi_3^2 + \phi_4^2\right)\,, \tag{B.1.82}$$

$$\tau_{\{3,3,4\}} = 2\left(\phi_1^4 + \phi_2^4 + \phi_3^4 + \phi_4^4\right)\,, \tag{B.1.83}$$

$$\sigma_{\{3,3,4\}} = 2\left(\phi_1^6 + \phi_2^6 + \phi_3^6 + \phi_4^6\right)\,, \tag{B.1.84}$$

$$\omega_{\{3,3,4\}} = 2\left(\phi_1^8 + \phi_2^8 + \phi_3^8 + \phi_4^8\right)\,. \tag{B.1.85}$$

The duality between the 16–cell and the 8–cell can be expressed in terms of the following map between the polynomial invariants in the two bases

$$\begin{aligned}
\rho_{\{4,3,3\}} &= 8\,\rho_{\{3,3,4\}}\,,\\
\tau_{\{4,3,3\}} &= 12\,\rho^2_{\{3,3,4\}} - 16\,\tau_{\{3,3,4\}}\,,\\
\sigma_{\{4,3,3\}} &= 30\,\rho^3_{\{3,3,4\}} - 120\,\tau_{\{3,3,4\}}\rho_{\{3,3,4\}} + 128\,\sigma_{\{3,3,4\}}\,,\\
\omega_{\{4,3,3\}} &= 105\,\rho^4_{\{3,3,4\}} - 840\,\rho^2_{\{3,3,4\}}\tau_{\{3,3,4\}} + 1792\,\rho_{\{3,3,4\}}\sigma_{\{3,3,4\}} - 2176\,\omega_{\{3,3,4\}}\,.
\end{aligned} \tag{B.1.86}$$

The invariants $\tau_{\{3,3,4\}}$, $\sigma_{\{3,3,4\}}$ and $\omega_{\{3,3,4\}}$ appear respectively at order $k = 4, 6, 8$ so that the proper upper critical dimensions to study this theory are $d_c = 4, 3, {}^8\!/_3$.

In $d_c = 4$ the potential has two marginal couplings

$$U(\rho,\tau) = \frac{1}{4!}(X\,\rho^2_{\{3,3,4\}} + Y\,\tau_{\{3,3,4\}})\,, \tag{B.1.87}$$

and we find the following NLO beta functions

$$\beta_X = -\varepsilon X + 16X^2 + 4XY - \frac{416}{3}X^3 - \frac{176}{3}X^2Y - \frac{20}{3}XY^2\,, \tag{B.1.88}$$

$$\beta_Y = -\varepsilon Y + 6Y^2 - \frac{544}{3}X^2Y - \frac{368}{3}XY^2 + 16XY - \frac{68}{3}Y^3\,, \tag{B.1.89}$$

with anomalous dimension

$$\eta = \frac{16}{3}X^2 + \frac{8}{3}XY + \frac{2}{3}Y^2\,. \tag{B.1.90}$$

In $d_c = 3$ we have three marginal couplings and the marginal potential reads

$$U(\rho,\tau,\sigma) = \frac{1}{6!}\left(X\,\rho^3_{\{3,3,4\}} + Y\,\rho^2_{\{3,3,4\}}\tau_{\{3,3,4\}} + Z\,\sigma_{\{3,3,4\}}\right)\,, \tag{B.1.91}$$

and for simplicity we give only the LO beta funtions

$$\beta_X = -2X\varepsilon + \frac{1088}{15}X^2 + \frac{64}{5}XY + \frac{8}{15}Y^2\,, \tag{B.1.92}$$

$$\beta_Y = -2Y\varepsilon + \frac{1408}{15}XY + 32XZ + \frac{208}{15}Y^2 + \frac{16}{3}YZ\,, \tag{B.1.93}$$

$$\beta_Z = -2Z\varepsilon + \frac{128}{3}XZ + \frac{128}{5}Y^2 + \frac{128}{3}YZ + \frac{40}{3}Z^2\,, \tag{B.1.94}$$

with

$$\eta = \frac{1024}{225}X^2 + \frac{512}{225}XY + \frac{32}{45}XZ + \frac{32}{75}Y^2 + \frac{16}{45}YZ + \frac{4}{45}Z^2\,. \tag{B.1.95}$$

Finally in $d_c = 8/3$ the marginal potential has five couplings

$$U(\rho,\tau,\sigma,\omega) = \frac{1}{8!}\left(X\,\rho^4_{\{3,3,4\}} + Y\,\rho^2_{\{3,3,4\}}\tau_{\{3,3,4\}} + Z\,\rho_{\{3,3,4\}}\sigma_{\{3,3,4\}} + W\,\tau^2_{\{3,3,4\}} + T\,\omega_{\{3,3,4\}}\right)\,, \tag{B.1.96}$$

with LO beta functions given by

$$\beta_X = -3\varepsilon X + \frac{1376}{7}X^2 + \frac{36}{35}WX + \frac{1032}{35}YX + \frac{9}{7}ZX + \frac{37}{35}Y^2 + \frac{3}{28}YZ\,, \tag{B.1.97}$$

$$\begin{aligned}\beta_Y = {} & -3\varepsilon Y + \frac{148}{5}Y^2 + \frac{1}{2}TY + \frac{208}{35}WY + \frac{1376}{5}XY + \frac{68}{7}ZY + \frac{45}{56}Z^2 \\ & + 6TX + \frac{1824}{35}WX + \frac{3}{14}WZ + \frac{444}{7}XZ\,,\end{aligned} \tag{B.1.98}$$

$$\begin{aligned}\beta_Z = {} & -3Z\varepsilon + \frac{64}{35}W^2 + \frac{768}{7}XW + \frac{1952}{35}YW + \frac{120}{7}ZW + \frac{7424}{105}Y^2 + \frac{205}{14}Z^2 \\ & + 96TX + 28TY + \frac{15}{2}TZ + \frac{1216}{7}XZ + 80YZ\,,\end{aligned} \tag{B.1.99}$$

$$\begin{aligned}\beta_W = {} & -3\varepsilon W + \frac{36}{7}W^2 + TW + 64XW + \frac{944}{35}YW + \frac{43}{7}ZW + \\ & + \frac{2008}{105}Y^2 + \frac{15}{56}Z^2 + TY + \frac{54}{7}YZ\,,\end{aligned} \tag{B.1.100}$$

$$\begin{aligned}\beta_T = {} & -3\varepsilon T + \frac{35}{2}T^2 + 68WT + 64XT + 80YT + 55ZT + \frac{1968}{35}W^2 + \frac{270}{7}Z^2 \\ & + \frac{640}{7}WY + \frac{648}{7}WZ + \frac{544}{7}YZ\,.\end{aligned} \tag{B.1.101}$$

The anomalous dimension reads

$$\eta = \frac{1}{280}T^2 + \frac{1}{70}TW + \frac{2}{35}TX + \frac{1}{35}TY + \frac{1}{70}TZ + \frac{19}{1225}W^2 + \frac{176}{1225}WX + \frac{76}{1225}WY + \frac{1}{35}WZ + \frac{256}{245}X^2 + \frac{128}{245}XY + \frac{8}{49}XZ + \frac{108}{1225}Y^2 + \frac{17}{245}YZ + \frac{31}{1960}Z^2 . \quad \text{(B.1.102)}$$

24–Cell $\{3,4,3\}$

The 24–cell is peculiar to the $N = 4$ case. The independent polynomial invariants appear at order $k = 2, 6, 8, 12$ and they read

$$\rho_{\{3,4,3\}} = 12(\phi_1^2 + \phi_2^2 + \phi_3^2 + \phi_4^2) , \quad \text{(B.1.103)}$$

$$\tau_{\{3,4,3\}} = 12[\phi_1^6 + 5\left(\phi_2^2 + \phi_3^2 + \phi_4^2\right)\phi_1^4 + 5\left(\phi_2^4 + \phi_3^4 + \phi_4^4\right)\phi_1^2 + \phi_2^6 + \phi_3^6 + \phi_4^6 + 5\phi_3^2\phi_4^4 + 5\phi_3^4\phi_4^2 + 5\phi_2^4\left(\phi_3^2 + \phi_4^2\right) + 5\phi_2^2\left(\phi_3^4 + \phi_4^4\right)] , \quad \text{(B.1.104)}$$

$$\sigma_{\{3,4,3\}} = 4[3\phi_1^8 + 28\left(\phi_2^2 + \phi_3^2 + \phi_4^2\right)\phi_1^6 + 70\left(\phi_2^4 + \phi_3^4 + \phi_4^4\right)\phi_1^4 + 28\left(\phi_2^6 + \phi_3^6 + \phi_4^6\right)\phi_1^2 + 3\phi_2^8 + 3\phi_3^8 + 3\phi_4^8 + 28\phi_3^2\phi_4^6 + 70\phi_3^4\phi_4^4 + 28\phi_3^6\phi_4^2 + 28\phi_2^6\left(\phi_3^2 + \phi_4^2\right) + 70\phi_2^4\left(\phi_3^4 + \phi_4^4\right) + 28\phi_2^2\left(\phi_3^6 + \phi_4^6\right)] , \quad \text{(B.1.105)}$$

$$\omega_{\{3,4,3\}} = 12([\phi_1^{12} + 22\left(\phi_2^2 + \phi_3^2 + \phi_4^2\right)\phi_1^{10} + 165\left(\phi_2^4 + \phi_3^4 + \phi_4^4\right)\phi_1^8 + 308\left(\phi_2^6 + \phi_3^6 + \phi_4^6\right)\phi_1^6 + 165\left(\phi_2^8 + \phi_3^8 + \phi_4^8\right)\phi_1^4 + 22\left(\phi_2^{10} + \phi_3^{10} + \phi_4^{10}\right)\phi_1^2 + \phi_2^{12} + \phi_3^{12} + \phi_4^{12} + 22\phi_3^2\phi_4^{10} + 165\phi_3^4\phi_4^8 + 308\phi_3^6\phi_4^6 + 165\phi_3^8\phi_4^4 + 22\phi_3^{10}\phi_4^2 + 22\phi_2^{10}\left(\phi_3^2 + \phi_4^2\right) + 165\phi_2^8\left(\phi_3^4 + \phi_4^4\right) + 308\phi_2^6\left(\phi_3^6 + \phi_4^6\right) + 165\phi_2^4\left(\phi_3^8 + \phi_4^8\right) + 22\phi_2^2\left(\phi_3^{10} + \phi_4^{10}\right)] . \quad \text{(B.1.106)}$$

It is natural to consider the critical behavior of this system at the upper critical dimensions $d_c = 3, {}^8/_3, {}^5/_2, {}^{12}/_5$. Since they show a critical behavior which is not $\mathtt{O(N)}$-like, we report the cases $d_c = {}^5/_2$ and $d_c = {}^{12}/_5$.

We start considering the case $d_c = {}^5/_2$. The marginal potential reads

$$U(\rho, \tau, \sigma) = \frac{1}{10!}\left(X\,\rho_{\{3,4,3\}}^5 + Y\,\rho_{\{3,4,3\}}^2\tau_{\{3,4,3\}} + Z\,\sigma_{\{3,4,3\}}\rho_{\{3,4,3\}}\right) , \quad \text{(B.1.107)}$$

and the corresponding LO beta functions are

$$\beta_X = -4\varepsilon X + \frac{104398848}{35}X^2 + \frac{173568}{7}XY + 768XZ + \frac{19876}{525}Y^2 + \frac{844}{225}YZ + \frac{5642}{6075}Z^2\,, \tag{B.1.108}$$

$$\beta_Y = -4\varepsilon Y + \frac{108822528}{35}XY + \frac{2039808}{5}XZ + \frac{3320064}{175}Y^2 + \frac{178816}{75}YZ - \frac{121184}{675}Z^2\,, \tag{B.1.109}$$

$$\beta_Z = -4\varepsilon Z + \frac{8552448}{5}XZ + \frac{4810752}{175}Y^2 + \frac{772096}{25}YZ + \frac{930496}{225}Z^2\,, \tag{B.1.110}$$

with anomalous dimension

$$\eta = \frac{8153726976}{1225}X^2 + \frac{28311552}{245}XY + \frac{2359296}{175}XZ + \frac{3219456}{6125}Y^2 + \frac{16384}{125}YZ + \frac{71168}{7875}Z^2\,. \tag{B.1.111}$$

Beside the `penta-O(4)` FP, there are two coincident 24-cell FPs characterised by the same anomalous dimension $\eta = 0.0000115365$.

Finally we consider the theory in $d_c = 12/5$. The marginal potential then is

$$U(\rho,\tau,\sigma,\omega) = \frac{1}{12!}\left(X\,\rho^6_{\{3,4,3\}} + Y\,\rho^3_{\{3,4,3\}}\tau_{\{3,4,3\}} + Z\rho^2_{\{3,4,3\}}\sigma_{\{3,4,3\}} + W\,\tau^2_{\{3,4,3\}} + T\,\omega_{\{3,4,3\}}\right)\,, \tag{B.1.112}$$

and the LO beta functions read

$$\begin{aligned}\beta_X = &-5\varepsilon X - \frac{1925}{1492992}T^2 + \frac{17}{576}TW + 560TX + \frac{263}{54}TY + \frac{1855}{3888}TZ - \frac{41567}{898128}W^2 \\ &+ \frac{43360}{231}WX - \frac{10313}{2079}WY - \frac{4094}{8019}WZ + \frac{304349184}{11}X^2 + \frac{1420800}{7}XY \\ &+ \frac{66560}{11}XZ + \frac{45352}{231}Y^2 + \frac{292}{297}YZ + \frac{25445}{16038}Z^2\,, \end{aligned} \tag{B.1.113}$$

$$\begin{aligned}\beta_Y = &-5\varepsilon Y + \frac{385}{1296}T^2 - \frac{2398}{243}TW - 157440TX - \frac{13076}{9}TY - \frac{36407}{243}TZ + \frac{537479}{37422}W^2 \\ &+ \frac{30136320}{77}WX + \frac{998576}{297}WY + \frac{155264}{891}WZ + \frac{2460450816}{77}XY \\ &+ \frac{37232640}{11}XZ + \frac{14161536}{77}Y^2 + \frac{6724864}{297}YZ - \frac{599872}{2673}Z^2\,, \end{aligned} \tag{B.1.114}$$

$$\begin{aligned}\beta_Z = &-5\varepsilon Z - \frac{385}{288}T^2 + \frac{2809}{27}TW + 1658880TX + 14624TY + \frac{39452}{27}TZ + \frac{123734}{2079}W^2 \\ &+ \frac{4423680}{11}WX + \frac{2310208}{231}WY + \frac{92992}{33}WZ + 20348928XZ + \frac{22076928}{77}Y^2 \\ &+ \frac{9234944}{33}YZ + \frac{7956928}{297}Z^2\,, \end{aligned} \tag{B.1.115}$$

$$\begin{aligned}\beta_W = &-5\varepsilon W + \frac{77}{18}T^2 + \frac{2236}{27}TW + 3776TY + \frac{19712}{27}TZ + \frac{86072}{297}W^2 \\ &+ 2654208WX + \frac{8694016}{231}WY + \frac{559232}{99}WZ + \frac{43628544}{77}Y^2 \\ &+ \frac{7792640}{33}YZ + \frac{7189504}{297}Z^2\,, \end{aligned} \tag{B.1.116}$$

$$\begin{aligned}\beta_T = &-5\varepsilon T + \frac{2464}{3}T^2 + \frac{5536}{3}TW + 2654208TX + 92160TY + \frac{92288}{3}TZ + \frac{21760}{33}W^2 \\ &+ \frac{417792}{11}WY + \frac{770048}{33}WZ + \frac{7766016}{11}YZ + \frac{2265088}{11}Z^2\,, \end{aligned} \tag{B.1.117}$$

with anomalous dimension given by

$$\eta = \frac{429981696}{245}X^2 + \frac{1492992}{49}XY + \frac{124416}{35}XZ + \frac{34992}{245}Y^2 + \frac{1296}{35}YZ + \frac{99}{35}Z^2\,. \tag{B.1.118}$$

Apart from the `Hexa-O(4)` fixed point the system displays two `24-Cell` fixed points whose critical exponents are given in Section 2.4.

600-Cell $\{5,3,3\}$ – 120-Cell $\{3,3,5\}$

The independent invariants have very complicated expressions and they appear at order $2, 12, 20, 30$. The possible upper critical dimensions are therefore gievn by $d_c = {}^{12}/_{5}, {}^{20}/_{9}, {}^{15}/_{7}$. We think it is not illuminating to report here the explicit expressions for the invariants as well as for the corresponding beta functions, but we point out that they can be extracted following the main lines of reasoning given in the main text.

B.2 Beta functionals

We report here the multicomponent beta functionals for the cases $d_c = 5/2$ and $d_c = 12/5$. In particular, in the $d_c = 12/5$ case we refer to γ as the Euler's constant and to $\psi(z) = \Gamma'(z)/\Gamma(z)$ as the logarithmic derivative of the Gamma function.

$$d_c = \frac{5}{2}$$

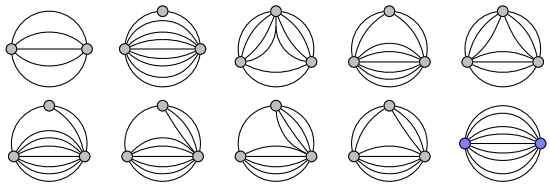

$$\begin{aligned}
\beta_V = & \frac{1}{30} V_{a_1a_2a_3a_4a_5} V_{a_1a_2a_3a_4a_5} \\
& + \frac{1}{7560} V_{a_1a_2} V_{a_1a_3a_4a_5a_6a_7a_8a_9a_{10}} V_{a_2a_3a_4a_5a_6a_7a_8a_9a_{10}} \\
& - \frac{1}{144}\sqrt{\frac{\pi}{2}}\Gamma\left(1/4\right)^2 V_{a_1a_2a_3a_4a_5a_6a_7a_8} V_{a_1a_2a_3a_4a_9a_{10}} V_{a_5a_6a_7a_8a_9a_{10}} \\
& + \frac{\Gamma\left(3/4\right)^2}{45\sqrt{2\pi}} V_{a_1a_2a_3a_4} V_{a_1a_2a_5a_6a_7a_8a_9a_{10}} V_{a_3a_4a_5a_6a_7a_8a_9a_{10}} \\
& - \frac{\pi\Gamma\left(1/4\right)^2}{216\Gamma\left(3/4\right)^2} V_{a_1a_2a_3a_4a_5a_6} V_{a_1a_2a_3a_7a_8a_9a_{10}} V_{a_4a_5a_6a_7a_8a_9a_{10}} \\
& + \frac{2}{945} V_{a_1a_2a_3} V_{a_1a_4a_5a_6a_7a_8a_9a_{10}} V_{a_2a_3a_4a_5a_6a_7a_8a_9a_{10}} \\
& + \frac{2}{135} V_{a_1a_2a_3a_4} V_{a_1a_5a_6a_7a_8a_9a_{10}} V_{a_2a_3a_4a_5a_6a_7a_8a_9a_{10}} \\
& - \frac{2}{45} V_{a_1a_2a_3a_4a_5} V_{a_1a_6a_7a_8a_9a_{10}} V_{a_2a_3a_4a_5a_6a_7a_8a_9a_{10}} \\
& + \frac{1}{45}\left[-4+\pi-\log(4)\right] V_{a_1a_2a_3a_4a_5} V_{a_1a_2a_6a_7a_8a_9a_{10}} V_{a_3a_4a_5a_6a_7a_8a_9a_{10}} \\
(\beta_Z)_{a_1a_2} = & -\frac{1}{56700} V_{a_1a_3a_4a_5a_6a_7a_8a_9a_{10}a_{11}} V_{a_2a_3a_4a_5a_6a_7a_8a_9a_{10}a_{11}}
\end{aligned} \tag{B.2.1}$$

$$d_c = \frac{12}{5}$$

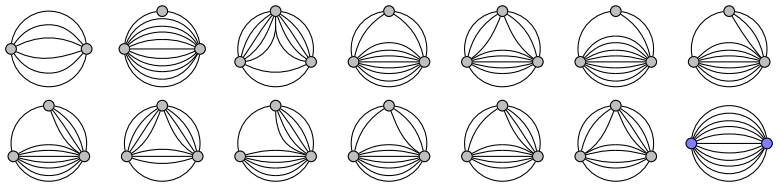

$$\begin{aligned}
\beta_V = {} & \frac{1}{144} V_{a_1a_2a_3a_4a_5a_6} V_{a_1a_2a_3a_4a_5a_6} \\
& + \frac{1}{580608} V_{a_1a_2} V_{a_1a_3a_4a_5a_6a_7a_8a_9a_{10}a_{11}a_{12}} V_{a_2a_3a_4a_5a_6a_7a_8a_9a_{10}a_{11}a_{12}} \\
& - \frac{\Gamma\left(1/5\right)^3 \Gamma\left(4/5\right)}{5760\Gamma\left(\frac{2}{5}\right)} V_{a_1a_2a_3a_4a_5a_6a_7a_8a_9a_{10}} V_{a_1a_2a_3a_4a_5a_{11}a_{12}} V_{a_6a_7a_8a_9a_{10}a_{11}a_{12}} \\
& - \frac{\Gamma\left(-2/5\right) \Gamma\left(1/5\right) \Gamma\left(4/5\right)^2}{32256\Gamma\left(2/5\right)^2 \Gamma\left(8/5\right)} V_{a_1a_2a_3a_4} V_{a_1a_2a_5a_6a_7a_8a_9a_{10}a_{11}a_{12}} V_{a_3a_4a_5a_6a_7a_8a_9a_{10}a_{11}a_{12}} \\
& + \frac{5\left[-5+\gamma-\psi\left(1/5\right)+2\psi\left(3/5\right)\right]}{5184} V_{a_1a_2a_3a_4a_5a_6} V_{a_1a_2a_3a_7a_8a_9a_{10}a_{11}a_{12}} V_{a_4a_5a_6a_7a_8a_9a_{10}a_{11}a_{12}} \\
& + \frac{25}{870912} V_{a_1a_2a_3} V_{a_1a_4a_5a_6a_7a_8a_9a_{10}a_{11}a_{12}} V_{a_2a_3a_4a_5a_6a_7a_8a_9a_{10}a_{11}a_{12}} \\
& + \frac{25}{145152} V_{a_1a_2a_3a_4} V_{a_1a_5a_6a_7a_8a_9a_{10}a_{11}a_{12}} V_{a_2a_3a_4a_5a_6a_7a_8a_9a_{10}a_{11}a_{12}} \\
& + \frac{25}{24192} V_{a_1a_2a_3a_4a_5} V_{a_1a_6a_7a_8a_9a_{10}a_{11}a_{12}} V_{a_2a_3a_4a_5a_6a_7a_8a_9a_{10}a_{11}a_{12}} \\
& - \frac{5\Gamma\left(1/5\right) \Gamma\left(2/5\right)^3}{41472\Gamma\left(4/5\right)^3} V_{a_1a_2a_3a_4a_5a_6a_7a_8} V_{a_1a_2a_3a_4a_9a_{10}a_{11}a_{12}} V_{a_5a_6a_7a_8a_9a_{10}a_{11}a_{12}} \\
& - \frac{5}{1728} V_{a_1a_2a_3a_4a_5a_6} V_{a_1a_7a_8a_9a_{10}a_{11}a_{12}} V_{a_2a_3a_4a_5a_6a_7a_8a_9a_{10}a_{11}a_{12}} \\
& - \frac{\Gamma\left(-1/5\right) \Gamma\left(1/5\right) \Gamma\left(4/5\right)}{6048\Gamma\left(2/5\right) \Gamma\left(7/5\right)} V_{a_1a_2a_3a_4a_5} V_{a_1a_2a_6a_7a_8a_9a_{10}a_{11}a_{12}} V_{a_3a_4a_5a_6a_7a_8a_9a_{10}a_{11}a_{12}} \\
& + \frac{5\left[-5+\gamma-\psi\left(1/5\right)+\psi\left(2/5\right)+\psi\left(4/5\right)\right]}{3456} V_{a_1a_2a_3a_4a_5a_6} V_{a_1a_2a_7a_8a_9a_{10}a_{11}a_{12}} V_{a_3a_4a_5a_6a_7a_8a_9a_{10}a_{11}a_{12}} \\
& - \frac{\Gamma(1/5)^2 \Gamma(2/5)}{1728\,\Gamma(4/5)} V_{a_1a_2a_3a_4a_5a_6a_7} V_{a_1a_2a_3a_8a_9a_{10}a_{11}a_{12}} V_{a_4a_5a_6a_7a_8a_9a_{10}a_{11}a_{12}} \\
(\beta_Z)_{a_1a_2} = {} & -\frac{1}{4790016} V_{a_1a_3a_4a_5a_6a_7a_8a_9a_{10}a_{11}a_{12}a_{13}} V_{a_2a_3a_4a_5a_6a_7a_8a_9a_{10}a_{11}a_{12}a_{13}}
\end{aligned} \tag{B.2.2}$$

B.3 The main ideas behind the functional perturbative RG

In this appendix we aim to give a short review of the key concepts behind the functional reformulation of the perturbative renormalization group. In a nutshell the functional perspective simplifies the computations of the beta functions and unfolds the general structure behind the ε-expansion, furnishing a preferred tool to the exploration of new universality classes. The presentation follows closely [103].

B.3.1 Loops, poles and regularization scheme

Let's consider the standard effective action Γ: in the background field approach the effective action can be computed in terms of the standard loop expansion as

$$\Gamma = S + \frac{1}{2}\mathrm{Tr}\log S^{(2)} + \frac{1}{8}S^{(4)}_{xyzw}G_{xy}G_{zw} - \frac{1}{12}S^{(3)}_{xyz}S^{(3)}_{abc}G_{xa}G_{yb}G_{zc} + \dots\,, \tag{B.3.1}$$

where the propagator is defined as $G_{xy} \equiv (S^{(2)})^{-1}_{xy}$ and integration over coordinates is understood. The corresponding graphical representation

$\Gamma =$ tree $+\ \frac{1}{2}$  $+\ \frac{1}{8}$ 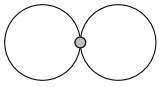 $-\ \frac{1}{12}$  $+\ \dots\,,$ (B.3.2)

makes it easier to visualize the expansion in Eq. (B.3.1) as a reorganization of perturbation theory according to the number of loops of connected vacuum diagrams. The vertex set at a given loop order L , namely the set of all possible vertices a L–loop diagram can have, is determined by Euler's formula

$$L = P - \mathcal{V} + 1\,, \tag{B.3.3}$$

where L is the number of closed loops, P is the number of internal lines (propagators) and $\mathcal{V}$ is the number of vertices. To demonstrate it, consider the subgraph where the $\mathcal{V}$ vertices are linked by just $\mathcal{V} - 1$ lines to create a minimal connected tree graph (this may of course be not unique). Then add the remaining $P - \mathcal{V} + 1$ lines between the various vertices to restore the complete graph; each addition creates a new loop.

The effective action Γ naturally contains divergent contributions which may arise in integrating over L undetermined loop momenta. The critical thing to re-

alise is that divergent integrals are meaningless; for unambiguous calculations, it is necessary to remove the divergences. There is no unique prescription on how to do this, and in the end, the exact method does not matter since they all lead to the same result. Different methods however may be more or less useful in doing calculations.

A technique is particularly useful in the study both of quantum field theory as applied to the theory of fundamental interactions and to the theory of critical phenomena, namely the dimensional continuation of Feynman diagrams. This leads also to a (perturbative) definition of a field theory in generic, non–integer, dimension d. Dimensional regularisation, the minimal subtraction scheme and the ε–expansion are based on it. In $\overline{\text{MS}}$ dimensional regularisation, divergent contributions appear as $1/\varepsilon$ poles, where ε measures the distance from the upper critical dimension, namely $d = d_c - \varepsilon$, and can be cancelled by adding new (counter) terms to the Lagrangian. On the other hand, from the RG perspective, $1/\varepsilon$ poles encodes the scale dependence of the theory and represent the primary object of interest in the renormalization procedure.

B.3.2 Upper critical dimensions

The renormalization group beta *functionals* β_V and β_Z describing the RG flow of the potential V and that of the wave–function renormalization functional Z, at any loop L, can be obtained considering

$$\Gamma^{(L)}_{\text{div}} = \frac{-1/L}{\varepsilon} \int d^{d_c}x \left\{ \beta_V^{(L)}(\phi) + \frac{1}{2}\beta_Z^{(L)}(\phi)(\partial\phi)^2 \right\} + O(1/\varepsilon^2)\,. \tag{B.3.4}$$

The key point of the functional approach is that divergencies are considered without specifying the functional form of the potential V and this is the rationale behind Eq. (B.3.4).

We now have to understand where $1/\varepsilon$ poles appear in the dimensionally regularised loop expansion (B.3.1). Typically the upper critical dimension d_c is defined as the dimension at which the coupling of the operator ϕ^m is canonically dimensionless and it is therefore expressed as $d_c = \frac{2m}{m-2}$ for $m \geq 2$. These are the dimensions where $1/\varepsilon$ poles appear in the dimensionally regularised loop expansion (B.3.1). It is interesting to notice that, since the perturbative expansion can be organised alternatively as an expansion in powers of the couplings that define the potential V, in the

ϕ^m	ϕ^3	ϕ^4	ϕ^5	ϕ^6	ϕ^7	ϕ^8	ϕ^9	ϕ^{10}	ϕ^{11}	ϕ^{12}	...
d_c	6	4	$10/3$	3	$14/5$	$8/3$	$18/7$	$5/2$	$22/9$	$12/5$	...
L_{LO}	1	1	3	2	5	3	7	4	9	5	...

Table B.1: Ginzburg Landau interactions ϕ^m with the corresponding upper critical dimensions d_c where $1/\varepsilon$ are present along with the corresponding leading loop–order L.

dimensional regularization scheme we can establish a one–to–one correspondence between terms of a certain loop order L in the beta functionals and those of fixed coupling order. The upper critical dimension d_c can be indeed related to the loop order L as $d_c = 2 + 2k/L$ for $k \geq 1$. In terms of this relation it is finally easy to understand at which loop orders L, a given theory ϕ^m receives contributions to its corresponding beta functionals, see Table B.1. This is of particular interest for another very important reason already mentioned in the main text, namely the fact that the leading and next–to–leading order contributions are *universal* [89], i.e., scheme–independent. We immediately notice that apart the cases $d_c = 6, 4, 3, 2$ all the other upper critical dimensions are rational and they have in general $L_{\mathrm{LO}} > 1$. This general analysis has a virtue: It permits to rapidly identify which are the critical dimensions d_c that allow for a continuation to an integer dimension $d = d_c - \varepsilon$, possibly describing a physically relevant universality class. As already remarked in the main text, the real surprise has been the identification of a new upper critical dimension relevant to the study of $d = 3$ univeralities: $d_c = 10/3$ whose leading order contribution appears a three loops. In the same spirit, all other theories ϕ^m with $m \geq 6$ are relevant to describe non–trivial critical behaviors in $d = 2$. As we shall see in a moment, the functional formalism is of great help in studying the scalar theories with rational critical dimension since no loop computation is really needed and the functional form of the beta functionals β_V and β_Z is completely fixed once d_c is given.

B.3.3 Beta functionals

From the loop expansion (B.3.1), we understand that monomials contributing to β_V are constructed in terms of derivatives $V^{(n)}$ of the potential, possibly linked by the appropriate powers of $V^{(2)}$ insertions in order to have proper vacuum diagrams. It is easy to understand that for a given loop order L, once the vertex set has been fixed,

the functional form of the monomials is very constrained since dimensionally they must match the dimension of β_V which is obviously d_c. We therefore have

$$\mathcal{V}\left[d_c\left(1-\frac{n}{2}\right)+n\right]+2k=d_c\,, \tag{B.3.5}$$

and we one looks for solutions $k \in \mathbb{N}$. For example, at one loop the beta functional can be only of the form $(V^{(2)})^{\frac{d_c}{2}}$. At two loops we have that the vertex set is given by $(V^{(3)})^2$ and therefore the beta functional β_V can only be of the form $(V^{(3)})^2(V^{(2)})^k$. The exact monomials set is then rapidly understood in terms of Eq. (B.3.5). Let's consider to this purpose the possible (integer Ginzburg–Landau) upper critical dimensions at two loops, namely $d_c = 6, 4, 3$. Setting $\mathcal{V} = 2$ and $n = 3$ we find that the monomials contributing to $\beta_V^{L=2}$ are

$$(V^{(3)})^2(V^{(2)})^3 \qquad d_c = 6\,, \tag{B.3.6}$$
$$(V^{(3)})^2 V^{(2)} \qquad d_c = 4\,, \tag{B.3.7}$$
$$(V^{(3)})^2 \qquad d_c = 3\,. \tag{B.3.8}$$

The same reasoning applies to higher loop computations: The functional form of the beta functionals is fixed with the sole inputs of the loop order L and the critical dimension d_c.

The analysis of the functional form of β_Z proceeds analogously apart the fact that the vertex set is expanded since we now look at two point functions. Some examples are listed below in which only LO and NLO are considered.

- $d_c = 4$

$$\beta_V = A(V^{(2)})^2 + BV^{(2)}(V^{(3)})^2 + \dots \tag{B.3.9}$$
$$\beta_V = C(V^{(4)})^2 + D(V^{(4)})^3 + \dots \tag{B.3.10}$$

- $d_c = 10/3$ [1]

$$\beta_V = A_1(V^{(3)})^2 V^{(4)} + A_2 V^{(2)}(V^{(4)})^2 + \dots \tag{B.3.11}$$
$$\beta_V = D(V^{(5)})^2 + \dots \tag{B.3.12}$$

[1] Note that in this case we have two terms at LO.

We want to stress here the notable fact that thanks to the functional constraints, the functional forms of β_V and β_Z have been determined, modulo coefficients, without performing any loop computation.

B.3.4 Computing the coefficients

We are now left with the computation of the coefficients. For the whole family of *even* minimal models for which $d_c = \frac{2m}{m-1}$, the coefficients relative to the LO beta functionals can be obtained reconsidering the perturbative expansion in Eq. (B.3.1) as an expansion in terms of the couplings which define the potential V and the wavefunction Z. Since in this case the leading order correction is quadratic in the couplings the LO beta functionals read $\beta_V^{\mathrm{LO}} = A_n (V^{(n)})^2$ and $\beta_Z^{\mathrm{LO}} = D_n (V^{(2n)})^2$ which appear respectively at $(n-1)$ and $2(n-1)$ loops. The divergent part of the effective action reads in this case

$$\Gamma_{\mathrm{div}} = -\frac{1}{\varepsilon} \int \mathrm{d}^{\frac{2m}{m-1}} x \left\{ \frac{\Gamma(\frac{1}{n-1})^{n-1}}{(4\pi)^n n!} (V^{(n)})^2 - \frac{2(n-1)\Gamma(\frac{1}{n-1})^{2(n-1)}}{(4\pi)^{2n}(2n)!} (V^{(2n)})^2 \frac{1}{2} (\partial\phi)^2 \right\} , \tag{B.3.13}$$

from which one can extract the following coefficients for β_V^{LO} and β_Z^{LO}

$$A_n = \frac{1}{(4\pi)^n} \frac{n-1}{n!} \Gamma\left(\frac{1}{n-1}\right)^{n-1} , \tag{B.3.14}$$

$$D_n = \frac{1}{(4\pi)^{2n}} \frac{4(n-1)^2}{(2n)!} \Gamma\left(\frac{1}{n-1}\right)^{2(n-1)} . \tag{B.3.15}$$

One can easily check that, after rescaling, the $n = 2$ and $n = 3$ cases correctly reproduce the LO respectively for `Ising` and `Tri-Critical` universality classes. At NLO the computation of β_V^{NLO} for all unitary minimal models is a little bit more involved but the still easy to automatize. The result reads

$$\beta_V^{\mathrm{NLO}} = -\frac{1}{3} B_n \sum_{r+s+t=2n} K_{rst} V^{(r+s)} V^{(s+t)} V^{(t+r)} + B_n \sum_{s+t=n} L_{st} V^{(n)} V^{(n+s)} V^{(n+t)} , \tag{B.3.16}$$

with

$$B_n = \frac{(n-1)^2}{(4\pi)^{2n}}\Gamma\left(\frac{1}{n-1}\right)^{2(n-1)}, \tag{B.3.17}$$

$$K_{rst} = \frac{\Gamma(\frac{n-r}{n-1})\Gamma(\frac{n-s}{n-1})\Gamma(\frac{n-t}{n-1})}{\Gamma(\frac{r}{n-1})\Gamma(\frac{s}{n-1})\Gamma(\frac{t}{n-1})}, \tag{B.3.18}$$

$$L_{st} = n - 1 + \psi\left(\frac{1}{n-1}\right) - \psi\left(\frac{s}{n-1}\right) - \psi\left(\frac{t}{n-1}\right) + \psi(1), \tag{B.3.19}$$

reproduce the NLO respectively for `Ising` and `Tri-Critical`.

Finally as shown in Ref. [67], the LO non–unitary minimal models can be obtained from the NLO unitary ones for half integer $n = 3/2, 5/2, 7/2$. Then β_Z remain the same for unitary minimal models, namely $\beta_Z = D_n(V^{(2n)})^2$ and β_V contains only the first terms of Eq. (B.3.16).

B.3.5 Remarks on the multi-component generalisation

One of the most remarkable and striking consequences of the functional formalism is the fact that the expressions so derived for the beta functionals can be directly enhanced to their multi-component counterparts without performing any single additional computation. Few remarks are in order.

The basic idea is that the multi–component ($N > 1$) beta functionals β_V and β_Z must reduce to their single–component known cases in the $N = 1$ limit. If there is only one way to add indices to each monomial appearing in the $N = 1$ beta functionals, then the relative coefficients in the $N > 1$ case are univocally fixed. The monomials appearing in the beta functionals are basically of two types:

- Only vertices $V_{a_1 \ldots a_k}$ with $k > 2$, for which there is only one way to contract indices and we note that, since we are working in dimensional regularisation, self–contractions like $V_{aa\ldots a_k}$ do not contribute;

- mass insertions $V_{a_1 a_2}$ which are generated by the expansion of the propagators in the loop diagrams. Note that the monomial V_{aa} is not present in dimensional regularisation.

In the *even* case (apart the trivial LO $d_c = 4$ case), in the NLO beta functional β_V^{NLO}, there appears only one term involving $V_{a_1 a_2}$ and this term is linear in the mass

insertion (the general formula was derived in [65]). Because of this fact there is only one multi–component diagram generalizing this term, and we can univocally fix the coefficient. A useful example is the $d_c = 3$ case: the $N = 1$ beta functional is given by

$$\beta_V = \frac{1}{3}(V^{(3)})^2 + \frac{1}{6}V^{(2)}(V^{(5)})^2 - \frac{4}{3}V^{(3)}V^{(4)}V^{(5)} - \frac{\pi^2}{12}(V^{(4)})^3\,, \tag{B.3.20}$$

for which the NLO monomial $V^{(2)}(V^{(5)})^2$ is the only involving a mass insertion and the $V_{a_1a_2}$ can only connect the two five vertices. The vertices in other NLO monomials can be connected only following the loop diagram from which they come from. In this way we immediately reproduce the result given in [70].

In the *odd* case, as mentioned above, it is possible to derive a general formula for the $N = 1$ beta functional β_V only at LO (see Ref. [66]). Since this formula can be obtained by analytical continuation of the NLO *even* case, it involves only one $V_{a_1a_2}$ in only one monomial and, as before, its multi–component counterpart can be fixed univocally. The picture is different for the *odd* NLO case for which, apart the $d_c = 6$ case, no general functionals β_V and β_Z are known. In the $N = 1$ single–component $d_c = 6$ case, the beta functional is $\beta_V = a(V^{(2)})^3 + b(V^{(2)})^2(V^{(3)})^3$ and since $V^{(2)}$ are mass insertions and since the NLO is at two loop (vacuum sun set), there are three propagators where the three mass insertions can fit

$$(V^{(2)})^3(V^{(3)})^2 \to \alpha V_{ik}V_{kl}V_{lj}V_{iab}V_{jab} + \beta V_{ik}V_{kj}V_{lm}V_{ija}V_{lmb} + \gamma V_{ia}V_{jb}V_{kc}V_{abc}V_{ijk}\,, \tag{B.3.21}$$

and thus the knowledge of the $N = 1$ case only fixes the sum $\alpha + \beta + \gamma$. From Ref [70], it is clear indeed that the $\beta_V^{\rm NLO}$ in $d_c = 6$ has these three terms and that the constraint just derived is satisfied. In the case of the LO (*even* and *odd)* β_Z we have only one monomial with no $V_{a_1a_2}$ and the results of the *even* case agrees with CFT results [62]. The determination of the NLO contributions in the *odd* case will complete the knowledge of the universal data of one component scalar theories.

Part II

Active Matter

Invitation to Part II

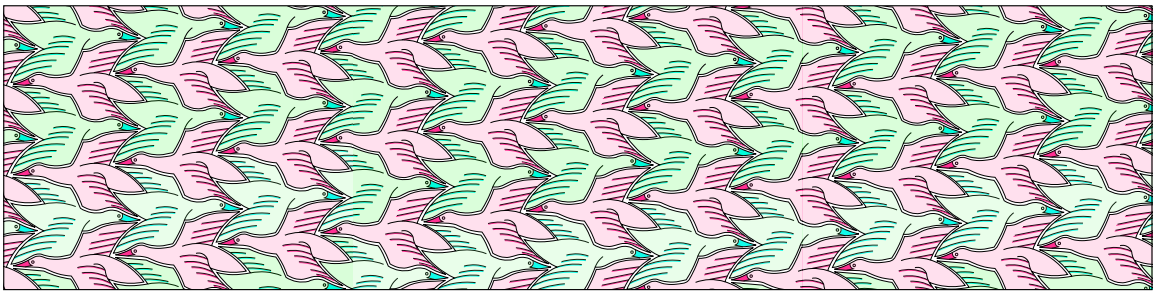

One of the great scientific challenges of our time is to understand how the stunning diversity and complexity of living systems emerge from the intertwined interactions among a large number of individual basic units. Group of animals such as schooling fish gyrating in vortices, swarming insects, or flocking birds revolving in the air, even though not guided by a single leader, they give rise to perfectly orchestrated and coordinated motion which might stabilize them against environmental disruptions. In the brain of an adult human, 10^{11} neurons and up to 10^{15} synaptic connections among them form an incredibly intricated and complex network which permits the electrical signals to propagate, affording an incredible diversity of operations among which learning, memorizing and talking to name just a few. Trillions of cells are born, live and die every minute in multicellular organisms, but still, they can coordinate their activity in countless ways to form assemblies of hierarchical order of complexity which sustain, and finally permit, their life itself. We could spend a lifetime studying an individual animal, neuron or cell without being able to deduce the astonishingly collective behavior they can give rise to. Nevertheless, the typically reductionist approach in biology, as an attempt to reduce biological phenomena to the behavior of molecules, has successfully led to the identification of most of the molecular building blocks shared, to a remarkable extent, by all forms of life on earth. Geneticists, in this respect, inferred the existence of genes as well as many of their properties and further studies clarified their role in DNA, which *per se* constitutes one of the greatest scientific discovery of the twentieth century. A biological function, however, can only rarely be attributed to an individual molecule and despite its enormous success, the reductionist approach offers no convincing clues on how systemic and collective properties emerge. Many of the most fascinating

phenomena of living systems are in fact intrinsically collective and they cannot be deduced from a meticulous inspection of their elementary components on an individual basis.

On the other hand, the enormous success of statistical physics in explaining the emergent collective phenomena in equilibrium and non–equilibrium systems, pushed physicists, in the last decades, to understand whether statistical physics could provide a useful language to shed light on the large–scale organization of biological systems [104–109]. At equilibrium, one of the most interesting aspects of many–particle systems is that complex collective behavior may emerge at a phase transition. That the intrinsic collective behavior of living systems would be a manifestation of collective phases as well as of transitions between them is a tempting hypothesis. Remarkably, phase transitions are a common theme in biology [110, 111]. Instead of embarking on a rather not–exhaustive list of examples, we consider fruitful to report the perhaps prototypical example of emergent collective behavior in a biological system: A flock of birds. Flocking is an outstanding example of a collective phase where simple interactions between thousands of birds give rise to spectacular and fascinating emergent behavior at larger scales. The remarkable degree of coordination and collective response typical of these flocks stimulated theoretical physicists to develop statistical mechanical models capable to describe these collective phenomena. On the one side Vicsek [112] proposed an individual–based model of self–propelled particles which mimics the tendency of biological subjects to move as other subjects in their neighborhood do, with some deviations treated as noise. On the other hand, Toner and Tu [113] proposed a continuum hydrodynamic description of the phenomenon, more intriguing and amenable to theoretical exploration. Both these models share the existence of a phase transitions from a coherent (ordered) flocking phase to an incoherent (disordered) swarming one. The already appealing scenario received more credit when methods have been developed to keep track of the trajectories of every bird in groups of more than one thousand as they are revolving in aerial displays [114, 115]. The minimally structured model, which is essentially equivalent to a model of spins in a magnet is, in fact, able to predict long–range correlations among fluctuations in flight direction which are in quantitative agreement with experimental data. Moreover, scale–free correlations in the orientation might be attributed to the spontaneous breaking of continuous ro-

tational symmetry in terms of Goldstone's theorem. In biological terms, criticality allows the flock to achieve maximal correlation across long distances with limited speed fluctuations. Long–range scale–invariant correlations are general features in systems exhibiting collective motion such as fish schools, insect swarms, herds of mammals, human crowds, bacterial colonies and groups of cells [116–123]. This typical trait shared by so many different living systems would represent the needing of self–organized groups to achieve large–scale coordination, and this can be accomplished operating close to a critical point. Sitting right at the borderline between ordered and disordered phases, i.e., at the very edge of a (continuous) phase transition, let the flock respond quicker to dangers that may visible to only a small fraction of individuals, spreading information fastly over long distances. This advantageous feature in flocks can be a common aspect of living systems that can exploit criticality to draw important functional advantages. The idea that evolution might have favored states close to the edge of a phase transition is certainly seducing since it suggests that operating near criticality could be a key strategy in biological organization [111].

That of a flock of birds is a remarkable example of how fruitful can be the interplay between biology and statistical physics for understanding the emergent collective behaviors typical of living systems. Many features at critical points are quite robust and largely independent of small–scale details, explaining why the typical scale–free behavior of birds is shared by many other living systems. Universality in biology has a very important consequence: It suggests that oversimplified models, in which many irrelevant details at the individual level are neglected and emphasis is put on the way they interact, can be fundamental for understanding collective aspects of living systems in relatively simple terms.

In the present chapter, we employ the same conceptual tools to study social unicellular organisms as well as multicellular ones, which may exhibit signatures of scale invariance and criticality in their collective behavior [122].

Chapter 3

Chemotaxis, growth and dynamic scaling laws

The emergent collective behavior typical of many, if not most, living systems exemplifies how local interactions can give rise to correlations that significantly exceed the microscopic scale set by individual units. When correlations are sufficiently long–ranged, in fact, the systems, active or passive, become insensitive to their microscopic details and their properties can be studied in terms of stylized models. There are at least two approaches to the construction of models in the continuum which can, therefore, be relevant for the description of the emergent collective properties of active as well as passive systems. Either one constructs them upon explicit coarse–graining a microscopic (i.e. at the particle–level) model or one writes down all the terms allowed by symmetries and conservation laws to a given order. Even if unambiguous, in the first approach there is no guarantee that the chosen microscopic model contains all the terms which are relevant for a general continuum theory. This is the case of chemotaxis which is going to be discussed in the present chapter. In the second approach, one buries the poor knowledge of the detailed microscopic dynamics in a few phenomenological parameters and write down every relevant (i.e., important) term at large length– and long time– scales. In practice, this means a gradient expansion where one retains the smallest possible number of space and time derivatives. In this respect, the chemotaxis theory to be described in this chapter is an example of the first bottom–up route while the hydrodynamic description of flocking of Toner and Tu [113] provides an example of the top–down one.

In general, the resulting continuum theories involve a set of order parameters that evolve according to (a set) of partial differential equation(s) whose deterministic version is often referred to as 'hydrodynamic' description. These equations typically describe the average behavior of the system and fluctuations are usually introduced in the form of a noise, transforming a model into a stochastic partial differential equation. A lesson learned from studying passive stochastic field theories is that they are typically constrained by time–reversal symmetry of the underlying microscopic dynamics [124]. This usually bears quite important consequences like the existence of a free energy functional of the order parameter, and correspondingly, of a unique Boltzmann distribution in steady–state as well as the validity of detailed balance and of the fluctuation–dissipation theorem. Typically, active materials that dissipate a continuous supply of energy by converting it into motion at the particle scale, are intrinsically not symmetric with respect to time–reversal and therefore they lack the aforementioned properties. In recent literature, several active field theories have been proposed to study, at the continuum level, systems of self–propelled particles of various types [125–127]. Casting non–equilibrium dynamical systems with many degrees of freedom in a field–theoretical language, allows one to use powerful techniques such as the scaling hypothesis and the renormalization group, originally developed to tackle problems in equilibrium condensed matter and statistical physics.

The hydrodynamic theory of Toner and Tu led the way [128], by applying field–theoretical renormalization group methods to study bird flocks in their ordered phase while the counterpart near–critical disordered phase of natural swarms has been recently analyzed in Refs. [129, 130]. A dynamical field theory that minimally extends Model B for diffusive phase separation of a scalar field by the addition of a time–reversal symmetry breaking term has been proposed and analyzed in Ref. [126] and later extended in Ref. [131]. A bottom–up scalar field theory relevant to describe collective phenomena emerging in a population of cells that grow and interact through the concentration field of chemicals they secrete has been proposed and analyzed by renormalization group means in Ref. [132]. In this chapter, we reconsider such a theory and we identify a nonlinear relevant term allowed by the underlying symmetries, which, however, was missing in the original proposal and which drastically changes the resulting phase diagram.

The quest for universal rules that describe emergent phenomena in living systems is a manifestation of the growing interest, in the biologically–oriented community of physicists, to go beyond mean–field descriptions. Statistical procedures like renormalization can identify precisely when and how collective phenomena start to become more significant paving the road to the understanding of universality in active matter systems. We believe that investigating the complex collective behavior of biological systems by renormalization–group means, is a natural course of action.

3.1 Introduction

The reaction of an organism to an external stimulus is in general called taxis: There are many different tactical responses in Nature, all of which are quite ubiquitous like chemotaxis, phototaxis, galvanotaxis, and phonotaxis just to name a few [133]. Chemotaxis describes the influence of chemical substances in the environment on the movement of mobile species. This can lead to strictly or partially oriented movement as well as partially tumbling movement. The movement can be towards larger concentrations of the chemical substance, in which case it is usually termed positive chemotaxis or chemoattraction, or towards regions of smaller chemical concentration in which case it is referred to as negative chemotaxis or chemorepulsion.

Chemotaxis can be considered as one of the primary mechanisms for the self–organization of biological systems. For example, ants secrete and deposit chemical pheromones which are used as means of communication among them, transmitting a variety of messages such as alarm, presence of food or lack of some particular job–related individuals. In this way, ants can form and sustain a colony. At a smaller scale, a myxamoebae population of *Dictyostelium*, during its life cycle, grows by cell division as long as there is sufficient food. Once food resources are exhausted, the myxamoebae spread all over the available domain; after a while, a cell starts to exude cyclic adenosine monophosphate which attracts the other myxamoebae, who start to move and to form an aggregate. The aggregate then moves towards light sources, form a fruiting body, spores are spread and the life cycle begins again [134]. Chemotaxis is also an important mean for cellular communication, which determines how cells arrange and organize for example in morphogenesis [135–137], tissue growth and homeostasis [138], wound healing [139] and cancer metastasis [140]

but also at smaller scales and for more primitive systems such as enzymes and synthetically active colloids [141, 142].

Phenomenological models describing chemotaxis as a directed motion guided by the chemical gradients [143–145] and undergoing stochastic fluctuations [146–149] have proven useful in studying chemotactic aggregation (collapse) [150, 151] of bacteria and collective behavior of synthetically active colloids [152, 153]. A common feature among all these models is that they all encode the essential long–range nature of the chemotactic interaction. It is not surprising, in fact, that the chemotactic interaction shares some of the features of other long–range interactions, such as the electrostatic and gravitational one, and the self–organization of chemotactic species resembles the formation of galaxies in astrophysics, as well as the large–scale structures formed by vortices in two–dimensional turbulence [154–157]. The interplay between birth and death of the living individuals of a colony as well as that of the chemical signals, adds another level of complexity to the collective properties of growing colonies [132, 158, 159].

In this chapter, we investigate via a renormalization group approach, the large–scale collective properties of systems of particles that interact via chemotaxis and which can undergo birth and decay processes. In doing so we follow a bottom–up strategy, starting from the original model of chemotaxis proposed by Keller and Segel [143, 144] (in which no birth and decay were considered) and introducing the corresponding coarse–grained field theory. Based on dimensional analysis and symmetry arguments, we introduce a novel chemotactic nonlinear term representing polarization–induced interactions which happens to break detailed balance. Such a term fundamentally changes the known phase diagram of chemotaxis [132] similarly as the introduction of a symmetry–allowed nonlinear term recently updated the essentially incomplete conserved KPZ theory [160–162]. The crucial feature of the novel Galilean–invariant Langevin equation is the non–renormalization of the effective noise and of the effective vertex function, which results in exact scaling exponents valid in all dimensions and to all orders in perturbation theory. We finally consider the logistic extension of the Langevin equation governing chemotaxis to account for birth and decay processes. We study how this interaction, which does not conserve the number of particles, modifies the phase diagram of the former conserved case, indicating possible motivations behind the runaway behavior observed.

Finally, we conclude with some remarks on the analogies between chemotaxis and KPZ–like theories suggesting possible implications of our analysis and we propose possible relevant directions for further studies.

3.2 Chemotaxis

Chemotactic aggregation in biological systems is usually studied in terms of the Keller–Segel (KS) model [143, 144], which provides a mean–field description of the phenomenon, able to capture the salient features of this interaction. The standard KS model is expressed as a reaction–diffusion system of two coupled differential equations which govern the evolution of the density $\rho(t, \vec{x})$ of the active particles considered, e.g. cells, and the concentration $c(t, \vec{x})$ of the secreted chemicals:

$$\partial_t \rho = \vec{\nabla} \cdot (D_\rho \, \vec{\nabla} \rho - \mu \, \rho \vec{\nabla} c) \,, \tag{3.2.1}$$

$$\partial_t c = D_c \, \nabla^2 c - k \, c + h \, \rho \,. \tag{3.2.2}$$

Equation (3.2.1) then describes the dynamics of the species, which diffuse with a diffusion coefficient D_ρ and, in addition to this diffusive motion, they move in the direction of the gradient of chemicals (chemotactic drift) with a particle current $\mu \, \rho \vec{\nabla} c$. The coefficient μ is called chemotactic sensitivity and it measures the strength of the influence of chemicals on the motion of the cells. The sensitivity μ can be either positive (chemoattraction) or negative (chemorepulsion): In the first case the species climb up the chemical gradient and eventually give rise to an aggregation process called chemotactic collapse; in the second case, instead, the chemicals act as a poison and the particles repel each other. The second equation in the KS model, Eq. (3.2.2), expresses the model assumption that the signal substance with concentration $c(t, \vec{x})$, besides diffusing with a diffusion coefficient D_c and degrading with a rate $k > 0$ as most chemicals do, is permanently produced by active particles with a rate $h > 0$. When the diffusion of chemicals is sufficiently fast compared to the species dynamics [163], one can make a quasi–stationary approximation $\partial_t c(t, \vec{x}) \simeq 0$ which leads to the following screened Poisson equation for the chemicals

$$\nabla^2 c - k_0 \, c = a \, \rho \,, \tag{3.2.3}$$

where we introduced $a \equiv h/D_c$ and $k_0 \equiv k/D_c$. This limit turns out to be physically reasonable and particularly useful in describing the long–time and large–distance properties of chemotaxis, which is the main purpose of the present Chapter.

It is essential to understand that the KS model given in Eqs. (3.2.1) and (3.2.2) is a deterministic mean–field model in which fluctuations are ignored. In order to go beyond such a description, it is convenient to adopt a microscopic description of chemotaxis [164], in which active particles are described on an individual basis, but the chemical signals are treated in the continuum limit. This is due to the clear length– and time–scale separation between microscopic orgnanisms and molecular fluids. A corpuscular description of the dynamics of the mobile species is obtained by considering N individual non–interacting particles moving in a d–dimensional space, coupled in terms of the following stochastic Langevin equations

$$\partial_t \vec{x}_i = \mu \vec{\nabla} c(t, \vec{x}_i(t)) + \sqrt{2D_\rho}\, \vec{\zeta}_i(t)\,, \tag{3.2.4}$$

$$\nabla^2 c = k_0\, c + a \sum_{i=1}^{N} \delta(\vec{x} - \vec{x}_i(t))\,, \tag{3.2.5}$$

where $\vec{x}_i$ describes the position of the particle i, which undergoes an overdamped motion in some medium feeling the effect of the chemicals, whose density field is indicated by c; $\zeta_i(t)$ is a white noise satisfying $\langle \zeta_i(t) \rangle = 0$ and whose correlation function reads $\langle \zeta_i(t)\zeta_j(t') \rangle = \delta_{ij}\delta(t - t')$. It is clear that within the mean–field approximation, one recovers the quasi–stationary KS model.

Self-gravitating brownian systems

Before focusing on the analysis of the model presented above, it is worth to point out some analogies between the KS model and an apparently unrelated physical system. To this purpose, consider a system of N Brownian particles immersed in a fluid. We assume that, on the particle i, the fluid exerts a friction force $-\xi\, \vec{v}_i$ and a stochastic force modelled by a white noise $\zeta_i(t)$ such that $\langle \zeta_i(t) \rangle = 0$ and $\langle \zeta_i(t)\zeta_j(t') \rangle = \delta_{ij}\delta(t - t')$. Such a stochastic force can model the classical Brownian motion, the turbulence induced by the fluid or any other stochastic effect. In addition, we assume that the particles interact with each other gravitationally. The corresponding stochastic

Langevin equation regulating the motion of each particle, with mass $m = 1$, is

$$\frac{d\vec{v}_i}{dt} = -\xi\,\vec{v}_i - \vec{\nabla}_i\Phi(\vec{r}_i) + \sqrt{2D}\,\vec{\zeta}_i(t)\,, \tag{3.2.6}$$

where Φ is the gravitational potential and we relate the inverse temperature $\beta \equiv 1/T$ to the friction term according to the Einstein relation $\xi = D\beta$. In the large–friction limit $\xi \to \infty$, i.e., overdamped motion or, equivalently, at large times $t \gg \xi^{-1}$, we can neglect the inertia of the particles in Eq. (3.2.6) and essentially recover the structure of Eq. (3.2.4). Performing a mean–field approximation we can write the so–called Smoluchowski–Poisson system of equations [154, 165, 166] satisfied by the density $\rho(t, \vec{x})$, namely

$$\partial_t\rho = \vec{\nabla}\cdot\left[\xi^{-1}(T\vec{\nabla}\rho + \rho\vec{\nabla}\Phi)\right]\,, \tag{3.2.7}$$

$$\nabla^2\Phi = 4\pi G\rho\,, \tag{3.2.8}$$

where G is the gravitational constant. Clearly, the Smoluchowsky–Poisson system of Eqs. (3.2.7) and (3.2.8) describing self–gravitating Brownian particles in the high friction limit and the Keller-Segel model of chemotaxis in Eqs. (3.2.1) and (3.2.2) in the absence of degradation of chemicals $k_0 = 0$, are equivalent. In particular we have the correspondonce $\Phi \leftrightarrow 4\pi Gc/a$, $\beta \leftrightarrow \mu a/(4\pi GD)$ and $\xi \leftrightarrow 4\pi G/(a\mu)$: The concentration of the secreted chemical c plays the role of the gravitational potential Φ.

There are striking similarities between self–gravitating systems, bacterial populations and two–dimensional vortices: As already noted in Ref. [157], such similarities can be attributed to the the long–range nature of the interactions governing their respective behaviors and to the fact that they interact via a field produced by the distribution of the individuals themselves via a Poisson equation. In this respect, we consider particularly interesting to elevate these analogies to the level of universality, and to reinterpret the results of the renormalization–group analysis presented below for chemotaxis in the case of gravitating systems.

3.3 Coarse–grained field theory of chemotaxis

Since we are interested in the long–time and large–scale behavior of the system, it is convenient to move from a microscopic description, where active walkers are considered on an individual basis, to a field description where a smoothly varying density of walkers is considered. Fluctuations can be included following the approach indicated by D.S. Dean in Ref. [167], which yields a coarse–grained field theory for the density distribution of chemotactic species [157]. Due to its fundamental role, we briefly review that approach for the KS model in Appendix C.1. Upon coarse–graining, the Langevin equation governing the density of particles is given by

$$\partial_t \rho = \vec{\nabla} \cdot \left(D_\rho \vec{\nabla} \rho - \mu_1 \, \rho \vec{\nabla} \phi - \mu_2 \vec{\nabla} (\vec{\nabla} \phi)^2 \right) + \zeta \,, \tag{3.3.1}$$

$$-\nabla^2 \phi = a \, \rho \,, \tag{3.3.2}$$

where $\rho(t, \vec{x})$ is the deviation of the cell concentration $C = C_0 + \rho(t, \vec{x})$ from a background average value C_0,[1] and where $\phi(t, \vec{x})$ is the density of chemical agents released by the cells and present in the surrounding medium. We notice that assuming that the particles release chemicals at constant rate, they create a chemical background the average concentration of which is spatially uniform. As the particles sense only chemical gradients, ϕ may be considered as representing the fluctuations from this background field. Cell diffusivity is again denoted by D_ρ, while the chemotactic sensitivities $\mu_{1,2}$ measure the strength of the interaction between the cells and the chemicals field. In the following we set $a = 1$ without loss of generality.[2] The stochastic nature of the dynamics is accounted for by the noise ζ whose correlation function reads, in d spatial dimensions,

$$\langle \zeta(t, \vec{x}) \zeta(t', \vec{x}') \rangle = 2(\Omega_0 - \Omega_2 \nabla^2) \, \delta^d(\vec{x} - \vec{x}') \delta(t - t') \,, \tag{3.3.3}$$

where the coefficients Ω_0 and Ω_2 generically depend on the actual concentration C of particles, as they have to vanish in the possible absorbing states of the dynamics, resulting into multiplicative noise. However, here we are interested in investigating

[1] With abuse of notation we refer to fluctuations in the density of particles above a background value C_0 with the same name ρ as in Eq. (3.2.1), even if the latter has to be intended as C.

[2] Notice that this is achieved by a rescaling of the chemotactic coupling constants: $\mu_1 \to a\mu_1$ and $\mu_2 \to a^2 \mu_2$.

the behavior of fluctuations away from them and therefore we assume $C \simeq C_0$ in the noise which becomes additive.[3] In particular, the term proportional to Ω_2 corresponds to a noise in the particle current, and thus it conserves the particle number, while that proportional to Ω_0 corresponds to a noise in the particle density which does not conserve the total particle number. In Eq. (3.3.1), the term $\mu_1 \vec{\nabla} \cdot (\rho \vec{\nabla} \phi)$ on the right–hand side describes the chemotactic interaction whereby the particle density C receives a contribution $-\vec{\nabla} \cdot \vec{J}_\phi$ to its time derivative $\partial_t C$ because of the particle current $\vec{J}_\phi = \mu_1 C \vec{\nabla} \phi$ due to the particle motion in the direction of the gradient of the chemical concentration ϕ. As we have seen, this term naturally emerges from the microscopic derivation of the KS model and in its stochastic generalization [157]. The term $\mu_2 \nabla^2 (\vec{\nabla} \phi)^2$, instead, has never been anticipated on the basis of a microscopic derivation and generalization thereof but, on the other hand, it emerges naturally only upon coarse–graining such a microscopic dynamics, and retaining all those terms allowed by the dimensional analysis and which are compatible with the symmetries of the theory. In fact, even if this term is not included in the original Langevin equation by assuming $\mu_2 = 0$, it is effectively generated by fluctuations already at the lowest, one–loop order and therefore it needs to be accounted for in the effective description of the model. We are going to discuss on the microscopic physical interpretation of this term in section 3.3.2. Note that because of the Poisson equation (3.3.2), the terms proportional to μ_1 and μ_2 are linearly dependent in $d = 1$, but they yield different chemotactic contributions in higher dimensions. The resulting dynamics may locally conserve the particle density $\rho(t, \vec{x})$ such that its spatial integral, i.e., the total particle number is actually fixed to its initial value. This is the case, for example, of a colloidal dispersion in which each active colloid releases chemicals in the surrounding medium and moves according to the sensed gradient.

3.3.1 Symmetries of the conserved dynamics

We discuss here the symmetries of the chemotaxis model since they entail important consequences in the renormalization–group analysis of the model to be presented next. The Langevin Eq. (3.3.1), possesses a ϕ–shift symmetry and a 'Galilean' symmetry: The first is a direct consequence of the fact that the chemical field ϕ always

[3] In the vicinity of the critical point and provided that an expansion in powers of ρ of the various coefficients which depend on $C = C_0 + \rho$ with $C_0 \neq 0$ can be performed, multiplicative noise terms can be shown to be irrelevant in the renormalization–group sense (see Appendix C.1).

appears in terms of its gradient, which makes the Langevin equation trivially invariant under the shift $\phi \to \phi + \text{const}$; the second expresses the invariance of the dynamics under the transformation

$$\phi'(t', \vec{x}') = \phi(t, \vec{x} + t(\mu_1 - 2\mu_2)\,\vec{w}) - \vec{w} \cdot \vec{x}\,, \tag{3.3.4}$$

$$\rho'(t', \vec{x}') = \rho(t, \vec{x} + t(\mu_1 - 2\mu_2)\,\vec{w})\,, \tag{3.3.5}$$

where $\vec{w}$ is a generic boost vector. Under these transformations, in fact, the Langevin Eq. (3.3.1) satisfies the following equation

$$\partial_t \rho = \vec{\nabla} \cdot \left(D_\rho \vec{\nabla}\rho - \mu_1\, \rho \vec{\nabla}\phi - \mu_2 \vec{\nabla}(\vec{\nabla}\phi)^2 \right) + \zeta(t, \vec{x} + t(\mu_1 - 2\mu_2)\vec{w})\,, \tag{3.3.6}$$

and we clearly see that, while the deterministic part of Eq. (3.3.1) is left invariant by this transformation, the stochastic part is now subject to a shifted noise $\zeta(t, \vec{x} + t(\mu_1 - 2\mu_2)\vec{w})$. This implies that the correlation in the noise ζ', reads

$$\begin{aligned} \langle \zeta'(t_1, \vec{x}_1)\zeta'(t_2, \vec{x}_2)\rangle &= \langle \zeta'(t_1, \vec{x}_1 + t_1(\mu_1 - 2\mu_2)\vec{w})\, \zeta'(t_2, \vec{x}_2 + t_1(\mu_1 - 2\mu_2)\vec{w})\rangle\,, \\ &\equiv g(t_1 - t_2, \vec{x}_1 - \vec{x}_2 + (t_1 - t_2)(\mu_1 - 2\mu_2)\vec{w})\,, \end{aligned} \tag{3.3.7}$$

where g measures the noise correlations in the original equation. In the absence of temporal correlations, i.e., when $g(t, \vec{x}) = \delta(t)g(\vec{x})$, we evince that the noise correlations for the new noise ζ' are identical to that in the original equation, namely

$$g'(t, \vec{x}) = g(t, \vec{x} + t(\mu_1 - 2\mu_2)\vec{w}) = \delta(t)g(\vec{x} + t(\mu_1 - 2\mu_2)\vec{w})) = \delta(t)g(\vec{x})\,. \tag{3.3.8}$$

We conclude therefore that the stochastic Langevin equation (3.3.1) is invariant under the Galilean transformation only if the noise has no temporal correlations [168]. We anticipate here that, since the couplings μ_1 and μ_2 appear in the Galilean transformations of Eqs. (3.3.4) and (3.3.5), the diagrams contributing to their renormalization would vanish to all orders in perturbation theory, see section 3.4.1. Suppose, in fact, that we carry out some renormalization procedure (the details of which do not matter); the Galilean invariance, which is an exact symmetry of the microscopic dynamics, requires a cancellation of the terms involving the Galilean boost vector $\vec{w}$ on the l.h.s. of Eq. (3.3.6) with the corresponding ones on the r.h.s. If, as a result of the

renormalization, the nonlinearity μ_0 changes as $\mu_0 \to \mu^{\rm R}$, that cancellation would no longer occur. In short, any coefficient in front of the non–linear term (other than unity) would appear to break the Galilean invariance.

3.3.2 Dimensional Analysis

The essential statement of the dynamic scaling hypothesis can be summarised as follows: Space and time are tied together by the dynamic scaling exponent z and therefore their rescaling cannot proceed independently. A change in scale $\vec{x} \to b\,\vec{x}$ is accompanied, in fact, by $t \to b^z\,t$, $\rho \to b^\chi \rho$ and, in terms of the Poisson Eq. (3.3.2), by $\phi \to b^{\chi+2}\phi$ with b a rescaling parameter. The exponents χ and z contain the scaling information, and therefore the dynamic universality class, of the Langevin Eq. (3.3.1), and they can be studied first by a naive dimensional analysis. After this rescaling, in the conserved–noise, the Langevin Eq. (3.3.1) transforms to

$$b^{\chi-z}\,\partial_t\rho = D_\rho\,b^{\chi-2}\,\nabla^2\rho - \mu_1\,b^{2\chi}\,\vec{\nabla}(\rho\vec{\nabla}\phi) - \mu_2\,b^{2\chi}\,\nabla^2(\vec{\nabla}\phi)^2 + b^{-(d+2+z)/2}\,\zeta\,, \quad (3.3.9)$$

where we used Eq. (3.3.3) with $\Omega_0 = 0$ to determine the scaling of the noise $\zeta(t,\vec{x})$; Accordingly under this transformation the parameters are scaled as

$$D_\rho \to b^{z-2}\,D_\rho\,, \qquad \Omega_2 \to b^{-d-2+z-2\chi}\,\Omega_2\,, \qquad \mu_{1,2} \to b^{\chi+z}\,\mu_{1,2}\,. \quad (3.3.10)$$

In the absence of the nonlinearities (i.e., $\mu_1 = \mu_2 = 0$) the equation becomes scale invariant upon choosing $z_0 = 2$ and $\chi_0 = -d/2$. The nonlinearities μ_1 and μ_2, when added to this scale–invariant equation, have dimension $y_0 = (4-d)/2$, which identifies the upper critical dimension of the model to be $d_c = 4$: For $d > d_c$ the nonlinearities scale to zero and they are irrelevant, while for $d < d_c$ the nonlinearities are relevant and grow under rescaling. This change of behavior at d_c is captured by a renormalization–group analysis to be described next. The same dimensional analysis in the presence of the non–conserving noise only ($\Omega_2 = 0$) reveals that the upper critical dimension in this case is $d_c = 6$. We are going to discuss more about the non–conserved noise case in relation to possible logistic extensions of the Langevin Eq. (3.3.1), see Sec. 3.6.

Before discussing the renormalization–group analysis of the model, we motivate the functional form of the non–linearities in the Langevin equation (3.3.1). One

can wonder which general form an interaction term compatible with the symmetries of the model assumes. Naively, upon coarse–graining of the microscopic KS model one is led to identify the term $\mu_1 \vec{\nabla}(\rho \vec{\nabla}\phi)$ as the only interaction term [132]. An analysis of the symmetry–allowed interaction terms marginal at d_c, reported in Appendix C.4, reveals that a second term must be included in the description of the coarse–grained model, i.e., $\mu_2 \nabla^2 (\vec{\nabla}\phi)^2$. While the physical interpretation of the chemotactic interaction term μ_1 is rather direct, the newly introduced interaction term μ_2 can be related to the average–density current as a result of the dipolar moments induced by the chemical field: In the case of polarizable particles, such a term can be attributed to the background current originating from the coupling between the chemical gradient and the polarization induced by the gradient itself.

To clarify this point, let's imagine that the active particles considered so far are indeed cells, characterized by their complex structure. Chemical receptors are distributed on the membrane of the cell and, as it is typically the case, their distribution is a function of the chemical gradient in its surrounding. These receptors, naturally tend to adjust the direction of motion of the cell in such a way to align with the direction of gradient, either along or opposite to it. For relatively small gradients, the induced dipole momentum $\vec{n}$ of the distribution of the receptors can be assumed to be linearly proportional to the chemical gradient, namely $\vec{n} = \gamma \vec{\nabla}\phi$. At this order, the equation of motion (3.2.4) for the single chemotactic cell becomes

$$\partial_t \vec{x}_i = \mu \vec{\nabla}\phi + \gamma \vec{\nabla}(\vec{n} \cdot \vec{\nabla}\phi) + \sqrt{2D_\rho}\, \zeta_i(t)\,, \tag{3.3.11}$$

$$\sim \mu_1 \vec{\nabla}\phi + \mu_2 \vec{\nabla}(\vec{\nabla}\phi)^2 + \sqrt{2D_\rho}\, \zeta_i(t)\,. \tag{3.3.12}$$

The second term on the r.h.s. of the latter equation can describe the polarization mode of chemotaxis which is observed, for instance, in neutrophils [169] when the chemical field is considered in the continuum limit. When a colony of cells is considered, upon coarse–graining the microscopic dynamics in Eq. (3.3.12), the corresponding Dean formalism [167] gives rise to the Langevin Eq. (3.3.1), see Appendix C.1 for details.

3.3.3 A similar case: Conserved KPZ

A scenario which resembles the one just described for chemotaxis was recently analyzed in a different context in Ref. [162], where the essentially incomplete conserved KPZ equation was corrected by the introduction of a novel term, responsible for the emergence of a new growth phase, possibly ruled by a strong–coupling fixed point. It is worth to recall that conserved growth models are described by the following equation [161]

$$\partial_t \phi = -\vec{\nabla} \cdot \left[\vec{\nabla} \left(D_\phi \nabla^2 \phi + \lambda (\vec{\nabla} \phi)^2 \right) \right] + \zeta \,, \tag{3.3.13}$$

where $\phi(\vec{x}, t)$ indicates the height of the surface above the point $\vec{x}$ and ζ is a Gaussian conserved noise. The nonlinear term $\propto \lambda$ is typical in conserved growth models and it is formally identical to the one we introduced for chemotaxis; usually, it is attributed to non–equilibrium correction to the chemical potential [170]. The authors in Ref. [162] introduced a symmetry–allowed nonlinear gradient term of the form $\vec{\nabla} \cdot ((\nabla^2 \phi) \vec{\nabla} \phi)$ to generalize the conserved KPZ model (the novel model has been called conserved KPZ+); this term, on the other hand, is identical to the chemotactic interaction term μ_1 emerging from the KS model. From a purely mathematical point of view, the only difference between conserved chemotaxis and conserved KPZ is the fact that in the first case one looks at the evolution of the laplacian of the field ϕ, namely $\partial_t \nabla^2 \phi$, rather than that of the field itself. This rather innocent statement, however, bears quite important consequences. In the original conserved KPZ model proposed by Sun, Guo, and Grant in Ref. [161], it was stated that, as a consequence of the (generalized) Galilean symmetry (tilt symmetry), λ in Eq. (3.3.13) changes only trivially under renormalization; this led the authors to derive supposedly exact exponents. However, as it was noted in Ref. [171], the coordinate transformation proposed in Ref. [161] is mathematically ill–defined because it mixes coordinates and linear differential operators in a coordinate substitution rule, which implies that the critical exponents have to be corrected at order ε^2. This is not the case for chemotaxis: The fact that we look at the evolution of the operator $\nabla^2 \phi$, results in the fact that the Galilean transformations of Eqs. (3.3.4) and (3.3.5) are well defined and the non–renormalization of the vertex, as we shall see in the next section, leads to exact critical exponents.

3.3.4 Violation of the fluctuation–dissipation theorem

As anticipated at the beginning of the chapter, the dynamics of active particles, typically violates time–reversal symmetry by continuously converting fuel into motion. The absence of time–reversal symmetry, on the other hand, has various consequences such as the absence of a free–energy functional $\mathcal{F}[\rho, \phi]$, the violation of detailed balance and of the fluctuation–dissipation theorem. In the case of conserving deterministic dynamics, it is natural to investigate if the chemotaxis interaction terms μ_1 and μ_2 can be derived from a certain free–energy functional $\mathcal{F}$. The latter should appear in the dynamics as

$$\partial_t \rho(\vec{x}, t) = \vec{\nabla} \cdot \left(\rho(\vec{x}, t) \vec{\nabla} \frac{\delta \mathcal{F}[\rho, \phi]}{\delta \rho(\vec{x}, t)} \right), \tag{3.3.14}$$

where we assume the particle current to be proportional to the particle density ρ. While the term $\propto \rho$, typical of the Keller–Segel model, can be derived from the functional $\mathcal{F}_1 = \int \rho(t, \vec{x})\, \phi(t, \vec{x})$, the μ_2 term on the r.h.s. of Eq. (3.3.1) is not the derivative of any functional. The latter, in principle, it could be derived from a functional $\mathcal{F}_2 = \int \rho(t, \vec{x})\, (\vec{\nabla}\phi(t, \vec{x}))^2$. However, this would imply that the free-energy functional $\mathcal{F}$ satisfies

$$\frac{\delta^2 \mathcal{F}_2}{\delta \rho(\vec{x}') \delta \rho(\vec{x})} = 2 \left(\vec{\nabla} \phi(\vec{x}) \right) \cdot \frac{\delta \vec{\nabla} \phi(\vec{x})}{\delta \rho(\vec{x}')} = -2 \left(\vec{\nabla} \phi(\vec{x}) \right) \cdot \frac{\delta \vec{\nabla}' \phi(\vec{x}')}{\delta \rho(\vec{x})} \neq \frac{\delta^2 \mathcal{F}_2}{\delta \rho(\vec{x}) \delta \rho(\vec{x}')},$$

unless $\vec{\nabla}' \phi(\vec{x}') = -\vec{\nabla} \phi(\vec{x})$, which does not hold in the general case. Accordingly, we conclude that the introduction of the μ_2 non–linearity results in the violation of detailed–balance.

3.4 Renormalization–group analysis

The renormalization group can be considered as a set of scale transformations in terms of which universal scale–invariant properties of a system at its critical point can be obtained. The RG establishes a correspondence between the values of the effective couplings which define the model at different length– and time–scales: The original one and a new, thinned–out scale in which the microscopic fluctuations have been effectively integrated out, resulting in modified couplings at the

new scale. A RG transformation, in fact, unfolds in two stages: *i*) integration of the short–wavelength details and, *ii*) rescaling of fields, length and time. In Wilson's approach [6], the first operation is the so–called momentum–shell integration, which consists in integrating out the fluctuations over large values of the momentum k within a shell $\Lambda/b < k < \Lambda$, where $b > 1$ is a rescaling factor. As a result, the cutoff is shifted from its original value Λ to Λ/b but, in order to be able to compare theories with similar microscopic structure, the second operation consists in rescaling space and time in such a way to restore the original cutoff Λ. The compound effect of these two stages is to effectively change the various coupling constants describing the system, hence determining, after repeated transformations, a flow in the space of the (running) coupling constants themselves. At criticality, however, the running couplings are no longer affected by further renormalization transformations, representing fixed points of the RG transformation. Fixed points contain therefore all the relevant information about the large–distance and long–time scale–invariant behavior of the system.

3.4.1 Perturbative expansion

As we have seen in section 3.3.2, interesting dynamic effects are expected to arise from the interaction terms μ_1 and μ_2 below the upper critical dimension d_c; we must, therefore, have a systematic procedure for expanding the correlation functions in powers of the nonlinearities.[4] The perturbative expansion can be carried out in terms of the generating functional approach known as response function formalism [172], in terms of which averages of physical observables over the stochastic dynamics are rewritten as thermal averages over a functional measure. The great advantage of using this formalism is that the standard Feynman technique can be used to perform a diagrammatic loop expansion so that perturbation theory can be set up as in equilibrium statistical field theory. Details on this formalism are reviewed in Appendix C.2. The generating functional for correlation and response functions reads

$$Z[\mathbb{J}] = \int \mathcal{D}\Psi \, \mathrm{e}^{-\mathcal{S}[\Psi] + \int_{\hat{x}} \mathbb{J}^{\mathrm{T}}(\hat{x}) \cdot \Psi(\hat{x})} \,, \tag{3.4.1}$$

[4] The expansion turns out to be meaningful for $d \simeq d_c$, i.e., for $0 < \varepsilon \equiv 4 - d \ll 1$ in the conserved case and for $0 < \varepsilon \equiv 6 - d \ll 1$ in the non–conserved one.

where we adopt a matrix notation indicating the field content by $\Psi \equiv (\rho, \tilde{\rho}, \phi, \tilde{\phi})$, the corresponding sources by $\mathbb{J} \equiv (j_\rho, \tilde{j}_\rho, j_\phi, \tilde{j}_\phi)$ and the action $\mathcal{S}[\Psi]$, derived from Eqs. (3.3.1) and (3.3.2), reads

$$\mathcal{S}[\rho,\tilde{\rho},\phi,\tilde{\phi}] = \int_{\hat{x}} \left\{ \tilde{\rho} \left[\partial_t \rho - D_\rho \nabla^2 \rho + \mu_1 \vec{\nabla}(\rho \vec{\nabla}\phi) + \mu_2 \nabla^2 (\vec{\nabla}\phi)^2 \right] - \Omega_0 \tilde{\rho}^2 + \Omega_2 \tilde{\rho} \nabla^2 \tilde{\rho} \right\} + \int_{\hat{x}} \tilde{\phi} \left(-\nabla^2 \phi - a\, \rho \right) , \tag{3.4.2}$$

and we introduced the shorthand notation $\int_{\hat{x}} \equiv \int \mathrm{d}^d \vec{x}\, \mathrm{d}t$ and $\hat{x} = (t, \vec{x})$. We remind that within this formalism the functional integrals over the response fields $\tilde{\rho}$ and $\tilde{\phi}$ are performed along the imaginary axis, whereas ρ and ϕ are real fields.

The starting point to set up the perturbative expansion, as in equilibrium statistical physics, is the Gaussian theory, which can be obtained by setting to zero all the non–linearities present in the theory, i.e., $\mu_1 = 0$ and $\mu_2 = 0$. It is particularly convenient to reconsider the theory in Fourier space and to notice that the term in the second line of Eq. (3.4.2) — which involves a linear term in $\tilde{\phi}$ — can be integrated out and fixes the relationship between ϕ and ρ to be given by Eq. (3.3.2).[5] From the resulting action expressed solely in terms of $\tilde{\rho}$ and ρ, one can read off the corresponding expressions for the response function G_0 (bare propagator) and the noise correlation function Θ_0 (bare noise), which turn out to be,

$$G_0(\vec{k},\omega) = \langle \tilde{\rho}(-\vec{k},-\omega)\, \rho(\vec{k},\omega) \rangle_0 = (-i\tau\, \omega + D_\rho\, k^2)^{-1} , \tag{3.4.3}$$

$$\Theta_0(\vec{k}) = \langle \rho(-\vec{k})\, \rho(\vec{k}) \rangle_0 = 2(\Omega_0 + \Omega_2\, k^2) \left| G_0(\vec{k},\omega) \right|^2 . \tag{3.4.4}$$

Analogously, from the interaction part of the action (3.4.2), it is easy to infer the three–point vertex function Γ_0 (bare vertex) representing the $\tilde{\rho}\rho^2$–interaction at the symmetrized point [6]

$$\Gamma_0(\vec{k},\vec{q}) = \frac{\mu_1}{2} \left(\frac{\vec{k}\cdot\vec{q}}{q^2} + \frac{\vec{k}\cdot(\vec{k}-\vec{q})}{(\vec{k}-\vec{q})^2} \right) - \mu_2 \frac{k^2 \vec{q}\cdot(\vec{k}-\vec{q})}{q^2 (\vec{k}-\vec{q})^2} . \tag{3.4.5}$$

At this point it should be noticed that the symmetrization of the vertex implies that

[5] Recall that we set $a = 1$.

[6] We use the following Fourier convention: $f(t,\vec{x}) = \int_{\hat{k}} f(\omega,\vec{k})\, \mathrm{e}^{-i\vec{k}\cdot\vec{x}+i\omega t}$.

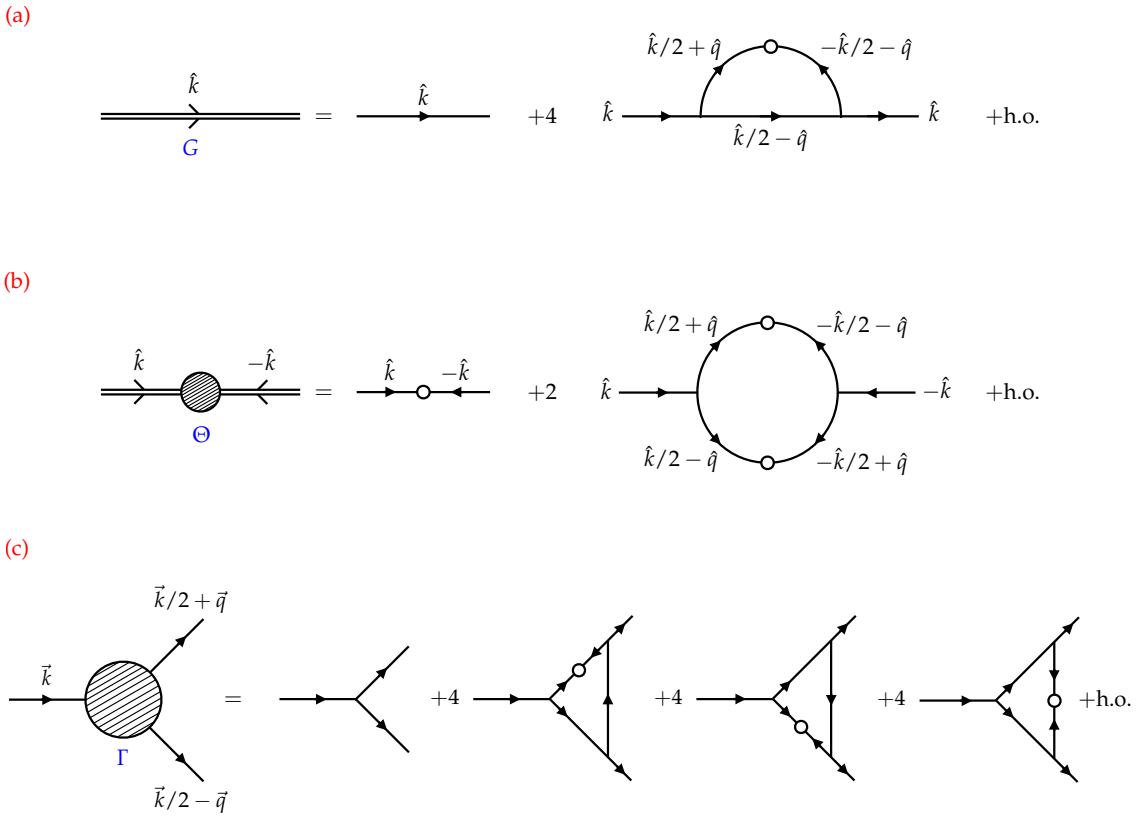

Figure 3.1: Diagrammatic representation of the one–loop (a) effective propagator or response function, (b) effective noise correlator and (c) effective vertex function. The combinatorial factors take into account possible noise contractions.

$\Gamma_0(\vec{k},\vec{q}) = \Gamma_0(\vec{k},\vec{k}-\vec{q})$ and on the other hand ensures that the momentum–shell regularization scheme adopted in this Chapter does not break the translational symmetry of the original action [173, 174]. In terms of the basic ingredients G_0, Θ_0 and Γ_0, the perturbative expansion can be systematically organized as a loop expansion to describe an effective propagator or response function G, an effective noise correlator Θ and an effective vertex function Γ as they result from nonlinear fluctuation corrections below the upper critical dimension. The corresponding one–loop diagrammatic representation is given in Fig. 3.1 .

3.4.2 Momentum–shell integrations

Lowest order one–loop corrections (integrals) are computed within the momentum-shell and as there are no singularities in this range of integration, only analytic corrections to the coupling constants result after the elimination of the fast modes.

Renormalization of the propagator

The effects of the nonlinearities μ_1 and μ_2 on the response function may be expressed in terms of the self-energy Σ by means of the standard Dyson equation $G(\vec{k},\omega) = G_0(\vec{k},\omega) + \Sigma(\vec{k},\omega)$. At one–loop in the diagrammatic expansion we have

$$\Sigma_1(\hat{k}) = \frac{8}{2!}\int_{\hat{q}}^{>} \Theta_0(\vec{k}/2+\vec{q})\Gamma_0(\vec{k},\vec{k}/2+\vec{q})\Gamma_0(\vec{k}/2-\vec{q},\vec{k})G_0(\hat{k}/2-\hat{q})\,, \tag{3.4.6}$$

where we have indicated $\int_{\hat{q}}^{>} \equiv \int_{-\infty}^{+\infty} d\omega \int_{\mathrm{S}} d^d\vec{q}$, where $\mathrm{S} = \{\vec{q} : \ \Lambda/b \leq |\vec{q}| \leq \Lambda\}$, and the combinatorial factor of four represents the various possible noise contractions leading to Fig. 3.1 (a). The self energy modifies the location of the poles of the propagator in the frequency plane, which we compute using residues; the d–dimensional integral over the internal momentum $\vec{q}$ is calculated in spherical coordinates taking advantage of the fact that, setting $b = \mathrm{e}^{\ell}$ and in the $\ell \to 0$ limit, that is for an infinitesimal RG transformation, the shell becomes infinitesimally thin and therefore the integral can be evaluated as the shell thickness $\Lambda\ell$ times the integrand evaluated at $q = \Lambda$, i.e., $\int_q^{>} f(q) = f(\Lambda)\Lambda\ell + O(\ell^2)$. From the resulting expression we can read–off the differential RG flow equation for the renormalized diffusion coefficient D_ρ^{R} which in the conserved case reads

$$\begin{aligned} D_\rho^{\mathrm{R}} &\equiv -\partial_{k^2} G^{-1}(\hat{k})\Big|_{\hat{k}=\hat{0}} \\ &= D_\rho \left[1 - \frac{K_d \ell \Lambda^{d-4}\Omega_2}{D_\rho^3}\left(\gamma_1\,\mu_1^2 + \gamma_2\,\mu_1\mu_2 + \gamma_3\,\mu_2^2\right)\right], \\ &= D_\rho \left[1 - \ell\left(\gamma_1\,\tilde{\mu}_1^2 + \gamma_2\,\tilde{\mu}_1\tilde{\mu}_2 + \gamma_3\,\tilde{\mu}_2^2\right)\right], \end{aligned} \tag{3.4.7}$$

where we introduced the following coefficients

$$\gamma_1 = \left(\frac{3}{4} - \frac{3}{2d}\right), \quad \gamma_2 = \left(2 - \frac{3d-6}{d(d+2)}\right), \quad \gamma_3 = \left(1 - \frac{4}{d}\right), \tag{3.4.8}$$

as well as the rescaled variables $\tilde{\mu}_{1,2} = \mu_{1,2}\sqrt{K_d \Lambda^{d-4} \Omega_2 / D_\rho^3}$ and we indicated by $K_d = S_d/(2\pi)^d$ where $S_d = 2\pi^d/\Gamma(d/2)$ is the area of a unit sphere in d dimensions. In the non–conserved case, the calculation proceeds as above and the renormalized diffusion coefficients read

$$D_\rho^{\mathrm{R}} = D_\rho \left[1 - \ell \left(\eta_1 \tilde{\mu}_1^2 + \eta_2 \tilde{\mu}_1 \tilde{\mu}_2 + \eta_3 \tilde{\mu}_2^2\right)\right] , \tag{3.4.9}$$

with the coefficients η_i given by

$$\eta_1 = \left(\frac{3}{4} - \frac{d+5}{d(d+2)}\right) , \quad \eta_2 = \left(2 - \frac{3d-12}{d(d+2)}\right) , \quad \eta_3 = \left(1 - \frac{6}{d}\right) , \tag{3.4.10}$$

and where the rescaled variables now reads $\tilde{\mu}_{1,2} = \mu_{1,2}\sqrt{K_d \Lambda^{d-6} \Omega_0 / D_\rho^3}$.

Non–Renormalization of the noise

The renormalization of the noise spectral density function Θ may in principle proceed analogously. However, a closer look at the diagram in Fig. 3.1 (b) reveals that the renormalization of the spectral density Θ must include at least two bare vertices with external momentum $\vec{k}$ and $-\vec{k}$. From Eq. (3.4.4) we see that the bare noise, in the limit $k \to 0$ scales as k^2 in the conserved noise case and as k^0 in the non–conserved noise one, and therefore we conclude that the one–loop renormalization produces only higher–order terms in the noise which can be safely discarded close to d_c. This result can be checked analytically by considering the one-loop correction Π_1 to the bare noise term Θ_0 which is given by the following integral

$$\Pi_1 = \frac{4}{2!} \int_{\hat{q}} \Theta_0(\vec{k}/2 + \vec{q}) \Theta_0(\vec{k}/2 - \vec{q}) \Gamma_0(\vec{k}, \vec{k}/2 + \vec{q}) \Gamma_0(-\vec{k}, -\vec{k}/2 - \vec{q}) . \tag{3.4.11}$$

The integral can be computed as explained for the renormalization of the propagator and yields the result $\Pi_1 = 0$. We conclude that there are no perturbative corrections to the noise from shell integrations at one–loop and therefore we have $\Theta^{\mathrm{R}} = \Theta_0$.

Non–renormalization of the vertex

The coupling constants μ_1 and μ_2 could in principle get a perturbative correction from the shell integration of the renormalized vertex. However, as already antici-

pated, by symmetry arguments one can already conclude that there are no corrections to the vertex to all orders in perturbation theory, namely we have that

$$\mu_1^R = \mu_1 \qquad \text{and} \qquad \mu_2^R = \mu_2\,. \tag{3.4.12}$$

We can formally prove this by constructing a Ward identity associated with the invariance under transformations (3.3.4) and (3.3.5), see section 3.3.1. The generating functional Γ of the vertex functions must accordingly remain invariant with respect to the combined variations,

$$\delta\rho = \rho(t',\vec{x}') - \rho(t,\vec{x}) = t(\mu_1 - 2\mu_2)\vec{w}\cdot\vec{\nabla}\rho\,, \tag{3.4.13}$$
$$\delta\tilde{\rho} = \tilde{\rho}(t',\vec{x}') - \tilde{\rho}(t,\vec{x}) = t(\mu_1 - 2\mu_2)\vec{w}\cdot\vec{\nabla}\tilde{\rho}\,, \tag{3.4.14}$$
$$\delta\phi = \phi(t',\vec{x}') - \phi(t,\vec{x}) = t(\mu_1 - 2\mu_2)\vec{w}\cdot\vec{\nabla}\phi - \vec{w}\cdot\vec{x}\,, \tag{3.4.15}$$
$$\delta\tilde{\phi} = \tilde{\phi}(t',\vec{x}') - \tilde{\phi}(t,\vec{x}) = t(\mu_1 - 2\mu_2)\vec{w}\cdot\vec{\nabla}\tilde{\phi}\,. \tag{3.4.16}$$

where the boost vector $\vec{w}$ is considered to be small. Since the Galilean boost vector $\vec{w}$ is arbitrary, then we have the following Ward identity

$$0 = \vec{w}\cdot\int_{\hat{x}}\left[t(\mu_1 - 2\mu_2)\left(\frac{\delta\Gamma}{\delta\rho}\vec{\nabla}\rho + \frac{\delta\Gamma}{\delta\tilde{\rho}}\vec{\nabla}\tilde{\rho} + \frac{\delta\Gamma}{\delta\phi}\vec{\nabla}\phi + \frac{\delta\Gamma}{\delta\tilde{\phi}}\vec{\nabla}\tilde{\phi}\right) - \vec{x}\,\frac{\delta\Gamma}{\delta\phi}\right]. \tag{3.4.17}$$

By taking functional derivatives and by invoking spatial and temporal translation invariance of the dynamics, one can relate vertex functions of different order. For example for the three point function one obtains in Fourier space

$$i(\mu_1 - 2\mu_2)\vec{q}\,'\,\partial_{\omega'}\Gamma_{\rho\tilde{\rho}}(\hat{q}') = \partial_{\vec{q}}\,\Gamma_{\phi\tilde{\rho}\rho}(\hat{q}=0;\hat{q}')\,, \tag{3.4.18}$$

and since the same identity holds for the renormalized vertex function as well, one concludes that the couplings are not renormalized to all orders. Due to the structure of the interaction vertices, the result is indeed confirmed by direct computation of the one–loop integrals contributing to the renormalization of the vertex represented in Fig. 3.1 (c) (see Appendix C.3).

3.4.3 Rescaling Space and Time

The compound effect of the shell integration is that the resulting theory is defined at new, smaller cutoff $\Lambda e^{-\ell}$. In order to compare the new theory with the original one, we rescale space and time as we did before, namely $\vec{x} \to e^{\ell}\vec{x}$ and therefore momentum $\vec{q} \to e^{-\ell}\vec{q}$ and $t \to e^{\ell z}t$. This choice is accompanied by rescaling the fields accordingly as $\rho \to e^{\ell\chi}\rho$ and $\tilde{\rho} \to e^{\ell\tilde{\chi}}\tilde{\rho}$, with additional corrections arising from shell integration that account for the anomalous behavior induced by the fluctuations below the critical dimension d_c, namely $\chi = (d+\eta)/2$ and $\tilde{\chi} = (d-\eta)/2$ where η is the anomalous dimension of the field ρ. Consequently the parameters D_ρ, Ω_2 (or Ω_0 in the non–conserved case) and $\mu_{1,2}$ are rescaled as in Eq. (3.3.10) with $b = e^{\ell}$, formally restoring the original cutoff, $\Lambda e^{-\ell} \to \Lambda$.

3.4.4 Beta functions and fixed–point equations

Combining the scaling equations (3.3.10) with $b = e^{\ell}$ in the limit $\ell \to 0$ with the renormalized equations obtained in Section 3.4.2, gives access to the following beta functions for the conserved chemotaxis model

$$\partial_\ell \mu_{1,2} = (z+\chi)\,\mu_{1,2}\,, \tag{3.4.19}$$

$$\partial_\ell D_\rho = (z-2)\,D_\rho - D_\rho\left(\gamma_1\,\tilde{\mu}_1^2 + \gamma_2\,\tilde{\mu}_1\tilde{\mu}_2 + \gamma_3\,\tilde{\mu}_2^2\right)\,, \tag{3.4.20}$$

$$\partial_\ell \Omega_2 = -(d+2-z+2\chi)\,\Omega_2\,, \tag{3.4.21}$$

The zeros of the beta functions determine the fixed points of the RG flow and they therefore have a crucial role in determining the critical properties of the theory. The exponents z and χ are adjusted so that the parameters are unchanged, namely $\partial_\ell D_\rho = \partial_\ell \Omega_2 = 0$, and therefore Eq. (3.4.19) indicates that the effective coupling constants $\tilde{\mu}_1$ and $\tilde{\mu}_2$ evolve under rescaling as

$$\partial_\ell \tilde{\mu}_{1,2} = \frac{1}{2}(4-d)\,\tilde{\mu}_{1,2} + \frac{3}{2}\,\tilde{\mu}_{1,2}\left(\gamma_1\,\tilde{\mu}_1^2 + \gamma_2\,\tilde{\mu}_1\tilde{\mu}_2 + \gamma_3\,\tilde{\mu}_2^2\right)\,. \tag{3.4.22}$$

This is the main result of our work and represents the one–loop renormalization group flow of the conserved chemotaxis model. The simple structure of the flow equations obtained is mainly due to the non–renormalization of the vertex function Γ and consequently of the coupling constants μ_1 and μ_2. Setting $\partial_\ell \mu_{1,2} = 0$

in Eq. (3.4.19), on the other hand, implies the identity $\chi + z = 0$. This identity is a consequence of the Galilean invariance of Eq. (3.3.1) in the presence of whatever correlations that preserve this symmetry, and it is valid to all orders in perturbation theory. The fixed point equations $\partial_\ell \tilde{\mu}_{1,2} = 0$ define the following lines of fixed points

$$\tilde{\mu}_2^* = -\frac{\gamma_2}{2\gamma_3}\,\tilde{\mu}_1^* \pm \frac{\sqrt{(\gamma_2^2 - 4\gamma_1\,\gamma_3)\,\tilde{\mu}_1^{*2} + \frac{4}{3}(d-4)\gamma_3}}{2\gamma_3}\,, \tag{3.4.23}$$

which are conics in the plane $\{\tilde{\mu}_1, \tilde{\mu}_2\}$ and their behavior is characterised by the discriminant $\Delta = [(\gamma_2/2)^2 - \gamma_1\,\gamma_3]$: when $\Delta > 0$, i.e., for $d > 1$, they are iperbolae, while in $d < 1$, when $\Delta < 0$, they are represented by an ellipse. The limiting case $\Delta = 0$ can be seen as an ellipse whose foci are at infinity and the lines of fixed points result in two straight parallel lines.

Analogously, a similar result holds in the presence of non–conserved noise, in which case we obtain the following beta functions

$$\partial_\ell \mu_{1,2} = (z + \chi)\,\mu_{1,2}\,, \tag{3.4.24}$$

$$\partial_\ell D_\rho = (z-2)\,D_\rho - D_\rho\left(\eta_1\,\tilde{\mu}_1^2 + \eta_2\,\tilde{\mu}_1\tilde{\mu}_2 + \eta_3\,\tilde{\mu}_2^2\right)\,, \tag{3.4.25}$$

$$\partial_\ell \Omega_0 = -(d - z + 2\chi)\,\Omega_0\,, \tag{3.4.26}$$

and the corresponding one–loop renormalization group flow of the dimensionless couplings is given by

$$\partial_\ell \tilde{\mu}_{1,2} = \frac{1}{2}(6-d)\,\tilde{\mu}_{1,2} + \frac{3}{2}\,\tilde{\mu}_{1,2}\left(\eta_1\,\tilde{\mu}_1^2 + \eta_2\,\tilde{\mu}_1\tilde{\mu}_2 + \eta_3\,\tilde{\mu}_2^2\right)\,, \tag{3.4.27}$$

with the corresponding lines of fixed points

$$\tilde{\mu}_2^* = -\frac{\eta_2}{2\eta_3}\,\tilde{\mu}_1^* \pm \frac{\sqrt{(\eta_2^2 - 4\eta_1\,\eta_3)\,\tilde{\mu}_1^{*2} + \frac{4}{3}(d-6)\eta_3}}{2\eta_3}\,, \tag{3.4.28}$$

for which the same qualitative features as for the conserved case hold. We emphasize here that, the qualitative description given above in terms of the discriminant Δ, however, requires the extrapolation of the flow equations to $d \simeq 1$. The perturbative calculation presented in the previous sections, and consequently the so–obtained re-

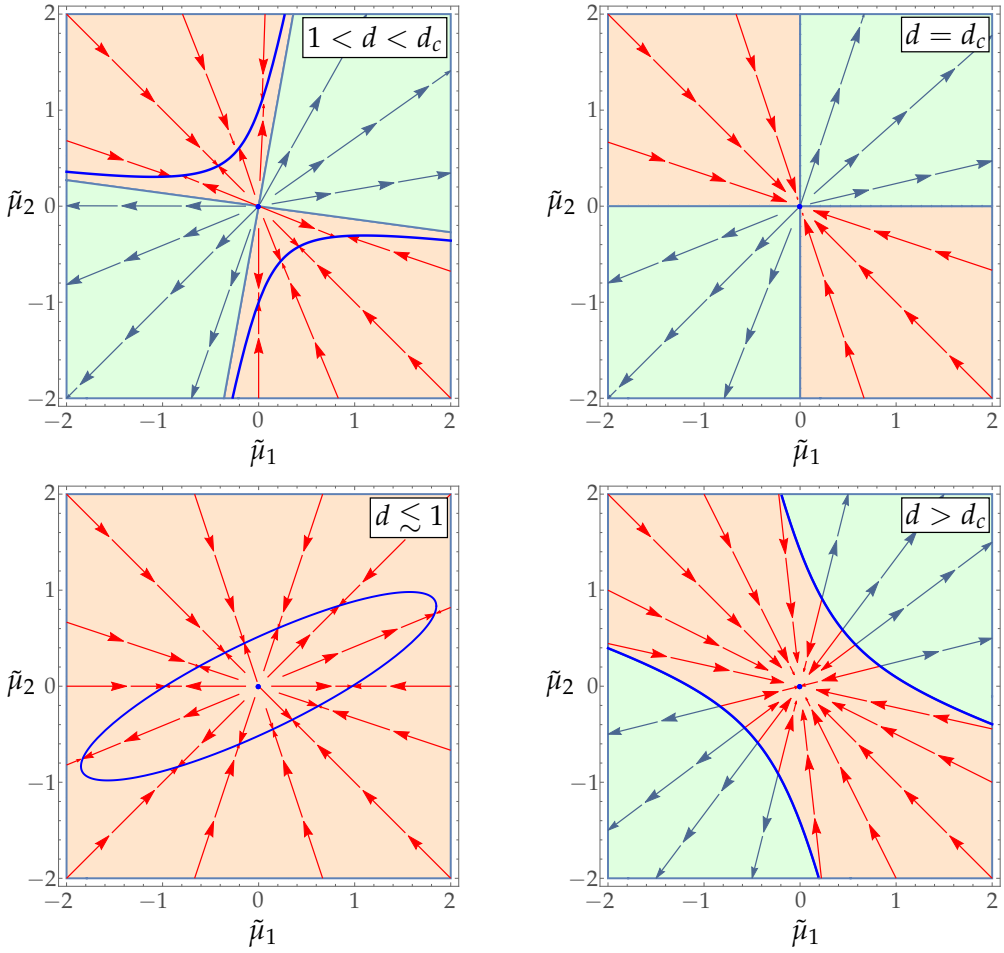

Figure 3.2: One–loop renormalization group flow of the chemotaxis model as a function of the spatial dimensionality d. In particular, the RG flow represented by Eq. (3.4.22) (and by Eq. (3.4.27) in the non–conserved case) is represented at $d = d_c$ (top right panel), for $1 < d < d_c$ (top left panel), $d \lesssim 1$ (bottom left panel) and for $d \geq d_c$ (bottom right panel). The blue lines are the fixed points given by Eq. (3.4.23) (and by Eq. (3.4.28) in the non–conserved case) while the orange and green areas mark respectively the attractive and repulsive regions of the phase diagram.

sults, should in fact be considered reliable only for $d \simeq d_c$, as a number of other terms become relevant at smaller d.

3.5 Analysis of the phase diagram

From the RG flow Eq. (3.4.22) we determine fixed points, which we recall are the points at which the parameters of the theory are unchanged under the RG transformation. Correspondingly, we study the RG flow in the $\{\tilde{\mu}_1, \tilde{\mu}_2\}$ plane as a function of the dimension d. The results for the RG flows are shown in Fig. 3.2. Apart from the Gaussian fixed point $\tilde{\mu}_1 = \tilde{\mu}_2 = 0$, whose exponents z_0 and χ_0 are determined in section 3.3.2, we find lines of fixed points defined by the conics of Eq. (3.4.23) and (3.4.28) along which the exact critical exponents are given, respectively, by

$$z^* = -\chi^* = \frac{d+2}{3} \qquad \text{conserved case}\,, \tag{3.5.1}$$

$$z^* = -\chi^* = \frac{d}{3} \qquad \text{non–conserved case}\,. \tag{3.5.2}$$

We note that the RG flow actually occurs along rays with constant ratio $r = \tilde{\mu}_1/\tilde{\mu}_2$. For $d > d_c$ the Gaussian fixed point is locally stable while the lines of fixed points are not: The basin of attraction of the Gaussian fixed point shrinks as d_c is approached from above. Below d_c the situation is reversed and the Gaussian fixed point becomes unstable while the lines of fixed points defined in Eq. (3.4.23) are stable. However, in $1 < d \leq d_c$, the latter are not globally attractive: Regions of the plane of the reduced couplings where the RG flow runs away to infinity are present (we notice that these regions exclude the $\tilde{\mu}_1 = 0$ axis). For $d \leq 1$ an interesting feature emerges: The lines of fixed points, change from hyperbolae to an ellipse, identifying a line of fixed points that is fully attractive. The limiting case $d = 1$ in which the lines of fixed points result in two straight parallel lines shares the same attractive behavior. We recall that $d = 1$ is the only case where the nonlinearities $\mu_{1,2}$ are indistinguishable. The scenario is really appealing and reminds us that observed for KPZ. In KPZ the upper critical dimension is $d_c = 2$ and $i)$ the Gaussian fixed point is stable for $d > 2$ and unstable for $d < 2$, $ii)$ a nontrivial fixed point is present and it is stable for $d < 2$ but unstable for $d > 2$, where the Gaussian fixed point has a finite basin of attraction, beyond which the flow runs away, $iii)$ the value of the coupling constant at the non-Gaussian fixed point diverges in the limit $d \to 2^-$ but $iv)$ in $d < 2$ the nontrivial fixed point is fully attractive. This latter point is the main qualitative difference since, in chemotaxis, the phase diagram exhibits a fully attractive line of

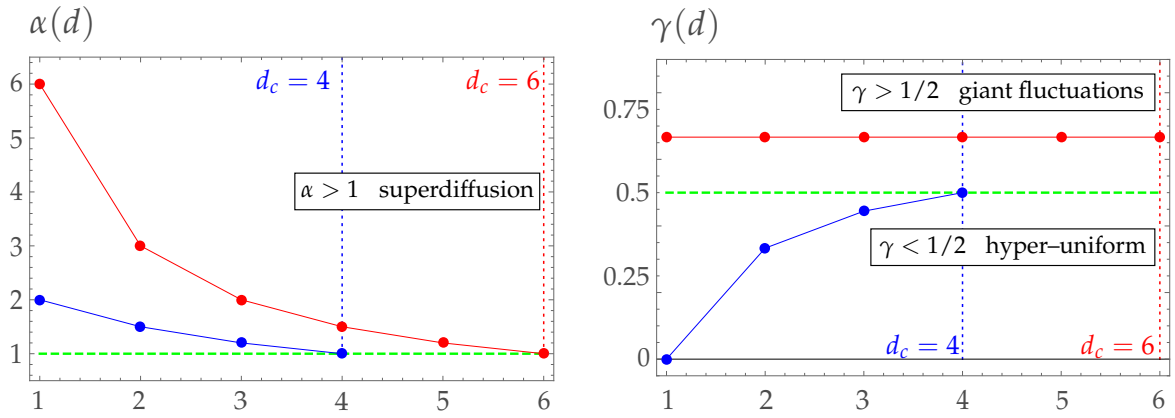

Figure 3.3: Exact critical exponents α (left panel) and γ (right panel) as a function of the dimension d, in the case of conserved noise (blue points) and non–conserved noise (red points). On the left, values of the critical exponents greater than $\alpha = 1$ (green dashed line) indicate a superdiffusive behavior of the particles at criticality; On the right, the green dashed line $\gamma = 1/2$ marks the distinction between giant fluctuations experienced by the particles in the non–conserved noise case, against a hyperuniform distribution typical of the conserved case.

fixed point only below $d = 1$ while feature *iii*) is present in chemotaxis only when $\tilde{\mu}_1 > 0$, namely for chemoattraction. In KPZ all this signifies the emergence of a non-perturbative strong–coupling fixed point. Albeit different, it is tempting to speculate that the runaway signifies the emergence of a strong–coupling fixed point in the theory of chemotaxis. However, at least two other scenarios are equally probable: The runaway behavior may be an artifact of the one–loop approximation or it may signal the transition to a phase ruled by a first–order phase transition.

Introducing the critical exponents α and γ according to $\Delta L^2 \sim t^\alpha$ and $\Delta N \sim N^\gamma$, where ΔL indicates the spatial extent of the density fluctuations in the colony and ΔN indicates the number fluctuations, the scaling relations $\Delta L \sim t^{1/z}$ and $\Delta N \sim L^{d+\chi}$ imply that $\alpha = 2/z$ and $\gamma = 1 + \chi/d$. From Fig. 3.3, where the values of these exponents are given, we conclude that the particles undergo superdiffusion, i.e. $\alpha > 1$, irrespectively of the nature of the noise. Moreover, compared to a Poisson distribution where $\gamma = 1/2$, the number fluctuations reveal a hyperuniform density distribution, i.e. $\gamma < 1/2$, in the presence of conserving noise. In the non–conserved noise, on the other hand, we observe giant number fluctuations, i.e., $\gamma > 1/2$. This last feature is shared among many active systems [175].

3.6 Logistic extensions

The discussion above focused on the case in which the particle density obeys a local conservation law; however, phenomena such as cell division may violate this conservation. The combined effect of cell division, death processes and the long–range chemotactic interaction among the living cells of a colony may be relevant to the description of the actual behavior of some biological species [176, 177] and it is the main topic of this Section.

As proposed in Ref. [132], in order to account birth and decay processes in the coarse-grained description of chemotaxis, we can extend phenomenologically the Langevin equation (3.3.1) as

$$(\partial_t - D_\rho \nabla^2 + \sigma)\rho = -\lambda\, \rho^2 - \mu_1 \vec{\nabla}\cdot(\rho\vec{\nabla}\phi) - \mu_2 \nabla^2(\vec{\nabla}\phi)^2 + \zeta\,, \tag{3.6.1}$$

where ϕ and ρ are still related by the Poisson equation (3.3.2), the linear and nonlinear growth terms are proportional respectively to σ and λ, namely the cells reproduce at a rate σ and they die at a rate λ and the Gaussian noise is still characterized by Eq. (3.3.3). In particular, the term proportional to σ naturally introduces a length scale ξ into the problem, analogous to a correlation length of the density fluctuations. In the absence of interactions $\xi \propto |\sigma|^{-1/2}$ and possible scale–invariant collective phenomena may emerge only upon tuning the value of σ to a critical value σ^* such that, correspondingly, ξ diverges. Considering the essentially number non–conserving nature of the interactions, only the non–conserved noise Ω_0 needs to be considered: Even if ω_0 is not included in the microscopic theory, the non–conserving noise is generated by the RG flow directly from the $\lambda\rho^2$ interaction and hence making the conserved noise Ω_2 irrelevant in the RG sense. Due to the breaking of the conservation law, however, the emerging scaling behavior differs from the one regarding simple non–conserved chemotaxis. In fact, the nonlinear growth term proportional to λ introduces a relevant perturbation which modifies the structure of the RG flow given by Eq. (3.4.27). The renormalization group procedure can be carried out exactly in the same way as for the simple chemotaxis theory, and the diagrams relevant to the one–loop renormalization are still the ones given in Fig. 3.1. In the next Section, we directly give the system of beta functions ruling the critical behavior of the extended chemotaxis theory and we leave analytical details to Appendix C.3. We

notice here that, even if, in the presence of the non–linear term $\propto \lambda\,\rho^2$, the Langevin Eq. (3.6.1) is still formally invariant with respect to the Galilean transformations in Eqs. (3.3.4), (3.3.5), the Ward identity in Eq. (3.4.2) simply holds as a general relationship between the couplings, and no exact exponents are obtained in this case.

3.6.1 Beta functions

The system of beta functions governing the theory of chemotaxis in presence of birth and decay processes is given by

$$\partial_\ell \sigma = z\,\sigma + \sigma\lambda\left[4\lambda + \mu_1\left(3+\frac{3}{d}\right) - \mu_2\left(2-\frac{14}{d}\right)\right], \tag{3.6.2}$$

$$\begin{aligned}\partial_\ell \lambda = {} & (z+\chi)\lambda + \\ & + \lambda\left\{4\lambda^2 - \lambda\left[\mu_1\left(5+\frac{6}{d}\right) + \mu_2\left(6-\frac{28}{d}\right)\right]\right. \\ & \left. + \mu_1^2\left(\frac{3}{2}+\frac{15}{2d}-\frac{9}{2(d+2)}\right) + \mu_1\mu_2\left(4-\frac{48}{d}+\frac{42}{d+2}\right) + \mu_2^2\left(2+\frac{58}{d}-\frac{90}{d+2}\right)\right\},\end{aligned} \tag{3.6.3}$$

$$\begin{aligned}\partial_\ell \mu_1 = {} & (z+\chi)\mu_1 + \lambda\left[\lambda(\mu_1-2\mu_2)\right. \\ & \left. - \mu_1^2\left(\frac{3}{4}-\frac{3}{2d}+\frac{3}{d+2}\right) + \mu_1\mu_2\left(1-\frac{16}{d}+\frac{28}{d+2}\right) + \mu_2^2\left(1+\frac{42}{d}-\frac{60}{d+2}\right)\right],\end{aligned} \tag{3.6.4}$$

$$\begin{aligned}\partial_\ell \mu_2 = {} & (z+\chi)\mu_2 + \\ & \lambda\left[\mu_1^2\left(\frac{1}{d}-\frac{3}{2(d+2)}\right) - \mu_1\mu_2\left(\frac{10}{d}-\frac{14}{d+2}\right) + \mu_2^2\left(\frac{24}{d}-\frac{30}{d+2}\right)\right],\end{aligned} \tag{3.6.5}$$

$$\begin{aligned}\partial_\ell D_\rho = {} & (z-2)D_\rho - D_\rho(a_1\,\mu_1^2 + a_2\,\mu_1\mu_2 + a_3\mu_2^2) \\ & + \lambda\,D_\rho\left[\frac{\mu_1}{4}\left(\frac{9}{d}-\frac{6}{d+2}-1\right) + \mu_2\left(\frac{3}{2}-\frac{23}{2d}+\frac{21}{d+2}\right) + \lambda\left(1-\frac{2}{d}\right)\right],\end{aligned} \tag{3.6.6}$$

$$\partial_\ell \Omega_0 = (z-d-2\chi)\Omega_0 + \Omega_0\lambda^2\,. \tag{3.6.7}$$

We immediately notice that the flows of $\mu_{1,2}$ are not simply given by the scaling contribution, as it is the case in Eq. (3.4.19), but they now also have a contribution from the interaction diagrams that are not vanishing when $\lambda \neq 0$ and depend in a nontrivial way on λ, μ_1 and μ_2. Another feature is that λ gives rise to corrections to σ. That is to say that, even if we start with $\sigma = 0$, a $\sigma \neq 0$ will be generated by the RG flow and the fixed–point condition of its flow gives a value for σ that is proportional to λ^2, which can be eliminated by a mass–shift in the usual way [178]. The couplings Ω_0, D_ρ and λ are also renormalized by the nonvanishing interaction diagrams.

3.6.2 Fixed–point equations and phase diagram

We immediately notice that when $\lambda = 0$, namely when the growth interaction is switched off in Eq. 3.6.1, and at the critical point, one immediately recovers the system of beta functions in Eqs. (3.4.24–3.4.26) describing the simple chemotaxis theory in the presence of a non–conserving noise, as expected. We, therefore, conclude that the phase diagram on the $\lambda = 0$ plane agrees with the one given in Fig. 3.2 with exact critical exponents given by Eq. (3.5.2).

Fixed–point equations are obtained first by adjusting the critical exponents χ and z so that $\partial_\ell D_\rho = \partial_\ell \Omega_0 = 0$ and then looking for solutions of the corresponding set of equations. The analytical form of the so–obtained fixed point equations is reasonably complicated and not particularly illuminating and we prefer to discuss directly the phase diagram, leaving analytical details in Appendix C.3.

We performed a preliminary analysis of the flow equations (3.6.2)–(3.6.7) according to which the plane $\lambda = 0$ results to be an unstable manifold with respect to perturbations in the λ direction. At first order in $\varepsilon = d_c - d$, with $\varepsilon \ll 1$, we have found no stable fixed point (besides the line of fixed points when λ is fine–tuned to $\lambda = 0$), and the flow is therefore characterized by runaway trajectories, which are usually associated either to non–perturbative fixed points or to first–order phase transitions. Even if the one–loop computation should be considered valid and reliable only in the neighborhood of d_c, that is for $\varepsilon \ll 1$, we analyzed the critical behavior of the system in $d = 2$: At this particular dimension it appears a (numerically) stable fixed point, which would indicate a putative second–order phase transition. However, this result suggests that further clarifications and studies should be performed within the non–perturbative RG framework and numerical simulations as well.

Lee–Yang theory: A consistency check

When the chemotactic terms are turned off ($\mu_1 = 0, \mu_2 = 0$), the model reduces to a relaxation model for a non–conserved order parameter ρ, known as the (dynamical) Lee–Yang model [179–181]. By imposing fluctuation–dissipation theorem via the requirement that $\tilde{\chi} = \chi + z$ [7] [182], one can fix the critical exponents z and χ so that $\partial_\ell D_\rho = \partial_\ell \Omega_0 = 0$, namely,

$$z = 2 + \frac{2}{d}\lambda^2\,, \qquad \chi = \frac{1}{2}(d-2) + \frac{(d-2)}{2d}\lambda^2\,. \tag{3.6.8}$$

Accordingly, we are left with the following beta function for the nonlinerity λ

$$\partial_\ell \lambda = \frac{1}{2}(6-d)\lambda + \left(\frac{5}{2} + \frac{3}{d}\right)\lambda^3\,, \tag{3.6.9}$$

whose fixed points are given by

$$\lambda^*_{\rm G} = 0\,, \qquad \lambda^*_{\rm LY} = \pm\frac{\sqrt{d-6}}{\sqrt{\frac{6}{d}+5}}\,. \tag{3.6.10}$$

The critical exponents z and χ in Eq. (3.6.8) at the non–trivial fixed–point $\lambda^*_{\rm LY}$ are therefore given by

$$z^*_{\rm LY} = \frac{12d}{5d+6} = 2 - \frac{\varepsilon}{18} + O(\varepsilon^2)\,, \tag{3.6.11}$$

$$\chi^*_{\rm LY} = \frac{3(d-2)d}{5d+6} = 2 - \frac{5\,\varepsilon}{9} + O(\varepsilon^2)\,, \tag{3.6.12}$$

which are indeed the known analytical values of the critical exponents of the dynamical Lee–Yang theory at order ε, see Refs. [181, 183]. This provides a consistency check of our analysis of the system of Eqs. (3.6.2)–(3.6.7) in the corresponding very well–known Lee–Yang limit to which they reduce when chemotactic interactions are neglected.

[7] We remind that the field variables scale as $\rho \to \mathrm{e}^{\ell\chi}\rho$ and $\tilde{\rho} \to \mathrm{e}^{\ell\tilde{\chi}}\tilde{\rho}$.

3.7 Conclusions and perspectives

We studied the large–scale and long–time behavior of a model of chemotactic particles by using dynamic renormalization–group technique. A new nonlinear interaction term with the same scaling properties as that of the well–known Keller–Segel term is introduced, capturing the effects of the polarization of the particles induced by the chemical gradient. We showed that when both the nonlinearities are non–zero, the RG flows for the effective couplings ($\tilde{\mu}_{1,2}$) have two loci of fixed–points in the shape of conics, the behavior of which is determined by the corresponding discriminant. Runaway regions are present in $d > 1$ and they can possibly be associated with a new strong–coupling phase captured either by a first–order phase transition or by non–perturbative fixed–points, the latter being less probable than the former. In $d \leq 1$ the loci of fixed points become fully attractive, suggesting that in $d = 1$, where the non–linearities are identical, we do not expect any runaway behavior. However, it should be noted that this statement results from the extrapolation of our results away from the upper critical dimension d_c, in the vicinity of which, on the other hand, they should be retained reliable. In either cases, the non–renormalization of the vertex function and noise correlator enables us to obtain the scaling exponents exactly, revealing super–diffusive particles with either hyperuniform populations (conserving noise) or giant number fluctuations (non–conserving noise). This model can be utilized to shed light on different phases of systems of chemotactic particles, including cells, bacteria or active colloids.

In the last part of the chapter, we have examined the dynamics in the presence of a birth and decay processes. The RG flows become considerably more complicated as the non–conserved growth term does not obey the Galilean symmetry as the chemotactic nonlinearities do, and hence all the coupling constants now have non–trivial flows. The growth nonlinearity gives rise to both chemotactic terms under rescaling even when one of them is absent in the microscopic theory, whereas in the absence of chemotaxis we recover the Lee–Yang cubic theory. At this order of perturbation theory, however, the flows run away towards inaccessible regions and a linear stability analysis confirms that the $\lambda = 0$ plane is unstable with respect to λ perturbation. On the other hand, the flow has been obtained assuming the linear growth term can be tuned to zero whereas the RG calculation shows that it will also exhibits runaway flows proportional to λ. This suggests that a characteristic

length–scale is introduced into the system, moving it away from the critical state where the dynamics is self–similar. The absence of stable fixed points in this case and the associated runaway behavior may indicate the presence of non–perturbative fixed points, that we intend to explore as a future perspective by means of a non–perturbative approach such as that discussed in chapter 1. We also speculate that the presence of the full multiplicative noise may result in the introduction of an absorbing state for the density of cells and nontrivial fixed points with $\lambda^* \neq 0$.

Active field theories, by the introduction of leading–order gradient terms breaking the detailed balance, allow for the emergence of new classes of models in which the breaking of time–reversal symmetry is intimately linked to the physics of interfaces. In this respect, the similarities with the conserved KPZ+ is striking, since as for chemotaxis, it results from the introduction of a symmetry–allowed gradient term of the form of the nonlinearity μ_1. The resulting phase diagrams are, in fact, qualitatively similar. However, even if there are several analogies between chemotaxis, conserved KPZ+, and standard KPZ, we exclude that this could be an indication of the presence of a strong–coupling fixed point as for KPZ, though tempting. In this respect, it would be interesting to consider the theory obtained by applying the Laplacian operator to the KPZ equation since, apart from the noise term, the resulting theory would be essentially identical to chemotaxis. Further perspectives are in the direction of exploring and understanding the implications of these analogies.

The self–gravitating Brownian gas model has a conceptual interest in physics because it represents the canonical counterpart of a Hamiltonian system of stars in Newtonian interaction. Self–gravitating systems have very special thermodynamics features, characterized by the non–equivalence of statistical ensembles. Furthermore, these systems experience a rich diversity of phase transitions associated with their natural tendency to undergo gravitational collapse [184, 185]. These analogies have also suggested interesting experiments with ultra–cold gases leading to the fascinating possibility of reproducing gravitational instabilities in the laboratory [186]. In this respect, we find intriguing the fact that the collapse of the self–gravitating Brownian gas is analogous to the chemotactic aggregation of bacterial populations in biology. As the novel chemotactic interaction μ_2 we introduced here for the first time, never appeared in the rich literature of chemotaxis models, and as fruitful it has been the connection with astrophysics, we intend to understand better the conse-

quences of the addition of such a new term in the description of the critical dynamics of self–gravitating systems, as well as its actual physical meaning in this context.

Appendix C

C.1 The stochastic Keller–Segel model

In this section, we present the stochastic model of chemotaxis [157], which generalizes the KS model, by taking into account fluctuations. In doing so we find useful to briefly review Dean's approach [167], in terms of which an exact kinetic equation satisfied by the density distribution of cells can be derived.

In full generality we can rewrite Eq. (3.2.4) as

$$\partial_t \vec{x}_i(t) = -\vec{\mathcal{F}}(t, \vec{x}_i) + \vec{\zeta}_i(t, \vec{x})\,, \tag{C.1.1}$$

where $\vec{\mathcal{F}}$ represents the deterministic part of the evolution, which may depend on $\vec{x}_i$ and its derivatives and $\zeta(t, \vec{x})$ is a Gaussian noise whose correlation function is expressed as

$$\langle \vec{\zeta}(t, \vec{x}) \vec{\zeta}(t', \vec{x}') \rangle = 2A_2 \delta(t - t') \delta^d(\vec{x} - \vec{x}') \rangle\,. \tag{C.1.2}$$

Consider the density field $C(t, \vec{x})$, expressed in terms of δ-functions, namely

$$C(t, \vec{x}) = \sum_{i=1}^{N} C_i(t, \vec{x}) = \sum_{i=1}^{N} \delta(\vec{x} - \vec{x}_i(t))\,, \tag{C.1.3}$$

where C_i is the density of a single particle. For an arbitrary function $f(\vec{x})$ defined on the coordinate space of the system, it is true that

$$f(\vec{x}_i(t)) = \int d\vec{x}\, C_i(t, \vec{x}) f(\vec{x})\,, \tag{C.1.4}$$

so that expanding the stochastic differential equation (C.1.1) using Ito's calculus [187]

we can write

$$\frac{df(\vec{x}_i)}{dt} = \int d\vec{x}\, C_i(t,\vec{x}) \left\{ \vec{\nabla} f(\vec{x}) \cdot [-\vec{\mathcal{F}}(t,\vec{x}) + \vec{\zeta}_i(t,\vec{x})] + A_2 \nabla^2 f(\vec{r}) \right\} , \tag{C.1.5}$$

and by integrating by parts the last integral, we obtain

$$\frac{df(\vec{x}_i)}{dt} = \int d\vec{x}\, f(\vec{x}) \left[-\vec{\nabla}(C_i(t,\vec{x})\vec{\zeta}_i(t,\vec{x})) + \vec{\nabla}(C_i(t,\vec{x})\vec{\mathcal{F}}(t,\vec{x})) + A_2 \nabla^2 C_i(t,\vec{x}) \right] . \tag{C.1.6}$$

On the other hand, from Eq. (C.1.4), we may also deduce that

$$\frac{df(\vec{x}_i)}{dt} = \int d\vec{x}\, f(\vec{x})\, \partial_t C_i(t,\vec{x}) , \tag{C.1.7}$$

so that comparing equations (C.1.4) and (C.1.6) we find (using the fact that f is an arbitrary function) that

$$\partial_t C_i(t,\vec{x}) = -\vec{\nabla}(C_i(t,\vec{x})\vec{\zeta}_i(t,\vec{x})) + \vec{\nabla}(C_i(t,\vec{x})\vec{\mathcal{F}}(t,\vec{x})) + A_2 \nabla^2 C_i(t,\vec{x}) . \tag{C.1.8}$$

Summing Eq. (C.1.8) over i and using the definition of the density C we obtain

$$\partial_t C(t,\vec{x}) = -\sum_{i=1}^{N} \vec{\nabla}(C_i(t,\vec{x})\vec{\zeta}_i(t,\vec{x})) + \vec{\nabla}(C(t,\vec{x})\vec{\mathcal{F}}(t,\vec{x})) + A_2 \nabla^2 C(t,\vec{x}) , \tag{C.1.9}$$

Now, the first term on the r.h.s. of Eq. (C.1.9) can be rewritten as [167]

$$-\sum_{i=1}^{N} \vec{\nabla}(C_i(t,\vec{x})\zeta_i(t,\vec{x})) = \vec{\nabla}(C^{1/2}(t,\vec{x})\zeta(t,\vec{x})) , \tag{C.1.10}$$

so that Eq. (C.1.9) finally reads

$$\partial_t C(t,\vec{x}) = \vec{\nabla}(C(t,\vec{x})\vec{\mathcal{F}}(t,\vec{x})) + A_2 \nabla^2 C(t,\vec{x}) + \vec{\nabla}\ (C^{1/2}(t,\vec{x})\vec{\zeta}(t,\vec{x})) . \tag{C.1.11}$$

We can now specify the deterministic part $\vec{\mathcal{F}}$ to be $\mathcal{F} = -\mu_1\, \vec{\nabla}\phi - \mu_2 \vec{\nabla} \cdot (\vec{\nabla}\phi)^2$, (see Eq. (3.3.12)), to conclude that the equation satisfied by the density of particles in the

presence of chemotaxis reads

$$\partial_t C = A_2 \nabla^2 C - \mu_1 \vec{\nabla}(C\vec{\nabla}\phi) - \mu_2 \vec{\nabla}(C\vec{\nabla}(\vec{\nabla}\phi)^2) + \vec{\nabla}(C^{1/2}\vec{\zeta})\,. \tag{C.1.12}$$

As pointed out by Dean, the noise in Eq. (C.1.12) appears not additively but multiplicatively. To simplify the multiplicative noise term, we have assumed that the density C fluctuates around a spatially constant background value C_0; hence, we make the substitution $C(t,\vec{x}) = C_0 + \rho(t,\vec{x})$ and expand in ρ/C_0 up to the lowest–order non–linearity. Expanding Eq. (C.1.12) we then have

$$\begin{aligned}\partial_t \rho = A_2\nabla^2\rho - \mu_1\vec{\nabla}(\rho\vec{\nabla}\phi) - \mu_1 C_0\nabla^2\phi - \mu_2 C_0\nabla^2(\vec{\nabla}\phi)^2 - \mu_2\vec{\nabla}(\rho\vec{\nabla}(\vec{\nabla}\phi)^2) \\ + \vec{\nabla}(C_0^{1/2}\zeta) + (4C_0)^{-1/2}\vec{\nabla}(\rho\zeta)\,.\end{aligned} \tag{C.1.13}$$

Important remark: The total number of particles is conserved, provided that the density field C in the boundary integral $\int_{\partial V}\hat{n}\cdot(C\vec{\nabla}\phi)$, where V is the volume over which the total number of particles is calculated and $\hat{n}$ is the normal versor identifying the surface ∂V, approaches zero sufficiently fast. This is true only if the density C is considered constant, i.e., $C \simeq C_0$, over a volume $V \propto t^{1/2}$, beyond which it drops to zero sufficiently fast. In the stationary limit considered and in the absence of degradation of chemicals, the first green term in Eq. (C.1.13) can be disregarded on this basis. The second green term is, with respect to the naive dimensional analysis of section 3.3.2, always irrelevant at d_c. Finally, the third green term represents a multiplicative noise which can be disregarded as irrelavant, if the additive noise is used to fix the dimensions of the Gaussian theory as in section 3.3.2. This essentially leads to Eq. (3.3.1) upon redefining $\mu_2 C_0 \to \mu_2$, $A_2 \to D_\rho$ and $C_0 A_2 \to -\Omega_2$.

C.2 Response function formalism

The response function formalism is a method to write stochastic differential equations as a field theory formulated by using path integrals. The main idea is that, when computing averages over the stochastic noise, among all possible field configurations, only those satisfying the original stochastic equation do contribute and one can select such configurations using a Dirac delta functional.

Suppose that a field variable ψ evolves according to a stochastic dynamics described at a mesoscopic level by the following Langevin equation

$$\partial_t \psi(t,\vec{x}) = -\mathcal{F}(\psi(t,\vec{x})) + \zeta(t,\vec{x})\,, \tag{C.2.1}$$

where $\mathcal{F}$ represents the deterministic part of the evolution and can depend on ψ and its derivatives and $\zeta(t,\vec{x})$ is a Gaussian noise whose correlation function is given by Eq. (C.1.2). In general one is interested in computing averages of functions $\mathcal{O}(\psi(t,\vec{x}))$ of the field $\psi(t,\vec{x})$ over the noise distribution:

$$\langle \mathcal{O}(\psi) \rangle = \int \mathcal{D}\zeta\; P(\zeta)\; \mathcal{O}(\psi_\zeta)\,, \tag{C.2.2}$$

where $\psi_\zeta(t,\vec{x})$ is the solution of Eq. (C.2.1) for the realization ζ of the noise. This average can be conveniently written as

$$\begin{aligned}
\langle \mathcal{O}(\psi) \rangle &= \int \mathcal{D}\zeta\; P(\zeta) \int \mathcal{D}\psi\; \delta(\psi - \psi_\zeta)\; \mathcal{O}(\psi)\,, \\
&= \int \mathcal{D}\zeta\; P(\zeta) \int \mathcal{D}\psi\; \delta(\partial_t \psi(t,\vec{x}) + A_1 \mathcal{F}(\psi(t,\vec{x})) - \zeta(t,\vec{x}))\; J(\psi)\mathcal{O}(\psi)\,, \\
&= \int \mathcal{D}\zeta\; P(\zeta) \int \mathcal{D}\psi \mathcal{D}[i\tilde{\psi}]\; e^{\int_{t,\vec{x}} -\tilde{\psi}[\partial_t \psi(t,\vec{x}) + A_1 \mathcal{F}(\psi(t,\vec{x})) - \zeta(t,\vec{x})]}\; J(\psi)\mathcal{O}(\psi)\,,
\end{aligned} \tag{C.2.3}$$

where we used the functional analogue of the usual identity

$$\delta(x - x_0) = \delta(g(x))|g'(x_0)|\,, \tag{C.2.4}$$

ad we have assumed that the function $g(x)$ has a unique zero. In Eq. (C.2.3) the Jacobian J is given by

$$J(\psi) = \left| \det\left(\partial_t + \frac{\partial \mathcal{F}(\psi)}{\partial \psi} - \zeta \right) \right|\,. \tag{C.2.5}$$

The field $\tilde{\psi}$ is called *response field* and may be interpreted as a Lagrange multiplier, since it is introduced to select given configurations of the field ψ. We can now exploit the identity $\det = \exp \mathrm{Tr} \log$, so that the determinant comes as an additional term in the exponential in Eq. (C.2.3). This term appears to be proportional to the inverse of

the operator $(\partial_t)\delta(t-t')$, namely $\theta(t-t')$, evaluated at $t=t'$. This constant $\theta(0)=\alpha$ depends on the precise (discrete) ordering of times. Though the actual choice is irrelevant, the simplest one (known as Ito's discretization choice) corresponds to setting $\alpha=0$, from which one obtains $J=1$. Once the Jacobian is set to unity, one can finally integrate in Eq. (C.2.3) over the Gaussian noise distribution and deduce the generating functional $Z[j,\tilde{j}]$ for correlation and response functions, i.e.,

$$Z[j,\tilde{j}] = \int \mathcal{D}\psi\mathcal{D}[i\tilde{\psi}]\; e^{-S[\psi,\tilde{\psi}]+\int_{t,\vec{x}}\; j\psi+\tilde{j}\tilde{\psi}}\,, \tag{C.2.6}$$

where we introduced the so-called *dynamical functional*

$$S[\psi,\tilde{\psi}] = \int_{t,\vec{x}} \left\{ \tilde{\psi}\left[\partial_t\psi + A_1\mathcal{F}(\psi)\right] - A_2\tilde{\psi}^2 \right\}\,. \tag{C.2.7}$$

We note here that, even if physical observables $\mathcal{O}$ are functions of ψ, it makes sense to consider observables depending also on $\tilde{\psi}$, e.g., as $\mathcal{O}(\psi,\tilde{\psi})$. The great advantage of the response function formalism is to provide a general framework to address the field-theoretical RG study of out of equilibrium models.

C.3 One–loop vertex diagrams

We report here the detailed structure of the one–loop vertex diagrams appearing in Fig. 3.1. The cases of conserved chemotaxis (both in presence of a conserved and non–conserved noise) and the non–conserved chemotaxis, when extended to include birth and decay processes, are characterized by the same diagrams. However, in the presence of the λ non–linearity, the vertex is renormalized and the actual momentum structure of the vertex has to be considered carefully (see below). This is how we actually realized that the theory originally proposed in Ref. [132] was lacking the interaction term μ_2: The latter is already generated at one–loop in the renormalization of the vertex and therefore it needs to be included in the description of the theory. The relevant diagrams are

$$\Gamma_1^{(a)}(\vec{k},\vec{k}/2+\vec{p}) = 4\int_{\hat{q}} \Gamma_0(\vec{k},\vec{k}/2+\vec{q})\Gamma_0(\vec{p}-\vec{q},\vec{k}/2+\vec{p})\Gamma_0(\vec{k}/2-\vec{q},\vec{p}-\vec{q}) \\ \Theta_0(\vec{k}/2+\vec{q})G_0(\hat{p}-\hat{q})G_0(\hat{k}/2-\hat{q})\,, \tag{C.3.1}$$

$$\Gamma_1^{(b)}(\vec{k},\vec{k}/2+\vec{p}) = 4\int_{\hat{q}} \Gamma_0(\vec{k},\vec{k}/2+\vec{q})\Gamma_0(\vec{k}/2+\vec{q},\vec{k}/2+\vec{p})\Gamma_0(\vec{q}-\vec{p},\vec{k}/2-\vec{p}) \\ \Theta_0(\vec{k}/2-\vec{q})G_0(\hat{k}/2+\hat{q})G_0(\hat{q}-\hat{p})\,, \tag{C.3.2}$$

$$\Gamma_1^{(c)}(\vec{k},\vec{k}/2+\vec{p}) = 4\int_{\hat{q}} \Gamma_0(\vec{k},\vec{k}/2+\vec{q})\Gamma_0(\vec{k}/2+\vec{q},\vec{k}/2+\vec{p})\Gamma_0(\vec{k}/2-\vec{q},\vec{k}/2-\vec{p}) \\ \Theta_0(\vec{p}-\vec{q})G_0(\hat{k}/2+\hat{q})G_0(\hat{k}/2-\hat{q})\,. \tag{C.3.3}$$

In order to compute the renormalization of the chemotactic terms μ_1 and μ_2, the dependence of Γ on the external momenta $\vec{k}$ and $\vec{p}$ has to be retained. To simplify the internal momentum integration, we perform a series expansion for large q and we focus on the computation of the pole in $1/q^{d_c}$, which is the term that is UV divergent (when $\Lambda \to \infty$) and gives rise to the renormalization of the coupling constants close to the critical dimension $d_c = 6$.[1] Moreover, to compute the renormalization of the chemotactic terms $\mu_{1,2}$, we use the fact that when evaluated at external momenta $\vec{k}$ and $\vec{p}$ such that $\vec{k}\cdot\vec{p} = k^2\cos\theta$, the vertex $\Gamma(\vec{k},\vec{k}/2+\vec{p}) = \Gamma_\theta$ depends only on the angle θ between the external momenta. We use this property to define and calculate the renormalized interaction terms as follows

$$\lambda_{\mathrm{R}} := -\,\Gamma(\vec{k},\vec{k}/2+\vec{p})\Big|_{\hat{k}=\hat{0}}\,, \tag{C.3.4}$$

$$\mu_1^{\mathrm{R}} := (\lambda_{\mathrm{R}}-\lambda) - \frac{9}{16}\Gamma_{\theta=\pi} + \frac{25}{16}\Gamma_{\theta=\pi/2}\,, \tag{C.3.5}$$

$$\mu_2^{\mathrm{R}} := \frac{5}{4}(\lambda_{\mathrm{R}}-\lambda) + \frac{15}{32}\Gamma_{\theta=\pi} + \frac{25}{32}\Gamma_{\theta=\pi/2}\,. \tag{C.3.6}$$

C.4 Power counting and upper critical dimension

Considering chemotactic particles which respond only to fluctuations in the chemical concentration field ϕ, the velocity $\vec{v}(t)$ of a single particle immersed in the field

[1] This approach is typical of dimensional regularization and particularly advantageous in the computation of the vertex diagrams. Scale–invariant properties, on the other hand, are invariant with respect to the renormalization scheme adopted.

n	p	q	Operator	Galilean invariant	Comments
0	0	4	∇^4	/	/
	1	3	$\nabla^3\nabla\phi$	yes	$\sim \nabla^2\rho$ (marginal in all dimensions).
	2	2	$\nabla^2(\nabla\phi)^2$	yes	New chemotactic term.
	3	1	$\nabla(\nabla\phi)^3$, $\nabla\left(\nabla\phi(\nabla\phi)^2\right)$	no	/
1	0	2	$\nabla^2\rho$	yes	$\sim \nabla^2\rho$ (marginal in all dimensions).
	1	1	$\nabla(\rho\nabla\phi)$	yes	Chemotactic term.

Table C.1: Allowed operators which are marginal at $d = d_c$.

ϕ can be generically expressed in terms of the following gradient expansion

$$\vec{v}(t) = \ell_1\vec{\nabla}\phi + \ell_2\vec{\nabla}(\vec{\nabla}^2\phi) + \cdots + \ell_3\vec{\nabla}(\vec{\nabla}\phi)^2 + \ell_4\vec{\nabla}(\vec{\nabla}^2\phi^2) + \dots\,, \tag{C.4.1}$$

where ℓ_i are coefficients. In constructing the corresponding Langevin equation, the gradient expansion is, on the other hand, not sufficient. Indeed, terms that appear as higher–order in this expansion (see Table C.1) may be relevant in the renormalization group (RG) sense, and therefore become dominant at criticality. One must, therefore, order the numerous terms arising from the gradient expansion on the basis of their scaling dimensions. Based on the naive scaling analysis of section 3.3.2, we can now systematically determine the relevance of the interaction terms that will be generated by the renormalization–group flow and appear in the Langevin equation. The general form of an interaction term is, schematically,

$$g_{npq}\,\rho^n\,(\nabla\phi)^p\,\nabla^q\,, \tag{C.4.2}$$

where we assume $n, p \geq 0$. Since we consider conserved dynamics, interaction terms must come as the divergence of a vector field and thus $q \geq 1$. Moreover, ϕ only comes with a gradient to enforce the shift symmetry $\phi \to \phi + \text{const.}$ and, finally, $p + q$ must be even to have a scalar quantity. The general coupling constant has the dimension

$$[g_{npq}]_0 = 2 + p - q - \frac{d}{2}(n + p - 1)\,, \tag{C.4.3}$$

and this interaction is relevant whenever $[g_{npq}]_0$ is positive. The upper critical dimension d_c is therefore obtained by maximising the following expression

$$d_c = \max \; 2\left(\frac{n+2p+1-q}{n+p-1}\right), \tag{C.4.4}$$

where $n+p \neq 1$. One obtains the upper critical dimension $d_c = 4$ in the case of a conserved noise. A similar procedure yields $d_c = 6$ in the case of a non–conserved noise ($\Omega_2 = 0$), as explained in section 3.3.2. We can finally consider all the terms which are marginal at $d_c = 4$ and the result is summarised in Table C.1. We conclude that the nonlinearities in the Langevin Eq. (3.3.1) are the only that should be considered.

Bibliography

[1] J. H. Conway, H. Burgiel and C. Goodman-Strauss, *The symmetries of things*. AK Peters/CRC Press, 2016.

[2] P. A. M. Dirac, *The evolution of the physicist's picture of nature*, *Scientific American* **208** (1963) 45.

[3] D. J. Gross, *The role of symmetry in fundamental physics*, *Proceedings of the National Academy of Sciences* **93** (1996) 14256.

[4] R. Batterman, *The Oxford handbook of philosophy of physics*. Oxford University Press, 2013.

[5] K. G. Wilson and M. E. Fisher, *Critical exponents in 3.99 dimensions*, *Phys. Rev. Lett.* **28** (1972) 240.

[6] K. G. Wilson and J. Kogut, *The renormalization group and the ϵ expansion*, *Physics Reports* **12** (1974) 75 .

[7] E. Ising, *Beitrag zur theorie des ferromagnetismus*, *Zeitschrift für Physik* **31** (1925) 253.

[8] A. Cappelli, C. Itzykson and J. B. Zuber, *The a-d-e classification of minimal and $a1(1)$ conformal invariant theories*, *Communications in Mathematical Physics* **113** (1987) 1.

[9] A. Cappelli, C. Otzykson and J.-B. Zuber, *Modular invariant partition functions in two dimensions*, *Nuclear Physics B* **280** (1987) 445 .

[10] A. B. Zamolodchikov, *Conformal Symmetry and Multicritical Points in Two-Dimensional Quantum Field Theory. (In Russian)*, *Sov. J. Nucl. Phys.* **44** (1986) 529.

[11] R. B. Potts, *Some generalized order-disorder transformations*, *Mathematical Proceedings of the Cambridge Philosophical Society* **48** (1952) 106–109.

[12] S. R. Broadbent and J. M. Hammersley, *Percolation processes: I. crystals and mazes*, *Mathematical Proceedings of the Cambridge Philosophical Society* **53** (1957) 629–641.

[13] G. Kirchhoff, *Ueber die auflösung der gleichungen, auf welche man bei der untersuchung der linearen vertheilung galvanischer ströme geführt wird*, *Annalen der Physik* **148** (1847) 497.

[14] P. W. Kasteleyn and C. M. Fortuin, *Phase Transitions in Lattice Systems with Random Local Properties*, *Physical Society of Japan Journal Supplement, Vol. 26. Proceedings of the International Conference on Statistical Mechanics held 9-14 September, 1968 in Koyto., p.11* **26** (1969) 11.

[15] C. Fortuin and P. Kasteleyn, *On the random-cluster model: I. introduction and relation to other models*, *Physica* **57** (1972) 536 .

[16] F. Y. Wu, *The potts model*, *Rev. Mod. Phys.* **54** (1982) 235.

[17] R. K. P. Zia and D. J. Wallace, *Critical behaviour of the continuous n-component Potts model*, *Journal of Physics A Mathematical General* **8** (1975) 1495.

[18] D. J. Amit, *Renormalization of the Potts model*, *Journal of Physics A Mathematical General* **9** (1976) 1441.

[19] C. Wetterich, *Exact evolution equation for the effective potential*, *Physics Letters B* **301** (1993) 90 [1710.05815].

[20] T. R. Morris, *The exact renormalization group and approximate solutions*, *International Journal of Modern Physics A* **09** (1994) 2411.

[21] P. D. Gennes, *Phenomenology of short-range-order effects in the isotropic phase of nematic materials*, *Physics Letters A* **30** (1969) 454 .

[22] P. G. D. Gennes, *Short range order effects in the isotropic phase of nematics and cholesterics*, *Molecular Crystals and Liquid Crystals* **12** (1971) 193.

[23] M. Weger and I. Goldberg, *Some lattice and electronic properties of the β-tungstens*, vol. 28 of *Solid State Physics*, pp. 1 – 177, Academic Press, (1974), DOI.

[24] B. Svetitsky and L. G. Yaffe, *Critical behavior at finite-temperature confinement transitions*, *Nuclear Physics B* **210** (1982) 423 .

[25] L. G. Yaffe and B. Svetitsky, *First-order phase transition in the $su(3)$ gauge theory at finite temperature*, *Phys. Rev. D* **26** (1982) 963.

[26] M. Caselle, G. Delfino, P. Grinza, O. Jahn and N. Magnoli, *Potts correlators and the static three-quark potential*, *Journal of Statistical Mechanics: Theory and Experiment* **2006** (2006) P03008.

[27] G. Delfino and P. Grinza, *Confinement in the q-state potts field theory*, *Nuclear Physics B* **791** (2008) 265 .

[28] L. Lepori, G. Z. Tóth and G. Delfino, *The particle spectrum of the three-state potts field theory: a numerical study*, *Journal of Statistical Mechanics: Theory and Experiment* **2009** (2009) P11007.

[29] A. B. Harris, T. C. Lubensky, W. K. Holcomb and C. Dasgupta, *Renormalization-Group Approach to Percolation Problems.*, *Phys.Rev. Lett.* **35** (1975) 1397.

[30] R. J. Baxter, *Potts model at the critical temperature*, *Journal of Physics C: Solid State Physics* **6** (1973) L445.

[31] A. D. Sokal, *The multivariate tutte polynomial (alias potts model)*, *Surveys in combinatorics 2005* **327** (2005) 173 [math/0503607].

[32] B. Nienhuis, A. N. Berker, E. K. Riedel and M. Schick, *First- and Second-Order Phase Transitions in Potts Models: Renormalization-Group Solution*, *Phys. Rev. Lett.* **43** (1979) 737.

[33] S. Alexander, *Continuous phase transitions which should be first order*, *Solid State Communications* **14** (1974) 1069.

[34] S. J. Jensen and O. G. Mouritsen, *Is the Phase Transition of the Three-State Potts Model Continuous in Three Dimensions?*, *Phys. Rev. Lett.* **43** (1979) 1736.

[35] H. W. J. Blöte and R. H. Swendsen, *First order phase transitions and the three state Potts model*, *Journal of Applied Physics* **50** (1979) 7382.

[36] H. J. Herrmann, *Monte Carlo simulation of the three-dimensional Potts model*, *Zeitschrift fur Physik B Condensed Matter* **35** (1979) 171.

[37] M. Fukugita and M. Okawa, *Correlation length of the three-state Potts model in three dimensions*, *Phys. Rev. Lett.* **63** (1989) 13.

[38] O. F. de Alcantara Bonfim, *Finite-size effects and phase transition in the three-dimensional three-state Potts model*, *Journal of Statistical Physics* **62** (1991) 105.

[39] R. Gavai, F. Karsch and B. Petersson, *A study of the correlation length near a first-order phase transition: The three-dimensional three-state potts model*, *Nuclear Physics B* **322** (1989) 738 .

[40] G. R. Golner, *Investigation of the Potts Model Using Renormalization-Group Techniques*, *Phys. Rev. B* **8** (1973) 3419.

[41] D. J. Amit and A. Shcherbakov, *The phase transition in the continuous Potts model*, *Journal of Physics C Solid State Physics* **7** (1974) L96.

[42] K. E. Newman, E. K. Riedel and S. Muto, *q-state potts model by wilson's exact renormalization-group equation*, *Phys. Rev. B* **29** (1984) 302.

[43] O. F. de Alcantara Bonfim, J. E. Kirkham and A. J. McKane, *Critical exponents to order ϵ^3 for φ^3 models of critical phenomena in 6-ϵ dimensions*, *Journal of Physics A Mathematical General* **13** (1980) L247.

[44] O. F. de Alcantara Bonfim, J. E. Kirkham and A. J. McKane, *Critical exponents for the percolation problem and the Yang-Lee edge singularity*, *Journal of Physics A Mathematical General* **14** (1981) 2391.

[45] R. J. Baxter, *Exactly solved models in statistical mechanics*. Elsevier, 2016.

[46] W. T. Tutte, *A contribution to the theory of chromatic polynomials*, *Canadian Journal of Mathematics* **6** (1954) 80–91.

[47] G. Grimmett, *The Random-Cluster Model*, *arXiv Mathematics e-prints* (2002) math/0205237 [math/0205237].

[48] H. Kunz and F. Y. Wu, *Site percolation as a potts model*, *Journal of Physics C: Solid State Physics* **11** (1977) L1.

[49] G. Delfino and P. Grinza, *Universal ratios along a line of critical points. The Ashkin-Teller model*, *Nuclear Physics B* **682** (2004) 521 [hep-th/0309129].

[50] R. G. Priest and T. C. Lubensky, *Critical properties of two tensor models with application to the percolation problem*, *Phys. Rev. B* **13** (1976) 4159.

[51] J. Berges, N. Tetradis and C. Wetterich, *Non-perturbative renormalization flow in quantum field theory and statistical physics*, *Phys. Rep.* **363** (2002) 223 [hep-ph/0005122].

[52] B. Delamotte, *An Introduction to the Nonperturbative Renormalization Group*, pp. 49–132. Springer Berlin Heidelberg, Berlin, Heidelberg, 2012. cond-mat/0702365.

[53] J. M. Martín-García, *xtensor: Fast abstract tensor computer algebra*, http://xact.es/xTensor/.

[54] L. Canet, B. Delamotte, D. Mouhanna and J. Vidal, *Optimization of the derivative expansion in the nonperturbative renormalization group*, *Phys. Rev. D* **67** (2003) 065004 [hep-th/0211055].

[55] P. Roberto, *An introduction to covariant quantum gravity and asymptotic safety*, vol. 3. World Scientific, 2017.

[56] L. Zambelli and O. Zanusso, *Lee-Yang model from the functional renormalization group*, *Phys. Rev. D* **95** (2017) 085001 [1612.08739].

[57] H. G. Ballesteros, L. A. Fernández, V. Martín-Mayor, A. Muñoz Sudupe, G. Parisi and J. J. Ruiz-Lorenzo, *Critical exponents of the three-dimensional diluted ising model*, *Phys. Rev. B* **58** (1998) 2740.

[58] A. Bunde and S. Havlin, *Fractals and disordered systems*. Springer Science & Business Media, 2012.

[59] Y. Deng, T. M. Garoni and A. D. Sokal, *Ferromagnetic Phase Transition for the Spanning-Forest Model ($q \to 0$ Limit of the Potts Model) in Three or More Dimensions*, *Phys. Rev. Lett.* **98** (2007) 030602 [cond-mat/0610193].

[60] J. A. Gracey, *Four loop renormalization of ϕ^3 theory in six dimensions*, *Phys. Rev. D* **92** (2015) 025012 [1506.03357].

[61] P. M. Stevenson, *Optimized perturbation theory*, *Phys. Rev. D* **23** (1981) 2916.

[62] A. Codello, M. Safari, G. P. Vacca and O. Zanusso, *Leading cft constraints on multi-critical models in $d > 2$*, *JHEP* **04** (2017) 127 [1703.04830].

[63] H. Coxeter, *Regular Polytopes*. Dover publications, 1973.

[64] L. Schläfli and H. Wild, *Theorie der vielfachen Kontinuität*, vol. 38. Springer-Verlag, 2013.

[65] J. O'Dwyer and H. Osborn, *Epsilon expansion for multicritical fixed points and exact renormalisation group equations*, *Annals Phys.* **323** (2008) 1859 [0708.2697].

[66] A. Codello, M. Safari, G. P. Vacca and O. Zanusso, *Functional perturbative rg and cft data in the ϵ-expansion*, *The European Physical Journal C* **78** (2018) 30.

[67] A. Codello, M. Safari, G. P. Vacca and O. Zanusso, *New universality class in three dimensions: the critical blume-capel model*, *Phys. Rev. D* **96** (2017) 081701.

[68] J. A. Gracey, *Renormalization of scalar field theories in rational spacetime dimensions*, 1703.09685.

[69] J. Cardy, *Scaling and renormalization in statistical physics*, vol. 5. Cambridge university press, 1996.

[70] H. Osborn and A. Stergiou, *Seeking fixed points in multiple coupling scalar theories in the ϵ expansion*, *Journal of High Energy Physics* **2018** (2018) 51.

[71] S. Rychkov and A. Stergiou, *General Properties of Multiscalar RG Flows in $d = 4 - \varepsilon$*, *SciPost Phys.* **6** (2019) 008 [1810.10541].

[72] E. Brezin, J. L. Guillou, J. Zinn-Justin and B. Nickel, *Higher order contributions to critical exponents*, *Physics Letters A* **44** (1973) 227 .

[73] L. Zambelli and O. Zanusso, *Lee-yang model from the functional renormalization group*, *Phys. Rev. D* **95** (2017) 085001.

[74] M. V. Kompaniets and E. Panzer, *Minimally subtracted six loop renormalization of $O(n)$-symmetric ϕ^4 theory and critical exponents*, *Phys. Rev.* **D96** (2017) 036016 [1705.06483].

[75] L. T. Adzhemyan, E. V. Ivanova, M. V. Kompaniets, A. Kudlis and A. I. Sokolov, *Six-loop ε expansion study of three-dimensional n-vector model with cubic anisotropy*, *Nucl. Phys.* **B940** (2019) 332 [1901.02754].

[76] A. Codello, M. Safari, G. P. Vacca and O. Zanusso, *Leading order CFT analysis of multi-scalar theories in d¿2*, *Eur. Phys. J.* **C79** (2019) 331 [1809.05071].

[77] J. S. Hager, *Six-loop renormalization group functions of $O(n)$-symmetric ϕ^6-theory and epsilon-expansions of tricritical exponents up to ϵ^3*, *J. Phys.* **A35** (2002) 2703.

[78] A. Codello, M. Safari, G. P. Vacca and O. Zanusso,*in preparation* (2018) .

[79] E. Brézin, J. C. Le Guillou and J. Zinn-Justin, *Discussion of critical phenomena for general n-vector models*, *Phys. Rev. B* **10** (1974) 892.

[80] D. Wallace and R. Zia, *Gradient properties of the renormalisation group equations in multicomponent systems*, *Annals of Physics* **92** (1975) 142 .

[81] J.-C. Toledano, L. Michel, P. Toledano and E. Brezin, *Renormalization-group study of the fixed points and of their stability for phase transitions with four-component order parameters*, *Phys. Rev. B* **31** (1985) 7171.

[82] L. Michel, *Renormalization-group fixed points of general n-vector models*, *Phys. Rev. B* **29** (1984) 2777.

[83] D. M. Hatch, H. T. Stokes, J. S. Kim and J. W. Felix, *Selection of stable fixed points by the toledano-michel symmetry criterion: Six-component example*, *Phys. Rev. B* **32** (1985) 7624.

[84] A. Pelissetto and E. Vicari, *Critical phenomena and renormalization group theory*, *Phys. Rept.* **368** (2002) 549 [cond-mat/0012164].

[85] R. P. Stanley, *Invariants of finite groups and their applications to combinatorics*, *Bull. Amer. Math. Soc. (N.S.)* **1** (1979) 475.

[86] M. Oshikawa, *Ordered phase and scaling in Z_n models and the three-state antiferromagnetic potts model in three dimensions*, *Phys. Rev. B* **61** (2000) 3430.

[87] F. Léonard and B. Delamotte, *Critical exponents can be different on the two sides of a transition: a generic mechanism*, *Phys. Rev. Lett.* **115** (2015) 200601.

[88] D. J. Amit and L. Peliti, *On dangerous irrelevant operators*, *Annals of Physics* **140** (1982) 207 .

[89] S. Weinberg, *The quantum theory of fields*, vol. 2. Cambridge university press, 1995.

[90] B. Nienhuis, E. K. Riedel and M. Schick, *q-state potts model in general dimension*, *Phys. Rev. B* **23** (1981) 6055.

[91] A. Aharony, *Critical behavior of anisotropic cubic systems*, *Phys. Rev. B* **8** (1973) 4270.

[92] A. Aharony and M. E. Fisher, *Critical behaviour of magnets with dipolar interactions. i. renormalization group near four dimensions*, *Phys. Rev. B* **8** (1973) 3323.

[93] D. J. Wallace, *Critical behaviour of anisotropic cubic systems*, *Journal of Physics C: Solid State Physics* **6** (1973) 1390.

[94] P. Calabrese, A. Pelissetto and E. Vicari, *Randomly dilute spin models with cubic symmetry*, *Phys. Rev. B* **67** (2003) 024418.

[95] S. R. Kousvos and A. Stergiou, *Bootstrapping Mixed Correlators in Three-Dimensional Cubic Theories*, 1810.10015.

[96] R. Ben Alì Zinati, A. Codello and G. Gori,*in preparation* (2019) .

[97] A. Stergiou, *Bootstrapping hypercubic and hypertetrahedral theories in three dimensions*, *Journal of High Energy Physics* **2018** (2018) 35.

[98] S. Yabunaka and B. Delamotte, *Surprises in $o(n)$ models: nonperturbative fixed points, large n limits, and multicriticality*, *Phys. Rev. Lett.* **119** (2017) 191602.

[99] S. Yabunaka and B. Delamotte, *Why might the standard large n analysis fail in the* $\mathrm{O}(n)$ *model: The role of cusps in fixed point potentials*, *Phys. Rev. Lett.* **121** (2018) 231601.

[100] D. Poland, S. Rychkov and A. Vichi, *The Conformal Bootstrap: Theory, Numerical Techniques, and Applications*, *Rev. Mod. Phys.* **91** (2019) 15002 [1805.04405].

[101] A. Codello, *Scaling solutions in a continuous dimension*, *Journal of Physics A Mathematical General* **45** (2012) 465006 [1204.3877].

[102] V. A. Fateev and A. B. Zamolodchikov, *Parafermionic Currents in the Two-Dimensional Conformal Quantum Field Theory and Selfdual Critical Points in Z(n) Invariant Statistical Systems*, *Sov. Phys. JETP* **62** (1985) 215.

[103] A. Codello, M. Safari, G. P. Vacca and O. Zanusso,*in preparation* (2019) .

[104] E. Schrödinger, *What is life? The physical aspect of the living cell and mind*. Cambridge University Press Cambridge, 1944.

[105] J. J. Hopfield, *Neural networks and physical systems with emergent collective computational abilities*, *Proceedings of the National Academy of Sciences* **79** (1982) 2554.

[106] H. Haken, J. A. S. Kelso and H. Bunz, *A theoretical model of phase transitions in human hand movements*, *Biological Cybernetics* **51** (1985) 347.

[107] D. J. Amit and D. J. Amit, *Modeling brain function: The world of attractor neural networks*. Cambridge university press, 1992.

[108] W. Bialek, *Biophysics: searching for principles*. Princeton University Press, 2012.

[109] K. Sneppen, *Models of life*. Cambridge University Press, 2014.

[110] G. H. Pollack and W.-C. Chin, *Phase transitions in cell biology*. Springer, 2008.

[111] M. A. Muñoz, *Colloquium: Criticality and dynamical scaling in living systems*, *Rev. Mod. Phys.* **90** (2018) 031001.

[112] T. Vicsek, A. Czirók, E. Ben-Jacob, I. Cohen and O. Shochet, *Novel type of phase transition in a system of self-driven particles*, *Phys. Rev. Lett.* **75** (1995) 1226.

[113] J. Toner and Y. Tu, *Long-range order in a two-dimensional dynamical* XY *model: How birds fly together*, *Phys. Rev. Lett.* **75** (1995) 4326.

[114] M. Ballerini, N. Cabibbo, R. Candelier, A. Cavagna, E. Cisbani, I. Giardina et al., *Interaction ruling animal collective behavior depends on topological rather than metric distance: Evidence from a field study*, *Proceedings of the National Academy of Sciences* **105** (2008) 1232.

[115] A. Cavagna, A. Cimarelli, I. Giardina, G. Parisi, R. Santagati, F. Stefanini et al., *Scale-free correlations in starling flocks*, *Proceedings of the National Academy of Sciences* **107** (2010) 11865.

[116] E. Bonabeau, D. d. R. D. F. Marco, M. Dorigo, G. Theraulaz et al., *Swarm intelligence: from natural to artificial systems*, no. 1. Oxford university press, 1999.

[117] J. Krause, G. D. Ruxton, G. D. Ruxton, I. G. Ruxton et al., *Living in groups*. Oxford University Press, 2002.

[118] D. J. Sumpter, *Collective animal behavior*. Princeton University Press, 2010.

[119] A. Sokolov, I. S. Aranson, J. O. Kessler and R. E. Goldstein, *Concentration dependence of the collective dynamics of swimming bacteria*, *Phys. Rev. Lett.* **98** (2007) 158102.

[120] S. Ramaswamy, *The mechanics and statistics of active matter*, *Annual Review of Condensed Matter Physics* **1** (2010) 323.

[121] F. Peruani, J. Starruß, V. Jakovljevic, L. Søgaard-Andersen, A. Deutsch and M. Bär, *Collective motion and nonequilibrium cluster formation in colonies of gliding bacteria*, *Phys. Rev. Lett.* **108** (2012) 098102.

[122] C. D. Nadell, V. Bucci, K. Drescher, S. A. Levin, B. L. Bassler and J. B. Xavier, *Cutting through the complexity of cell collectives*, *Proceedings of the Royal Society B: Biological Sciences* **280** (2013) 20122770.

[123] E. Méhes and T. Vicsek, *Collective motion of cells: from experiments to models*, *Integrative Biology* **6** (2014) 831.

[124] P. C. Hohenberg and B. I. Halperin, *Theory of dynamic critical phenomena*, *Rev. Mod. Phys.* **49** (1977) 435.

[125] J. Stenhammar, A. Tiribocchi, R. J. Allen, D. Marenduzzo and M. E. Cates, *Continuum theory of phase separation kinetics for active brownian particles*, *Phys. Rev. Lett.* **111** (2013) 145702.

[126] R. Wittkowski, A. Tiribocchi, J. Stenhammar, R. J. Allen, D. Marenduzzo and M. E. Cates, *Scalar φ^4 field theory for active-particle phase separation*, *Nature communications* **5** (2014) 4351.

[127] A. Tiribocchi, R. Wittkowski, D. Marenduzzo and M. E. Cates, *Active model h: Scalar active matter in a momentum-conserving fluid*, *Phys. Rev. Lett.* **115** (2015) 188302.

[128] J. Toner and Y. Tu, *Flocks, herds, and schools: A quantitative theory of flocking*, *Phys. Rev. E* **58** (1998) 4828.

[129] A. Cavagna, L. Di Carlo, I. Giardina, L. Grandinetti, T. S. Grigera and G. Pisegna, *Dynamical renormalization group approach to the collective behaviour of swarms*, `https://arxiv.org/pdf/1905.01227.pdf`.

[130] A. Cavagna, L. Di Carlo, I. Giardina, L. Grandinetti, T. S. Grigera and G. Pisegna, *Renormalization group crossover in the critical dynamics of field theories with mode coupling terms*, https://arxiv.org/pdf/1905.01228.pdf.

[131] F. Caballero, C. Nardini and M. E. Cates, *From bulk to microphase separation in scalar active matter: a perturbative renormalization group analysis*, *Journal of Statistical Mechanics: Theory and Experiment* **2018** (2018) 123208.

[132] A. Gelimson and R. Golestanian, *Collective dynamics of dividing chemotactic cells*, *Phys. Rev. Lett.* **114** (2015) 028101.

[133] M. Eisenbach, *Chemotaxis*. World Scientific Publishing Company, 2004.

[134] J. T. Bonner, *Cellular slime molds*, vol. 2127. Princeton University Press, 2015.

[135] B. L. Hogan, *Morphogenesis*, *Cell* **96** (1999) 225.

[136] F. Crick, *Diffusion in embryogenesis*, *Nature* **225** (1970) 420.

[137] P. Friedl and D. Gilmour, *Collective cell migration in morphogenesis, regeneration and cancer*, *Nature reviews Molecular cell biology* **10** (2009) 445.

[138] A. Tzur, R. Kafri, V. S. LeBleu, G. Lahav and M. W. Kirschner, *Cell growth and size homeostasis in proliferating animal cells*, *Science* **325** (2009) 167 [https://science.sciencemag.org/content/325/5937/167.full.pdf].

[139] L. Schneider, M. Cammer, J. Lehman, S. K. Nielsen, C. F. Guerra, I. R. Veland et al., *Directional cell migration and chemotaxis in wound healing response to pdgf-aa are coordinated by the primary cilium in fibroblasts*, *Cellular physiology and Biochemistry* **25** (2010) 279.

[140] D. Hanahan and R. A. Weinberg, *Hallmarks of cancer: The next generation*, *Cell* **144** (2011) 646 .

[141] E. Ben-Jacob, I. Cohen and H. Levine, *Cooperative self-organization of microorganisms*, *Advances in Physics* **49** (2000) 395 [https://doi.org/10.1080/000187300405228].

[142] H. Levine and W. Rappel, *The physics of eukaryotic chemotaxis*, *Physics today* **66** (2013) .

[143] E. F. Keller and L. A. Segel, *Initiation of slime mold aggregation viewed as an instability*, *Journal of Theoretical Biology* **26** (1970) 399 .

[144] E. F. Keller and L. A. Segel, *Model for chemotaxis*, *Journal of Theoretical Biology* **30** (1971) 225 .

[145] Y. Tsori and P.-G. de Gennes, *Self-trapping of a single bacterium in its own chemoattractant*, *Europhysics Letters (EPL)* **66** (2004) 599.

[146] R. Grima, *Strong-coupling dynamics of a multicellular chemotactic system*, *Phys. Rev. Lett.* **95** (2005) 128103.

[147] R. Golestanian, *Anomalous diffusion of symmetric and asymmetric active colloids*, *Phys. Rev. Lett.* **102** (2009) 188305.

[148] A. Sengupta, S. van Teeffelen and H. Löwen, *Dynamics of a microorganism moving by chemotaxis in its own secretion*, *Phys. Rev. E* **80** (2009) 031122.

[149] J. Taktikos, V. Zaburdaev and H. Stark, *Collective dynamics of model microorganisms with chemotactic signaling*, *Phys. Rev. E* **85** (2012) 051901.

[150] M. P. Brenner, L. S. Levitov and E. O. Budrene, *Physical mechanisms for chemotactic pattern formation by bacteria*, *Biophysical Journal* **74** (1998) 1677 .

[151] P.-H. Chavanis and C. Sire, *Anomalous diffusion and collapse of self-gravitating langevin particles in d dimensions*, *Phys. Rev. E* **69** (2004) 016116.

[152] R. Golestanian, *Collective behavior of thermally active colloids*, *Phys. Rev. Lett.* **108** (2012) 038303.

[153] J. A. Cohen and R. Golestanian, *Emergent cometlike swarming of optically driven thermally active colloids*, *Phys. Rev. Lett.* **112** (2014) 068302.

[154] P. H. Chavanis, J. Sommeria and R. Robert, *Statistical mechanics of two-dimensional vortices and collisionless stellar systems*, *The Astrophysical Journal* **471** (1996) 385.

[155] P.-H. Chavanis, M. Ribot, C. Rosier and C. Sire, *On the analogy between self-gravitating Brownian particles and bacterial populations*, *Banach Center Publ.* **66** (2004) 103 [cond-mat/0407386].

[156] P. H. Chavanis, *Nonlinear mean field fokker-planck equations. application to the chemotaxis of biological populations*, *The European Physical Journal B* **62** (2008) 179.

[157] P.-H. Chavanis, *A stochastic keller–segel model of chemotaxis*, *Communications in Nonlinear Science and Numerical Simulation* **15** (2010) 60 .

[158] K. Kruse, J. F. Joanny, F. Jülicher, J. Prost and K. Sekimoto, *Generic theory of active polar gels: a paradigm for cytoskeletal dynamics*, *The European Physical Journal E* **16** (2005) 5.

[159] J. Toner, *Birth, death, and flight: A theory of malthusian flocks*, *Phys. Rev. Lett.* **108** (2012) 088102.

[160] M. Kardar, G. Parisi and Y.-C. Zhang, *Dynamic scaling of growing interfaces*, *Phys. Rev. Lett.* **56** (1986) 889.

[161] T. Sun, H. Guo and M. Grant, *Dynamics of driven interfaces with a conservation law*, *Phys. Rev. A* **40** (1989) 6763.

[162] F. Caballero, C. Nardini, F. van Wijland and M. E. Cates, *Strong coupling in conserved surface roughening: A new universality class?*, *Phys. Rev. Lett.* **121** (2018) 020601.

[163] W. Jäger and S. Luckhaus, *On explosions of solutions to a system of partial differential equations modelling chemotaxis*, *Transactions of the american mathematical society* **329** (1992) 819.

[164] T. J. Newman and R. Grima, *Many-body theory of chemotactic cell-cell interactions*, *Phys. Rev. E* **70** (2004) 051916.

[165] G. Wolansky, *Comparison between two models of self-gravitating clusters: Conditions for gravitational collapse*, *Nonlinear Analysis: Theory, Methods and Applications* **24** (1995) 1119 .

[166] P.-H. Chavanis, C. Rosier and C. Sire, *Thermodynamics of self-gravitating systems*, *Phys. Rev. E* **66** (2002) 036105.

[167] D. S. Dean, *Langevin equation for the density of a system of interacting langevin processes*, *Journal of Physics A: Mathematical and General* **29** (1996) L613.

[168] E. Medina, T. Hwa, M. Kardar and Y.-C. Zhang, *Burgers equation with correlated noise: Renormalization-group analysis and applications to directed polymers and interface growth*, *Phys. Rev. A* **39** (1989) 3053.

[169] G. Servant, O. D. Weiner, P. Herzmark, T. Balla, J. W. Sedat and H. R. Bourne, *Polarization of chemoattractant receptor signaling during neutrophil chemotaxis*, *Science* **287** (2000) 1037.

[170] D. E. Wolf and J. Villain, *Growth with surface diffusion*, *Europhysics Letters (EPL)* **13** (1990) 389.

[171] H. K. Janssen, *On critical exponents and the renormalization of the coupling constant in growth models with surface diffusion*, *Phys. Rev. Lett.* **78** (1997) 1082.

[172] P. C. Martin, E. D. Siggia and H. A. Rose, *Statistical dynamics of classical systems*, *Phys. Rev. A* **8** (1973) 423.

[173] M. E. Peskin, *An introduction to quantum field theory*. CRC Press, 2018.

[174] M. Le Bellac, *Quantum and statistical field theory*. Clarendon Press Oxford, 1991.

[175] M. E. Cates, *Active Field Theories*, *arXiv e-prints* (2019) arXiv:1904.01330 [1904.01330].

[176] J. Toner, *Birth, death, and flight: A theory of malthusian flocks*, *Phys. Rev. Lett.* **108** (2012) 088102.

[177] A. N. Malmi-Kakkada, X. Li, H. S. Samanta, S. Sinha and D. Thirumalai, *Cell growth rate dictates the onset of glass to fluidlike transition and long time superdiffusion in an evolving cell colony*, *Phys. Rev. X* **8** (2018) 021025.

[178] U. C. Täuber, *Critical dynamics: a field theory approach to equilibrium and non-equilibrium scaling behavior*. Cambridge University Press, 2014.

[179] C. N. Yang and T. D. Lee, *Statistical theory of equations of state and phase transitions. i. theory of condensation*, *Phys. Rev.* **87** (1952) 404.

[180] T. D. Lee and C. N. Yang, *Statistical theory of equations of state and phase transitions. ii. lattice gas and ising model*, *Phys. Rev.* **87** (1952) 410.

[181] N. Breuer and H. K. Janssen, *Equation of state and dynamical properties near the yang-lee edge singularity*, *Zeitschrift für Physik B Condensed Matter* **41** (1981) 55.

[182] P. Calabrese and A. Gambassi, *Ageing properties of critical systems*, *Journal of Physics A: Mathematical and General* **38** (2005) R133.

[183] M. E. Fisher, *Yang-lee edge singularity and ϕ^3 field theory*, *Phys. Rev. Lett.* **40** (1978) 1610.

[184] T. Padmanabhan, *Statistical mechanics of gravitating systems*, *Physics Reports* **188** (1990) 285 .

[185] P.-H. Chavanis, *Phase transitions in self-gravitating systems*, *International Journal of Modern Physics B* **20** (2006) 3113.

[186] A. Artemiev, I. Mazets, G. Kurizki and D. O'dell, *Electromagnetically-induced isothermal" gravitational" collapse in molecular fermionic gases*, *International Journal of Modern Physics B* **18** (2004) 2027.

[187] C. W. Gardiner et al., *Handbook of stochastic methods*, vol. 3. springer Berlin, 1985.